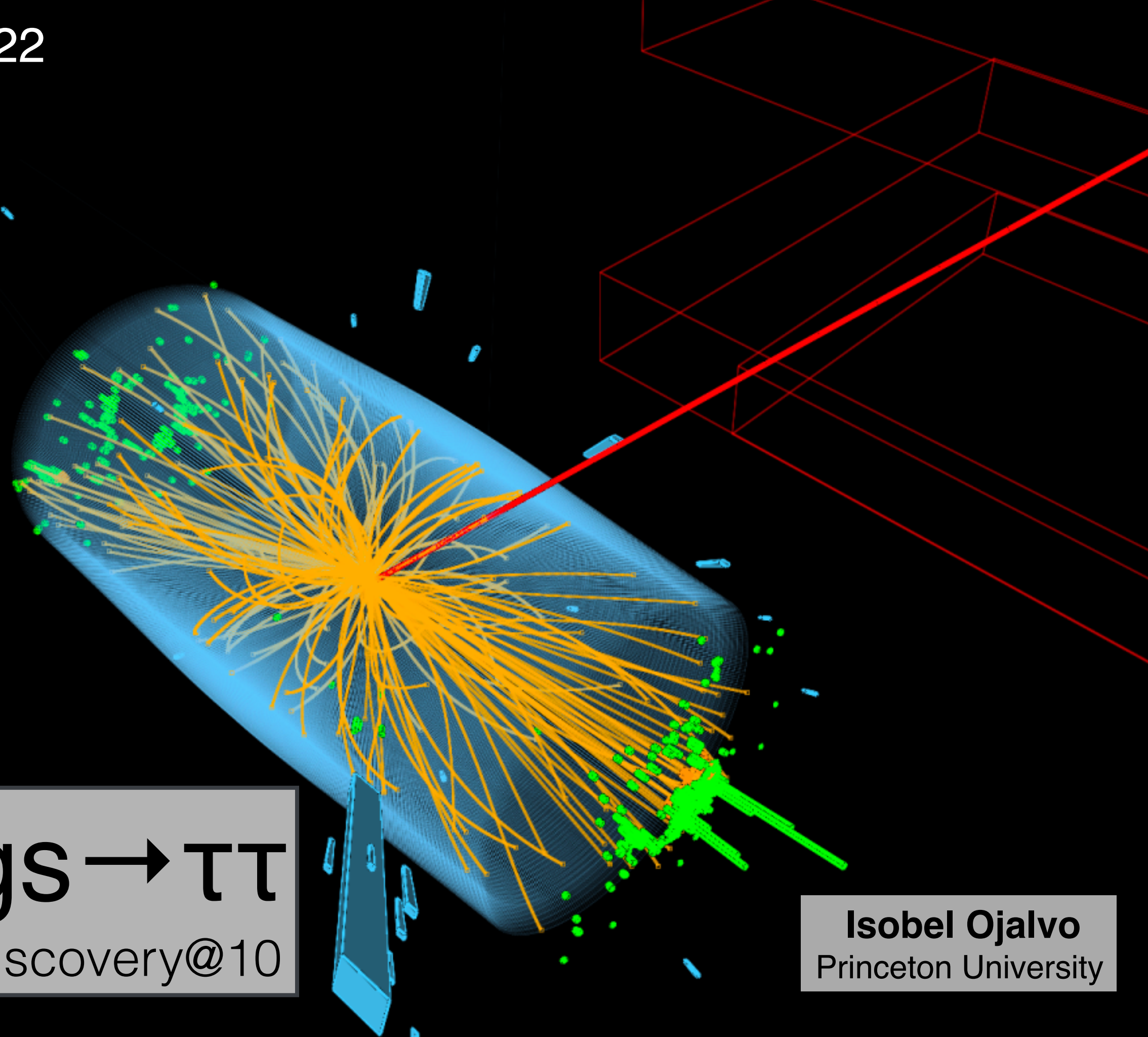


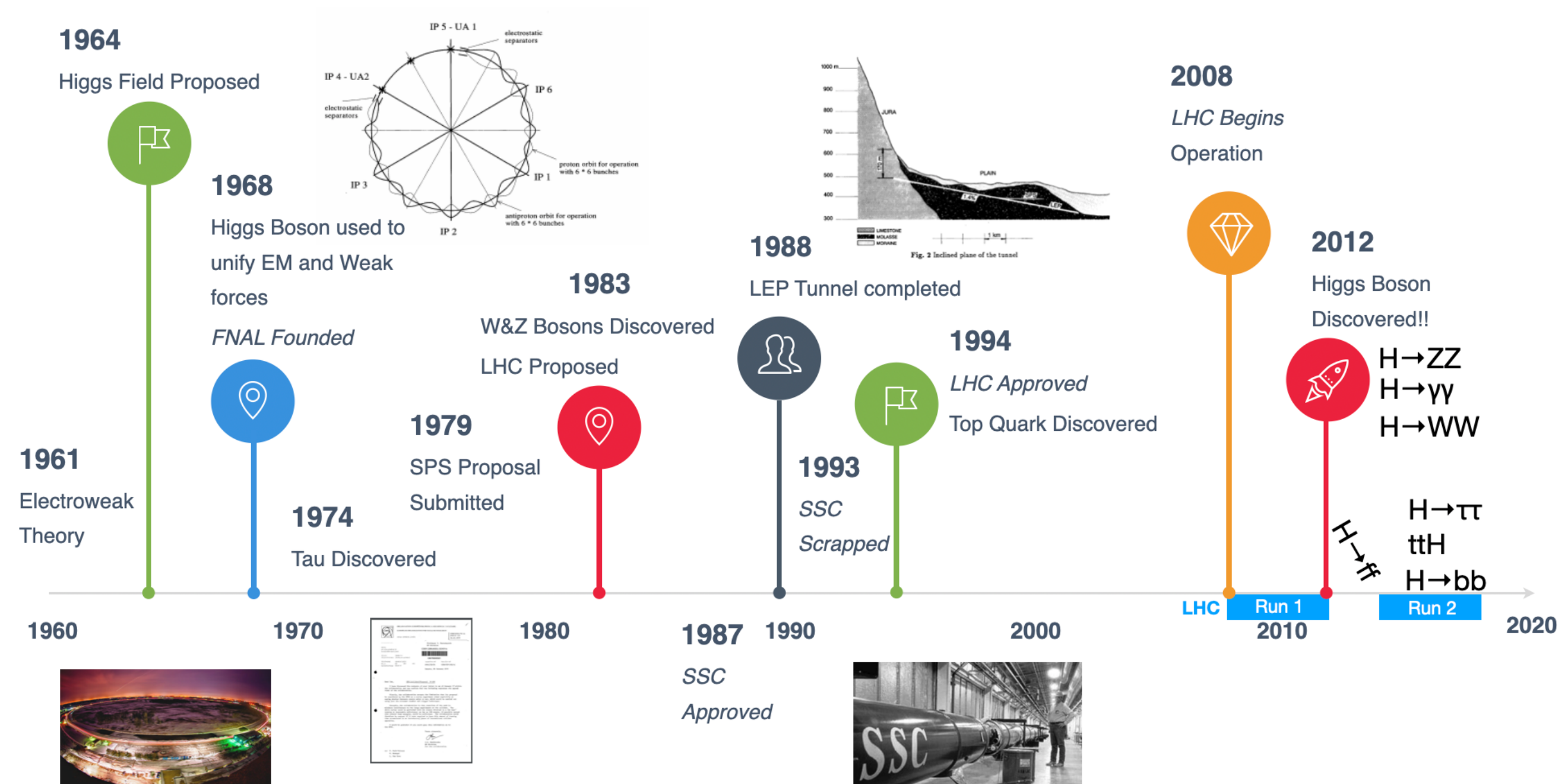
July 1, 2022



Higgs $\rightarrow \tau\tau$
Higgs Discovery@10

Isobel Ojalvo
Princeton University

A History of the Higgs



History of the Tau Lepton

Discovered by Martin L. Perl et al. (1974/1975)

- Stanford Positron Electron Accelerating Ring ([SPEAR](#)) — at SLAC
 - e+e- collider (CoM 7.4 GeV)
- Discovered via $e^+e^- \rightarrow \tau\tau \rightarrow \mu^\pm e^\mp vv$
- Search for a heavier lepton already underway at [ADONE](#) (Italy, 1.5 GeV CoM)
- M.L. Perl recognized the potential for discovery of a heavier lepton using SPEAR



Martin in the SPEAR Control Room in November 1974, following discovery of the J/Psi. Left to right, Gerson Goldhaber (LBL), Martin Perl, and Burton Richter.)

Tau Lepton was first of the **third generation** fermions discovered

- Followed by the discovery of the **bottom quark** (1977), the **top quark** (1995) and the **tau neutrino** (2000)

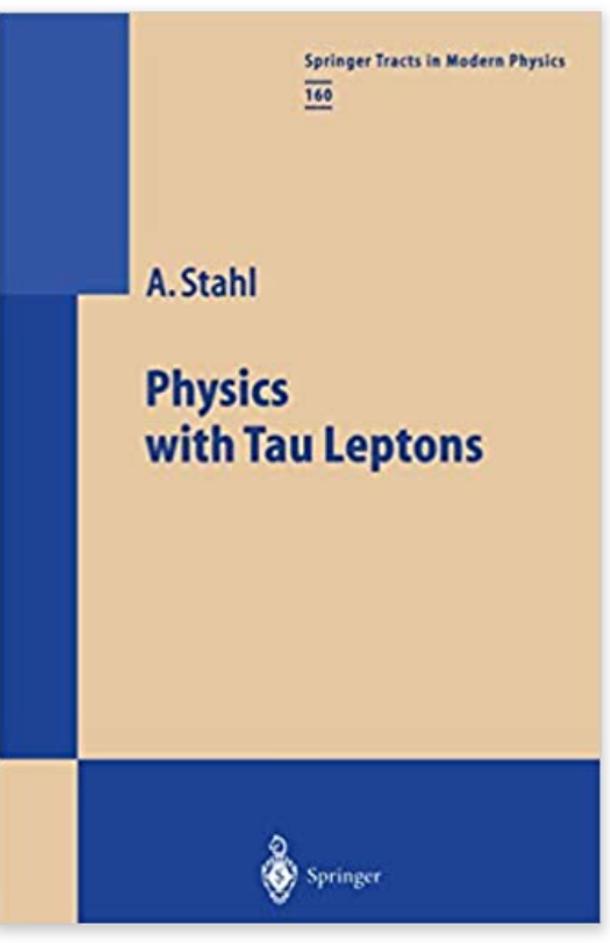
[link](#)



History of the Tau Lepton

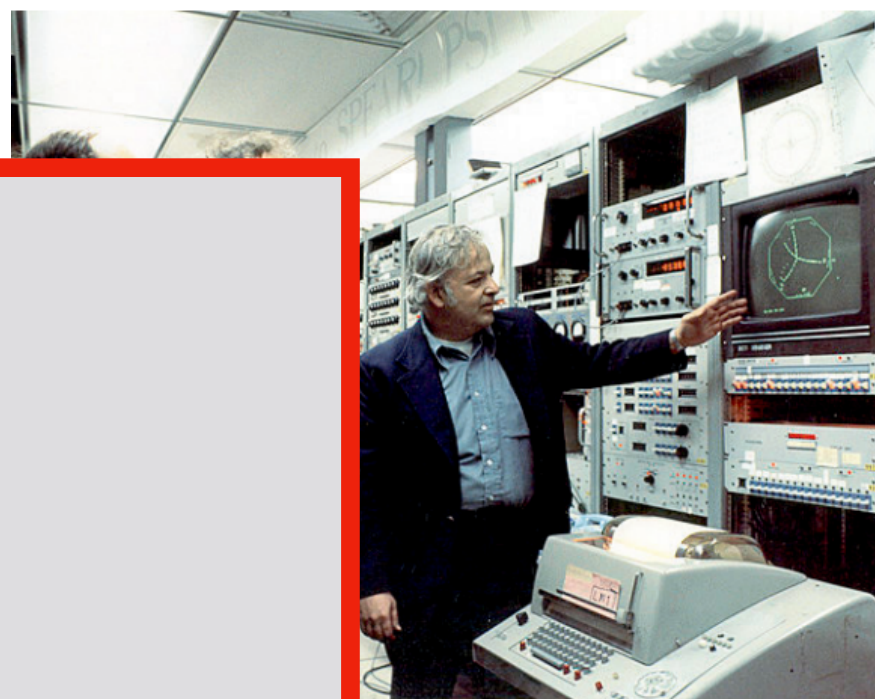
Discovered by Martin L. Perl et al. (1974/1975)

- Stanford Positron-Electron Ring (SPEAR)
 - e+e- coll.
- Discovered τ
- Search for a τ at SLAC underway at A
- M.L. Perl receives Nobel prize for discovery of a τ



Physics with Tau Leptons
by A. Stahl, published in 2001

“It is unclear whether or not one can study Tau Decays at the LHC”



SPEAR Control Room in 1974, following discovery of the τ (left, Gerson Goldhaber (LBL), right, Burton Richter.)

Tau Lepton was discovered
- Followed by the top quark (1995)

is discovered
977), the **top**

[link](#)



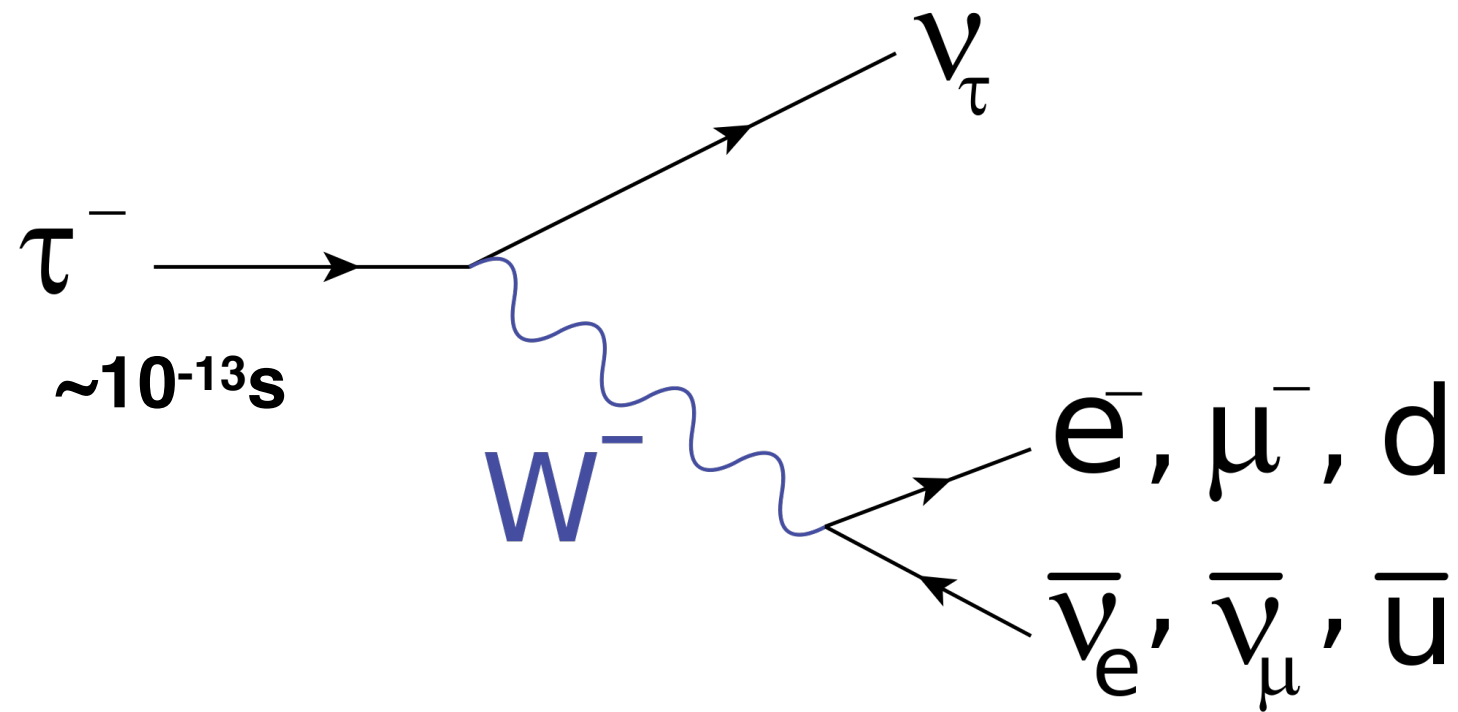
Basic Characteristics

Goal: Detect Taus Efficiently

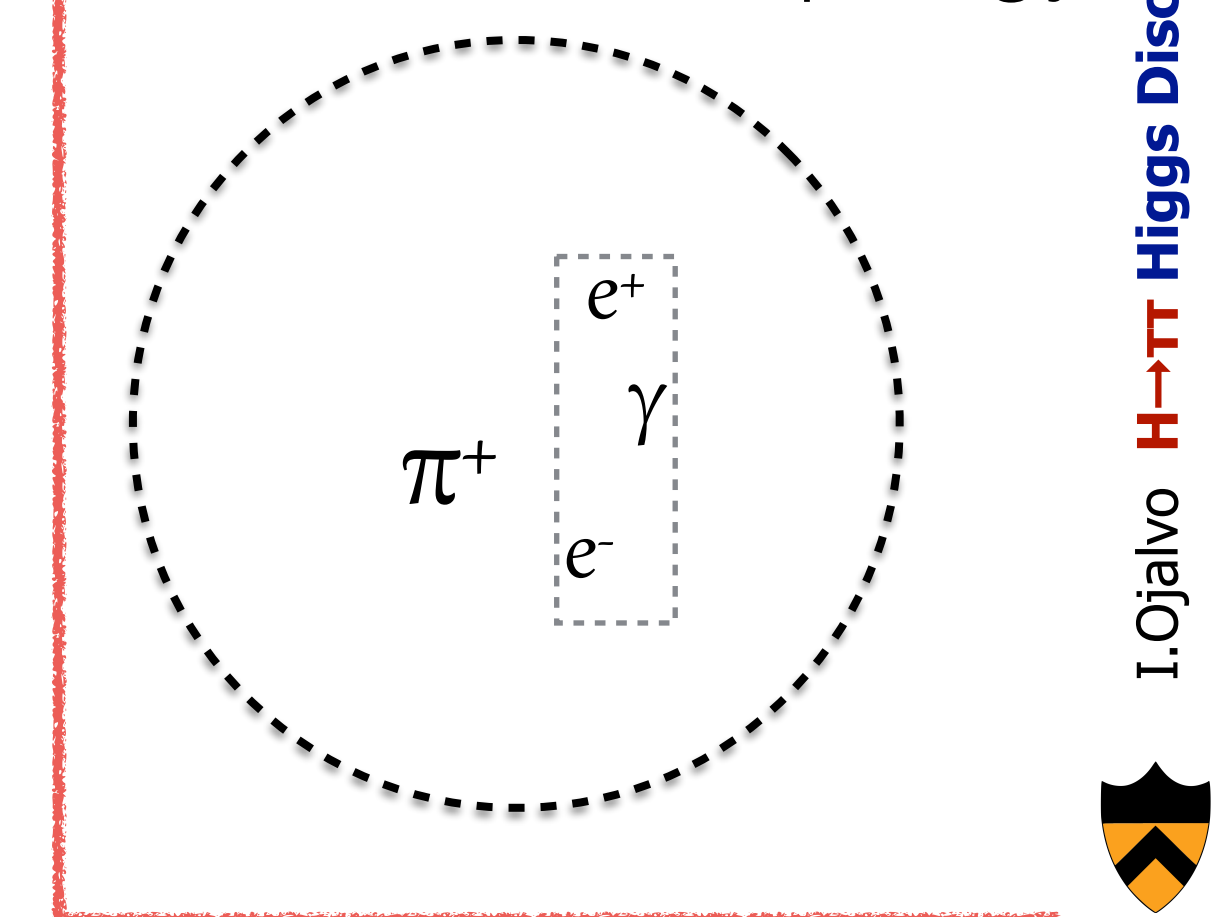
Weak Decay

- Leptonic e/muon + 2 ν
- Hadronic + ν
- Not Fully Reconstructed
(Missing Transverse Energy)

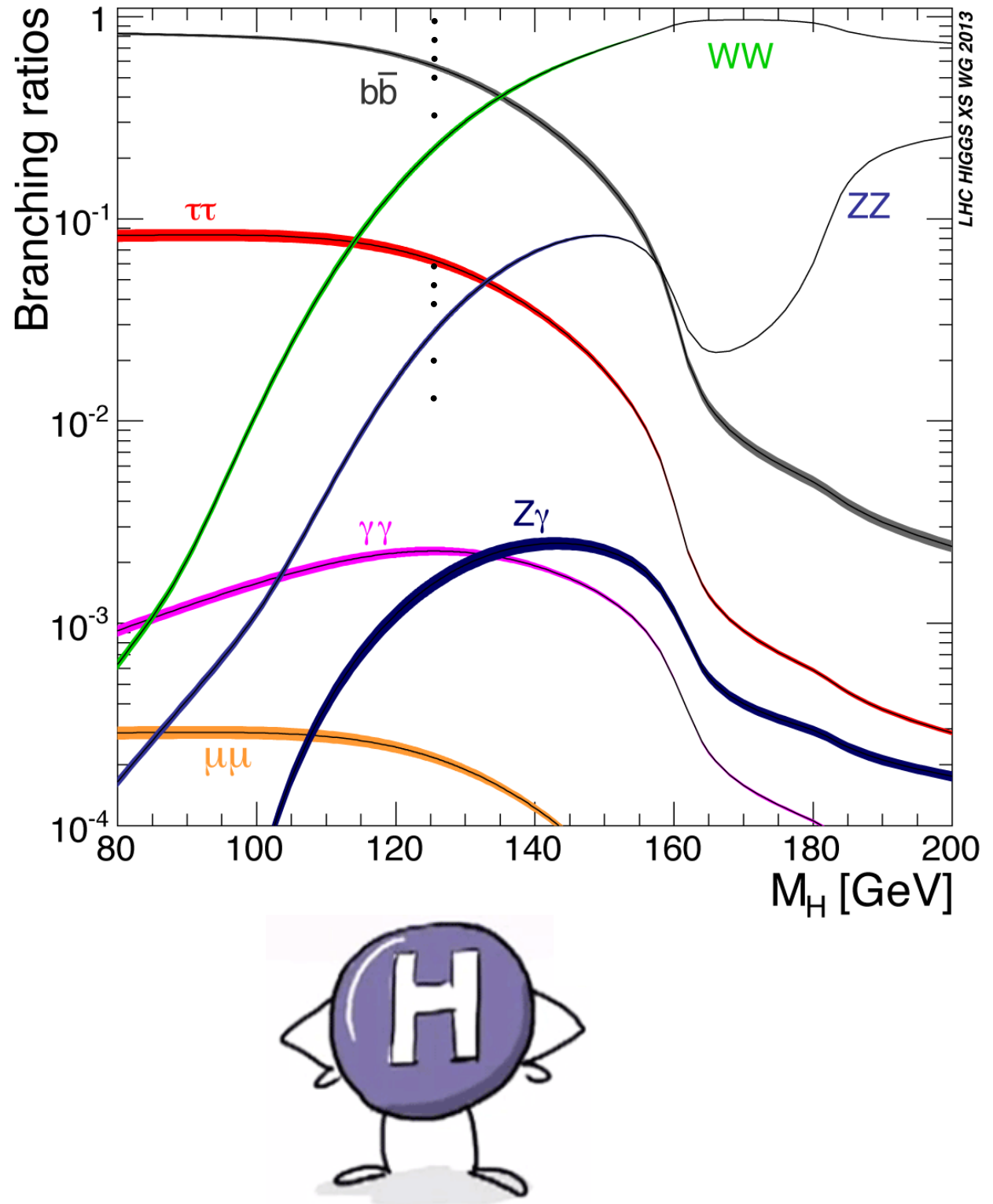
Decay Mode	Resonance	\mathcal{B} [%]
$\tau^- \rightarrow e^- \bar{\nu}_e \nu_\tau$		17.8
$\tau^- \rightarrow \mu^- \bar{\nu}_\mu \nu_\tau$		17.4
$\tau^- \rightarrow h^- \nu_\tau$		11.5
$\tau^- \rightarrow h^- \pi^0 \nu_\tau$	$\rho(770)$	26.0
$\tau^- \rightarrow h^- \pi^0 \pi^0 \nu_\tau$	$a_1(1260)$	10.8
$\tau^- \rightarrow h^- h^+ h^- \nu_\tau$	$a_1(1260)$	9.8
$\tau^- \rightarrow h^- h^+ h^- \pi^0 \nu_\tau$		4.8
Other hadronic modes		1.8
All hadronic modes		64.8



Hadronic Tau Topology



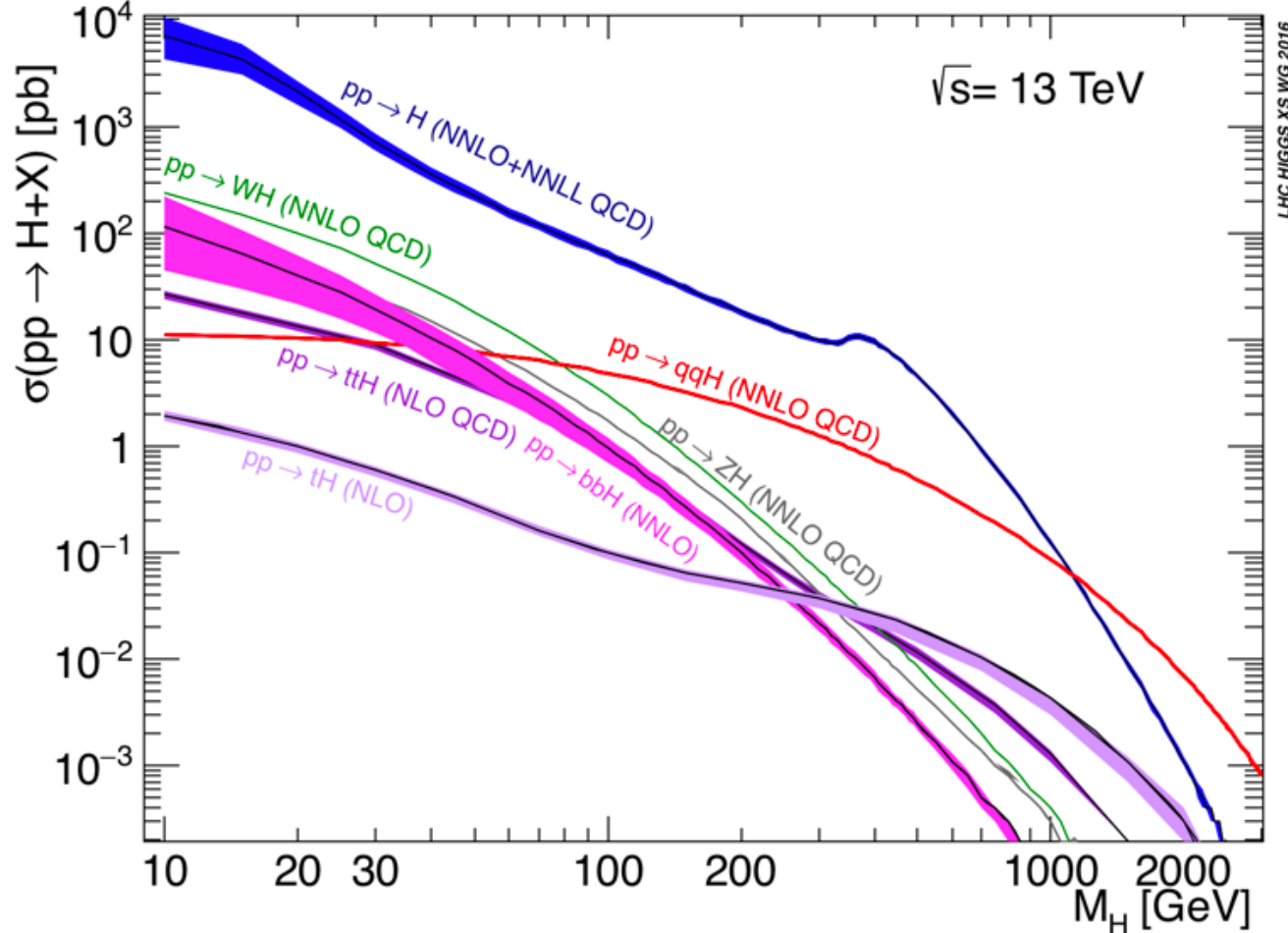
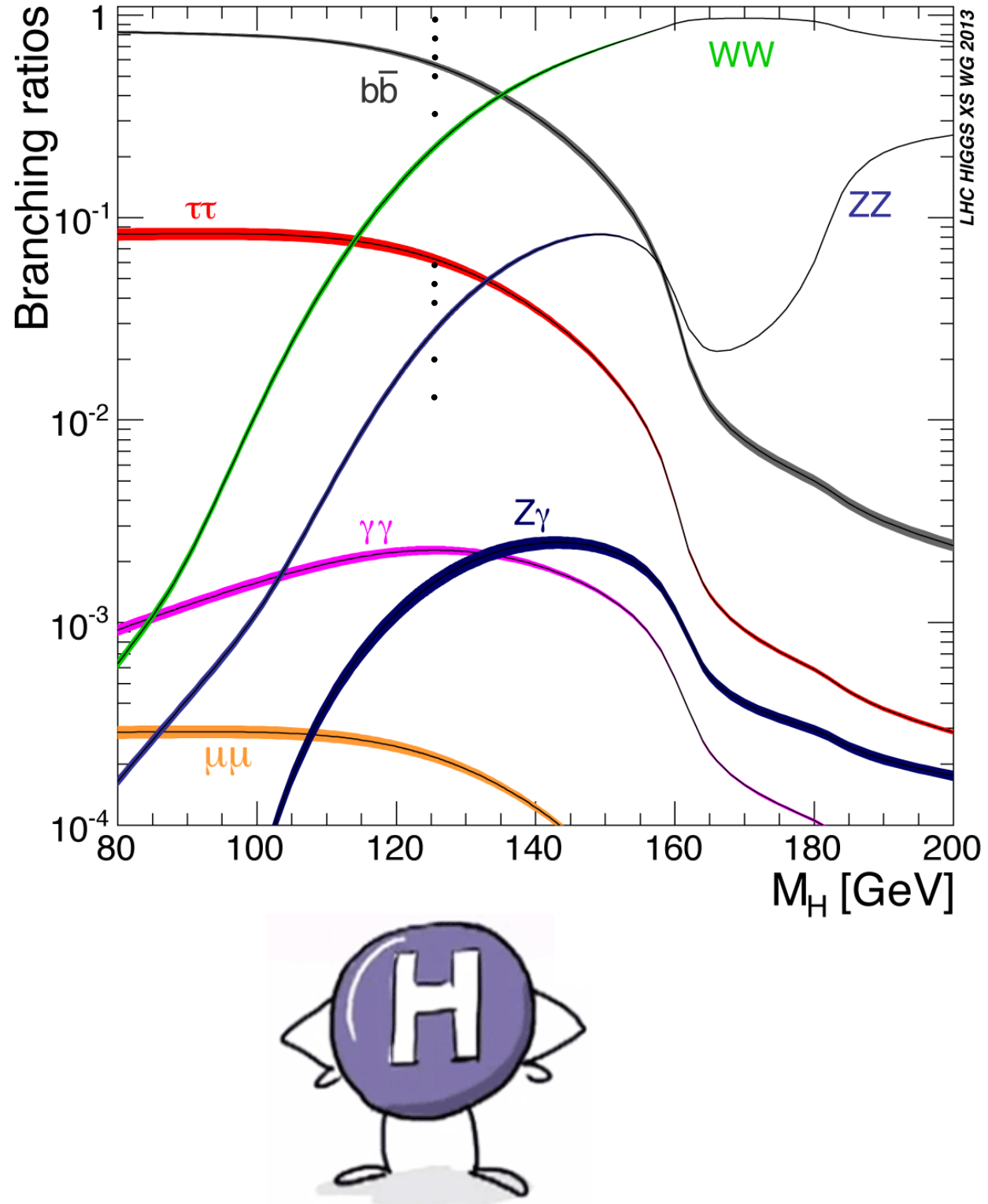
Studying the SM Higgs with τ's



- Lower branching fraction than bb but with a cleaner signature
 - Dedicated Triggers
 - Dedicated Reconstruction, ID
- Many production modes: ggH, VBF, VH, ttH



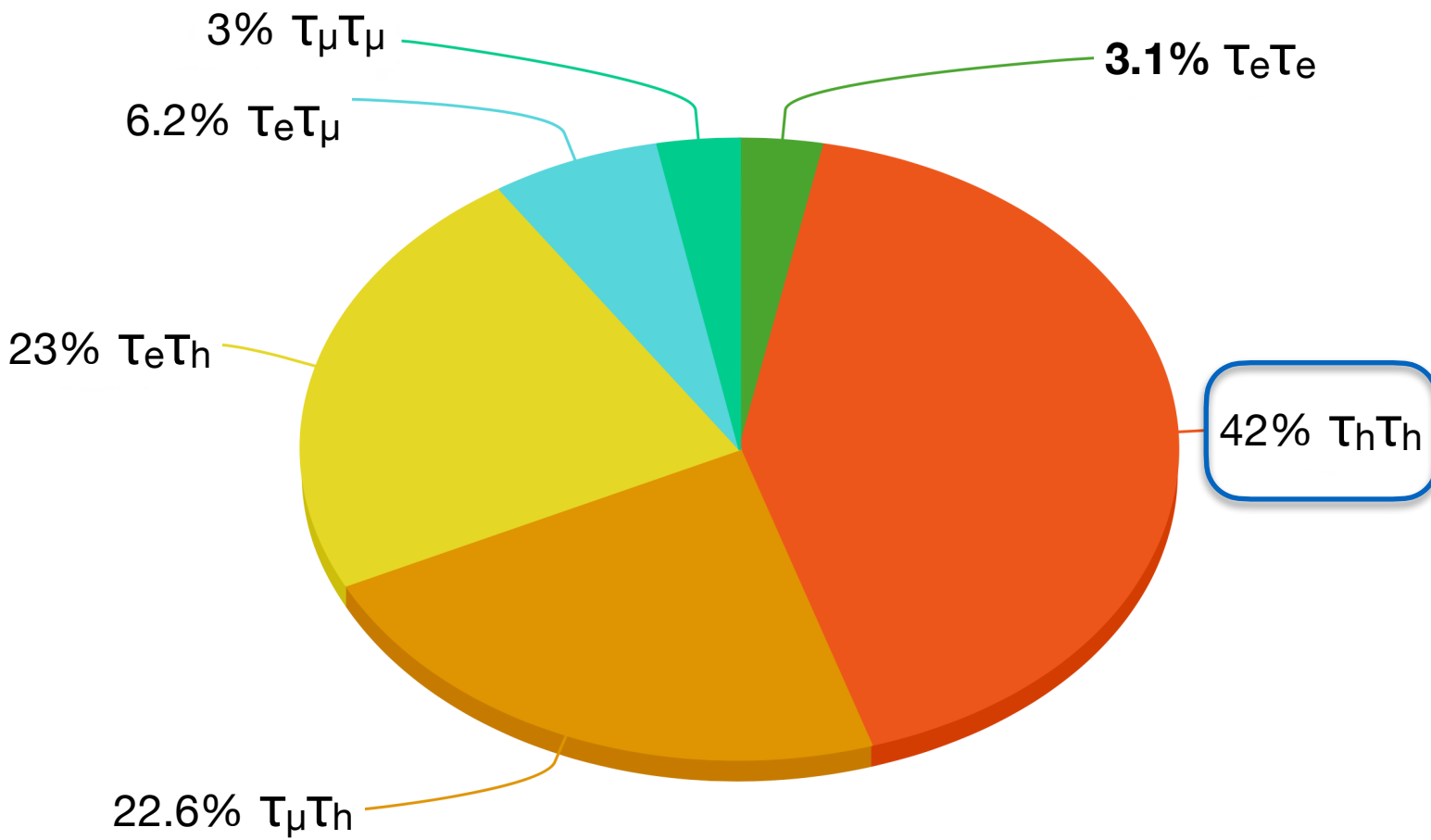
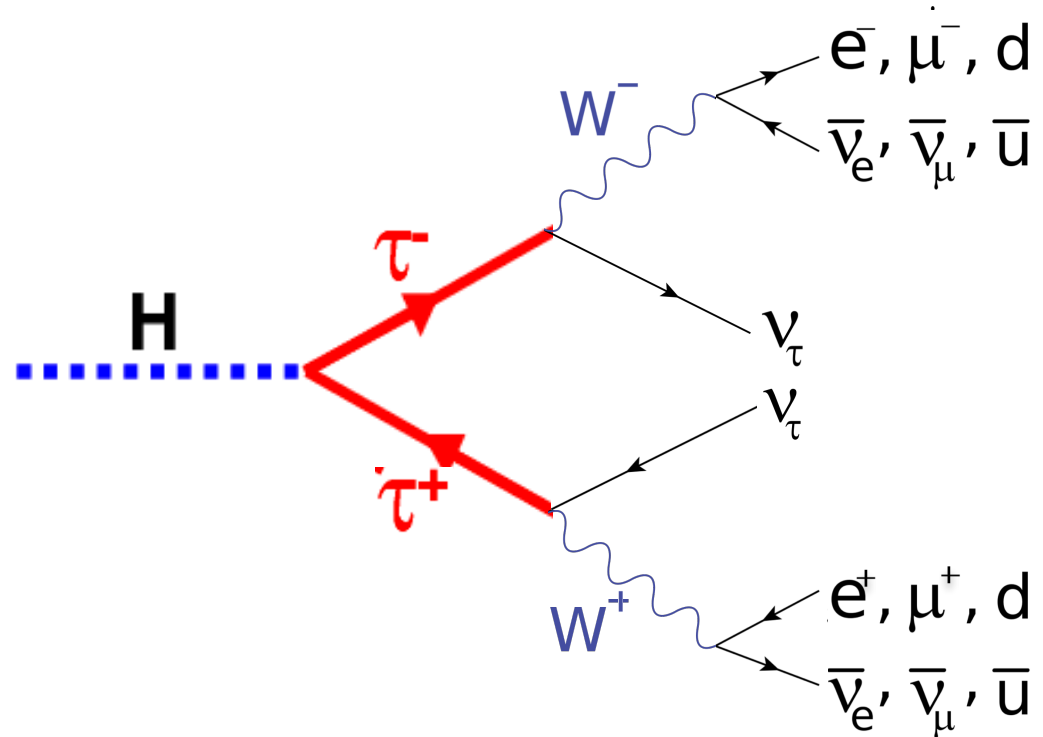
Studying the SM Higgs with τ's



- Many production modes:
 ggH , VBF , VH , ttH



How to Study $H \rightarrow \tau\tau$

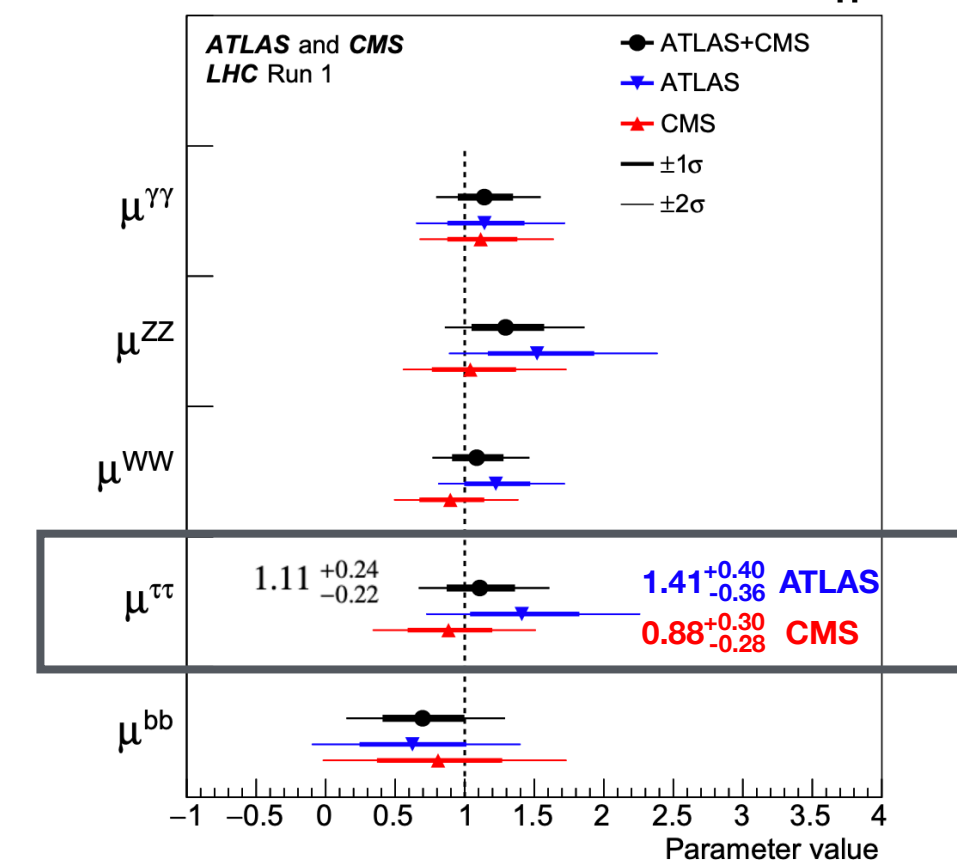
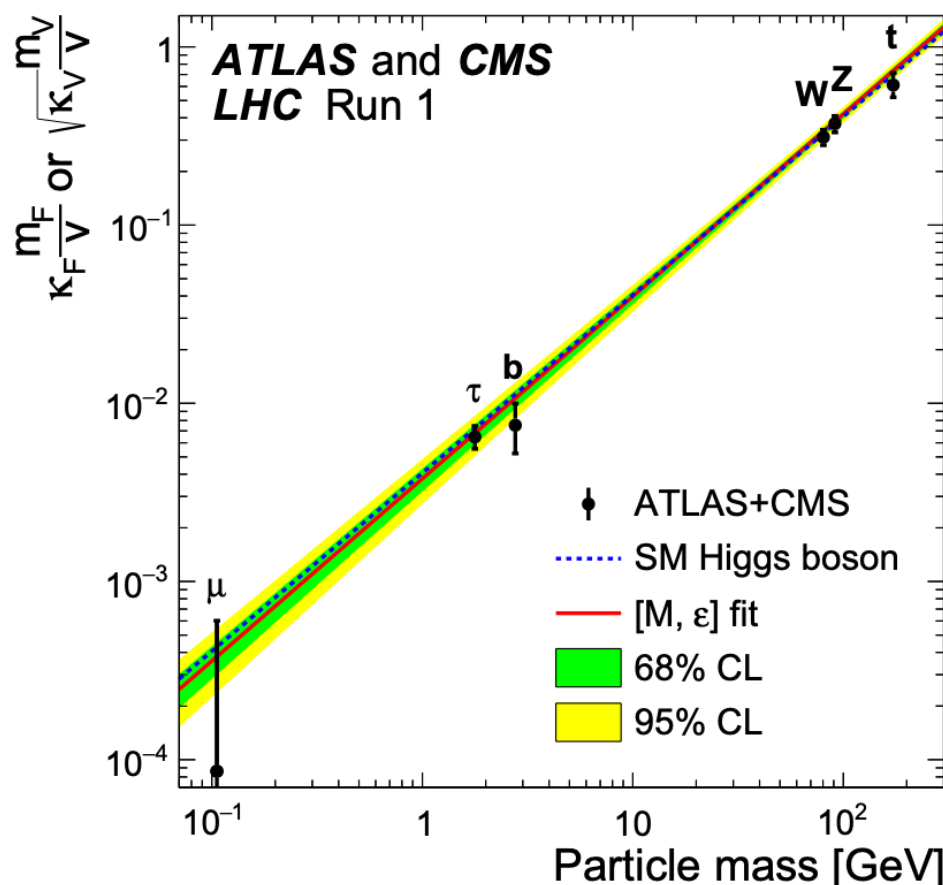
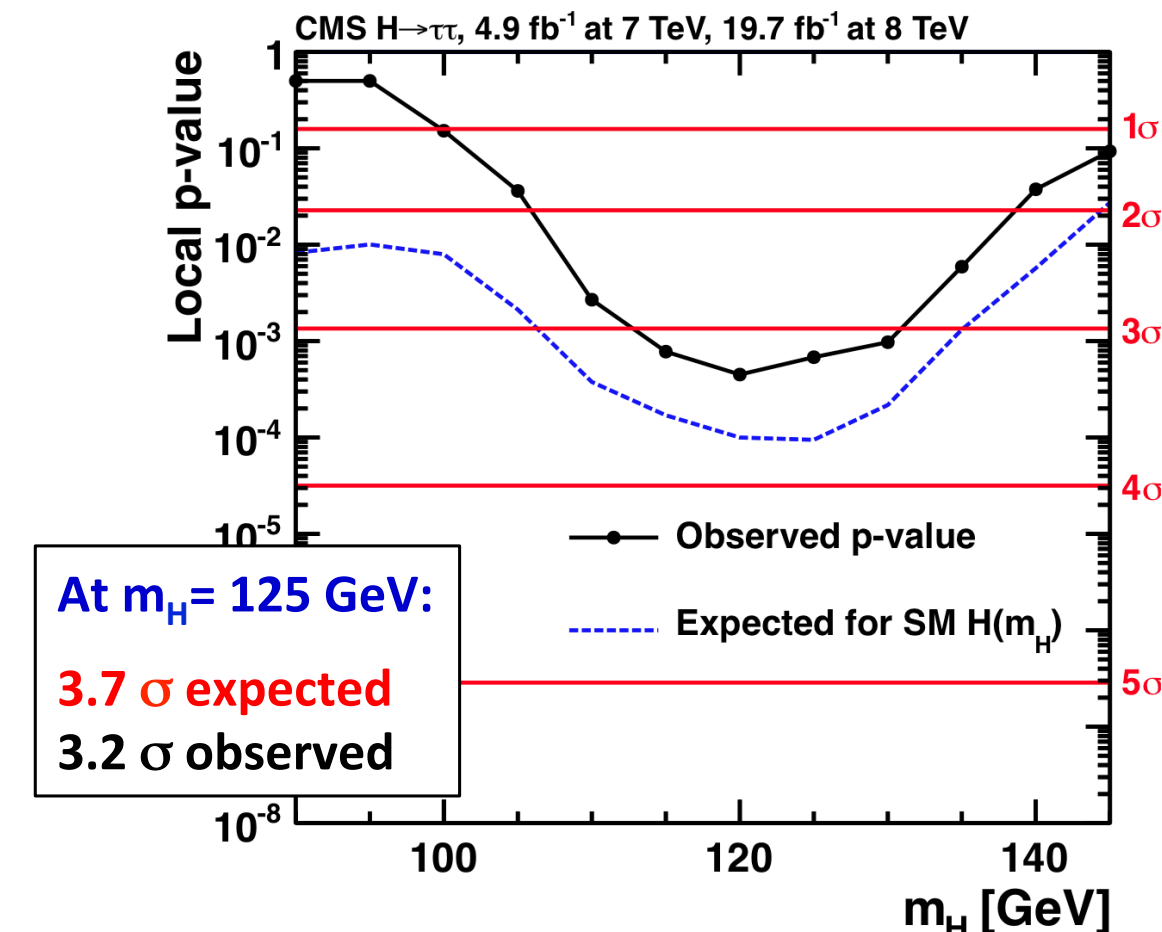
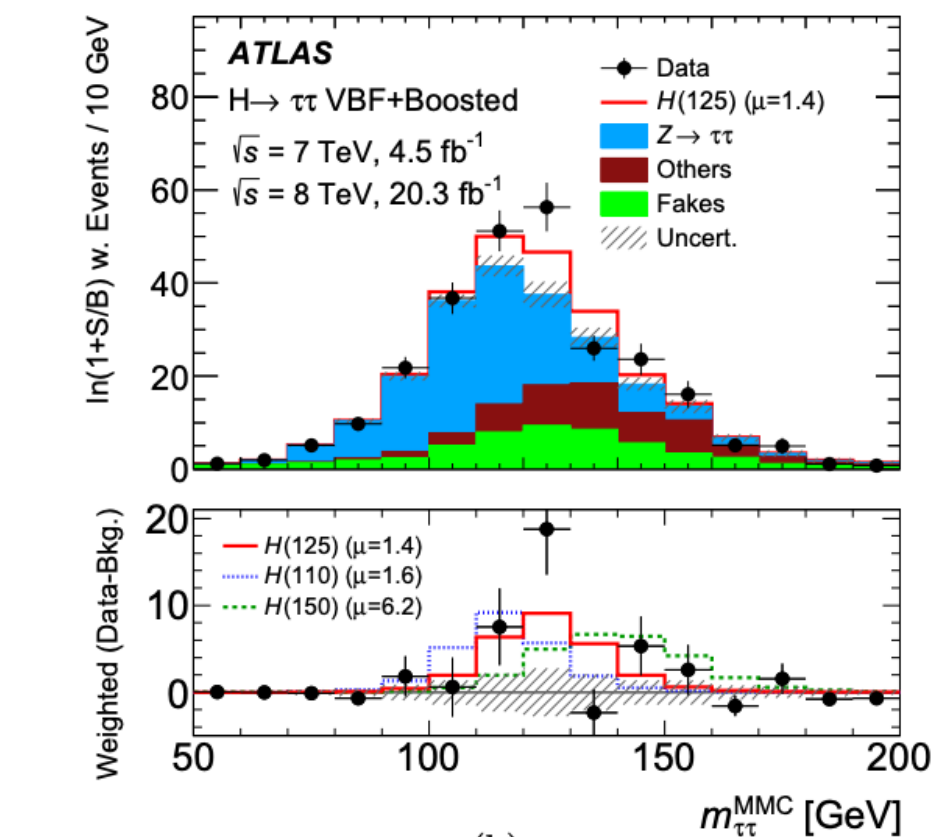


Variety of final states make this analysis complex a priori!

- To measure Essential to identify hadronic τ 's **online** and **offline**



End of Run-1 Combination



Level-1 Trigger at CMS

- CMS Level-1 trigger system composed of custom electronics designed and built in the early 2000's:
 - ASICs (RCT), Copper Cables, burn-once FPGAs (GCT)
- Legacy system used at CMS 2007-2012
- Phase-1 upgrade planned to handle LHC beyond Run-1, originally planned to be installed during Run-2
- CMS accelerated this program and installed the Phase-1 upgrade during LS-1 in two parts

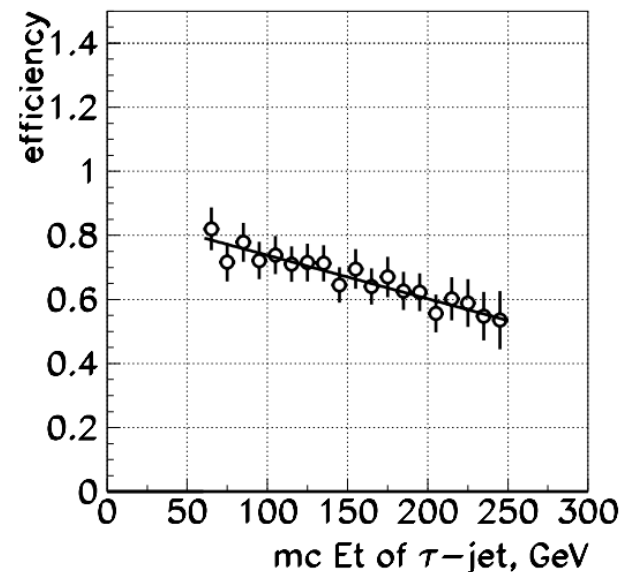
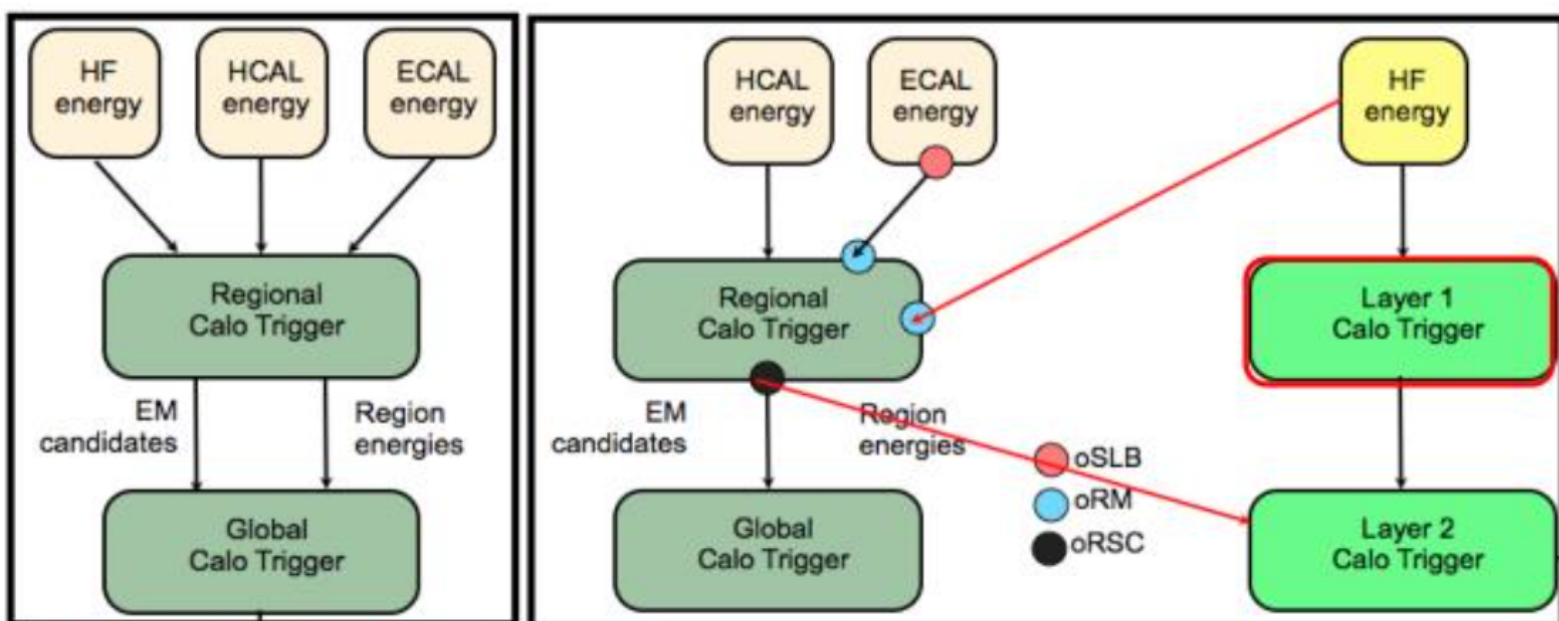
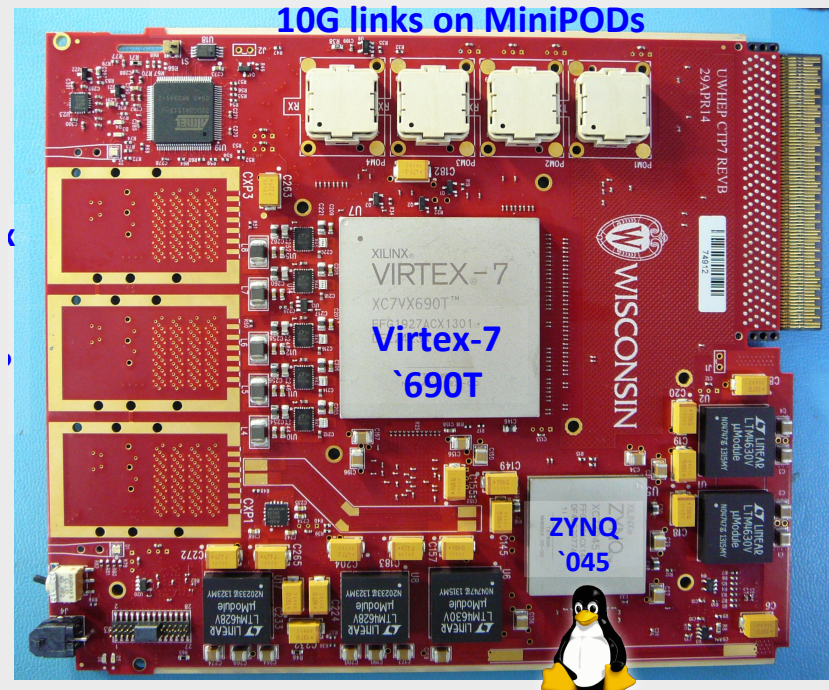


Figure 5: Efficiency of τ -jet identification with the L1 Tau algorithm as a function of the Monte-Carlo E_t of the τ -jet.

Phase-1 Trigger Upgrade



**Level 1:
Custom Hardware**

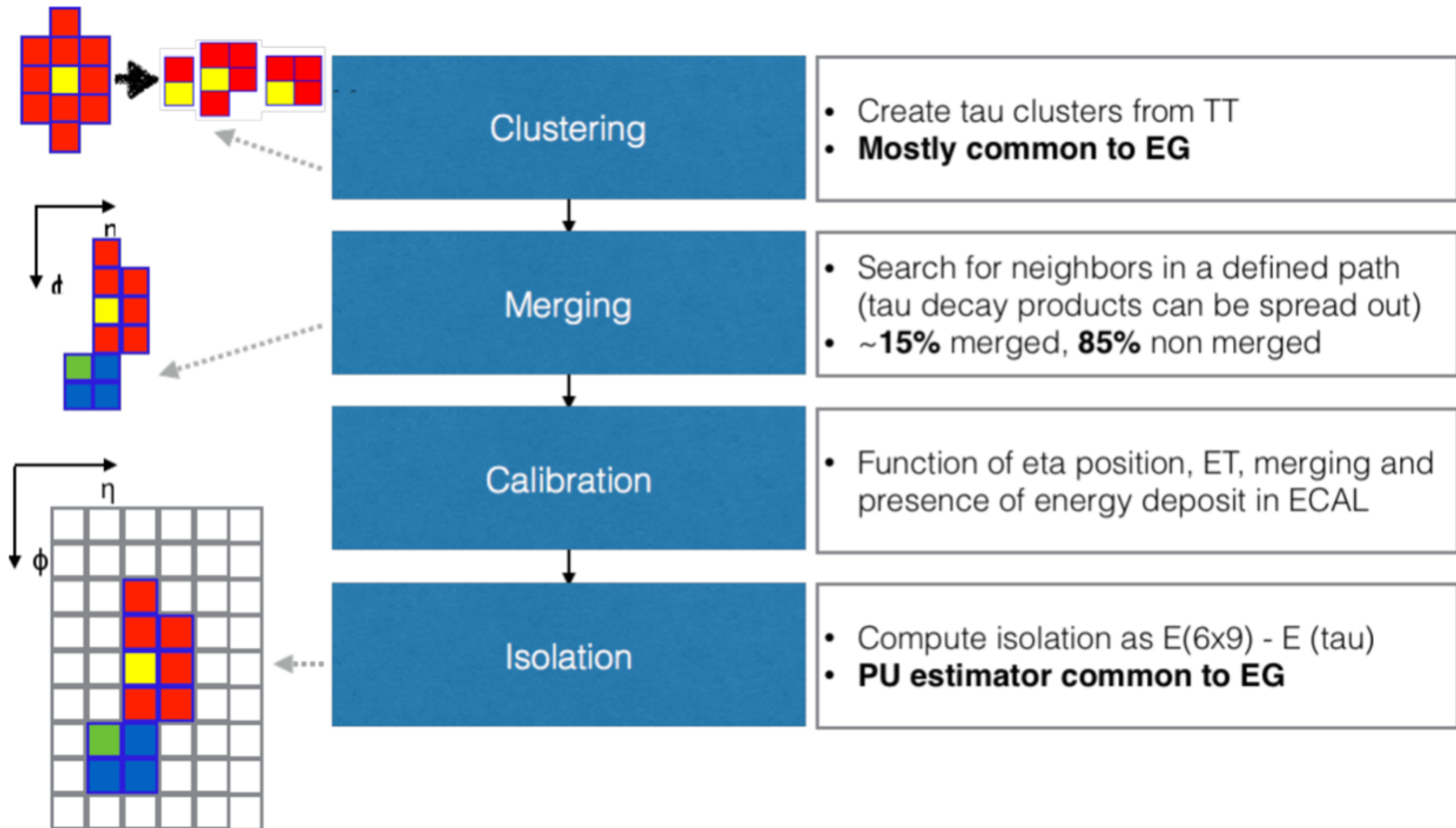


CTP7

**High Level
Trigger:
Computing
Farm**



Level-1 Tau Reconstruction



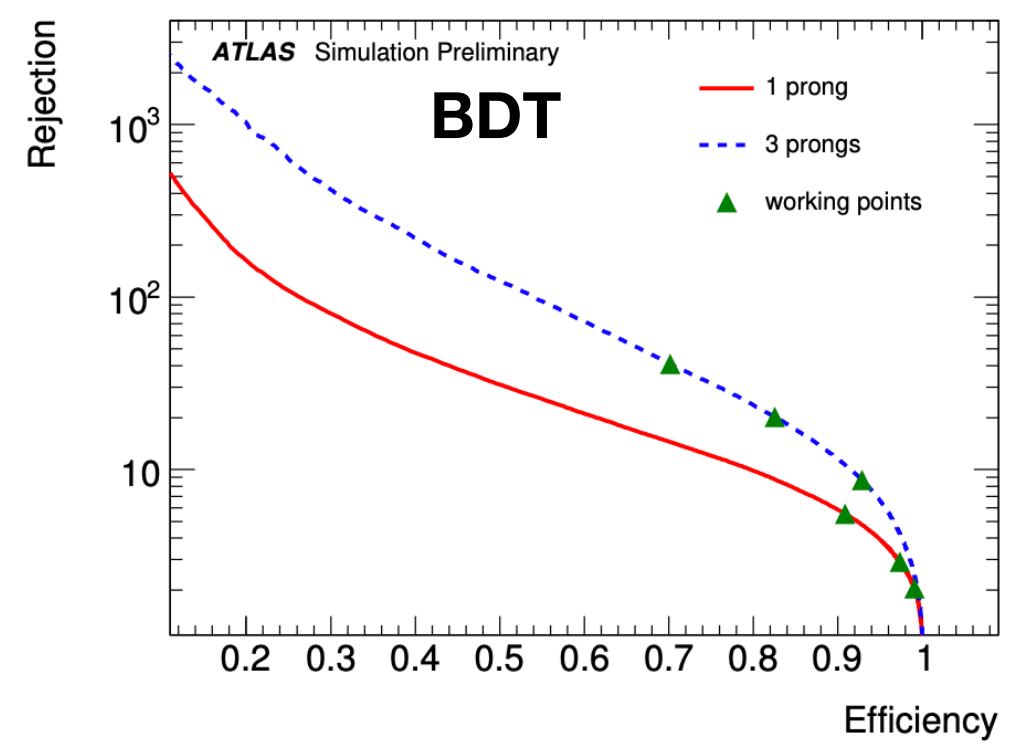
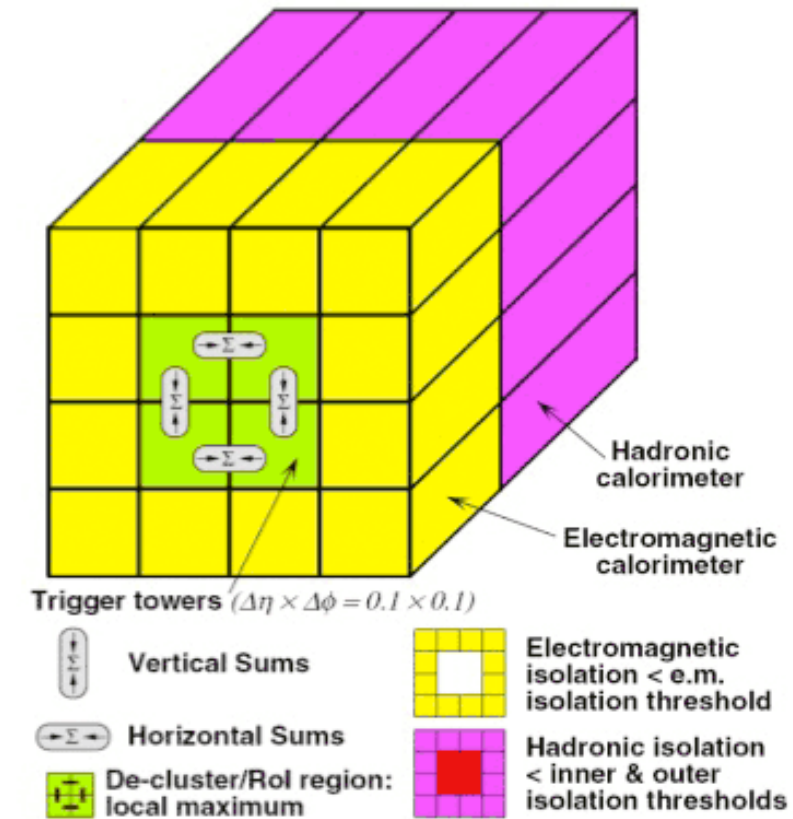
Triggering on Taus: ATLAS

Level-1:

- τ -candidate E_T calculated from the 2×2 core (red) in the HCAL
+ highest of the four sums in the core (green) of the ECAL
- Run 1: $E_T^{\text{EM isol}}[\text{GeV}] \leq (E_T[\text{GeV}]/10 + 1)$
Run 2: $E_T^{\text{EM isol}} < 4 \text{ GeV}$
- Topological selection to ensure di-cand objects are back to back

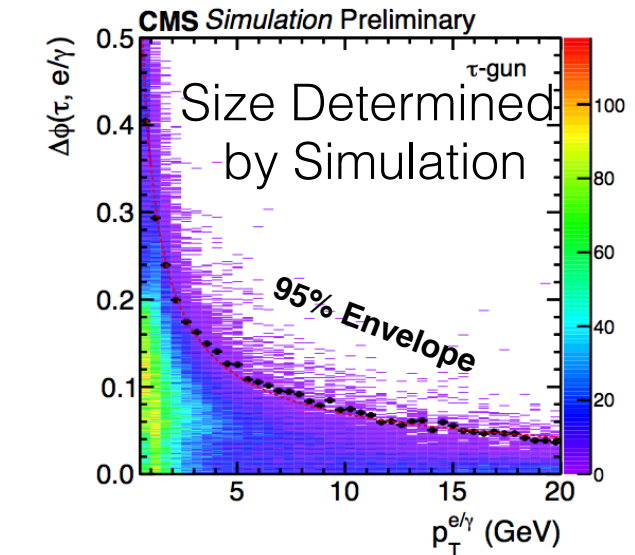
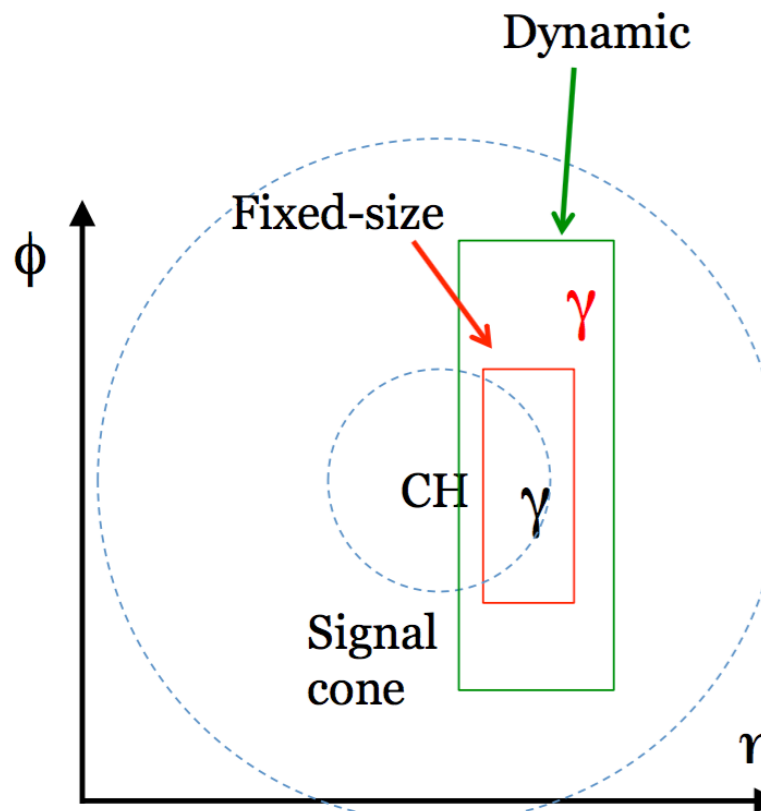
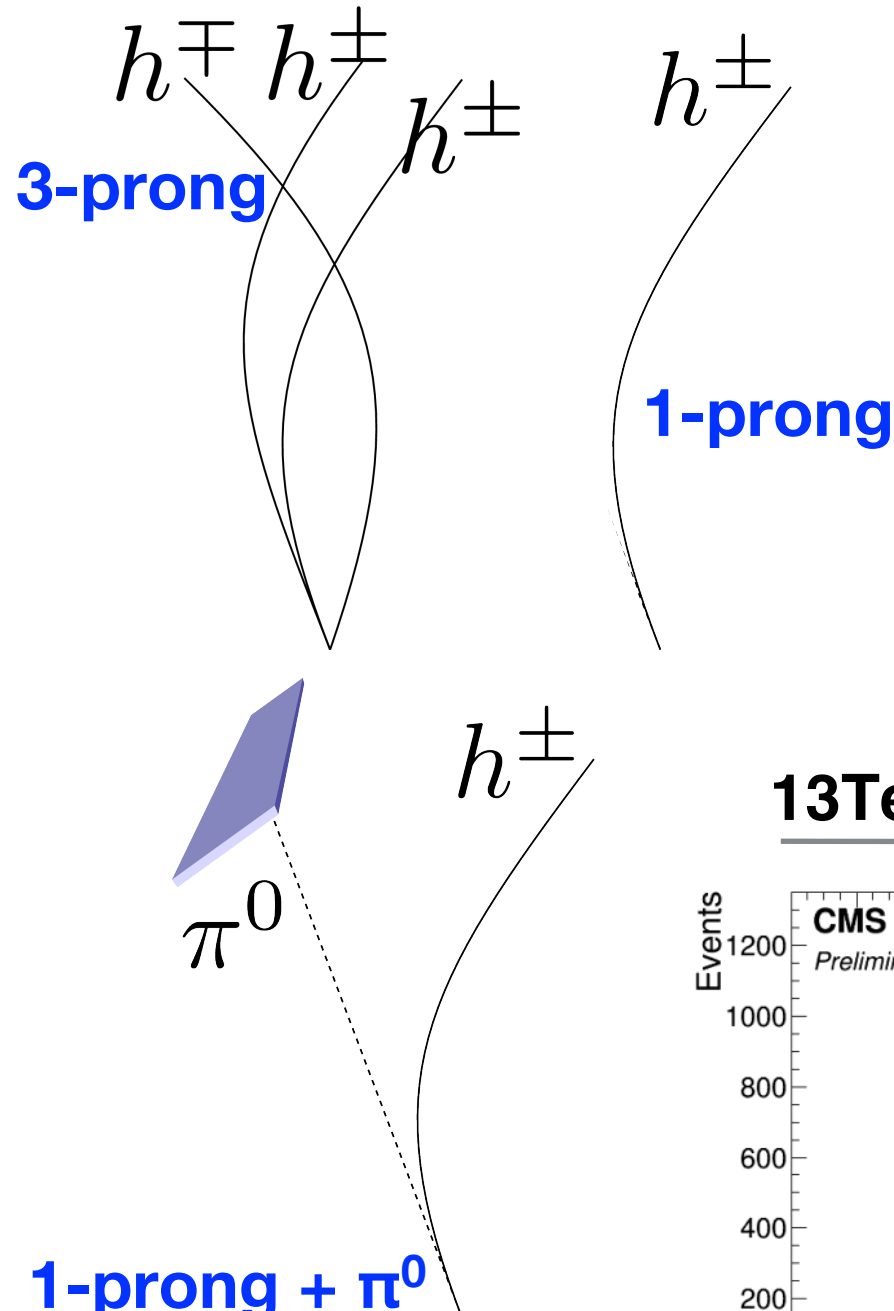
High Level Trigger:

- 1.) Calo-only selection (min calo p_T)
- 2.) Track selection:
$$1 \leq N_{\text{core}}^{\text{trk}} \leq 3, N_{\text{isol}}^{\text{trk}} \leq 1$$
- 3.) offline-like selection using BDT



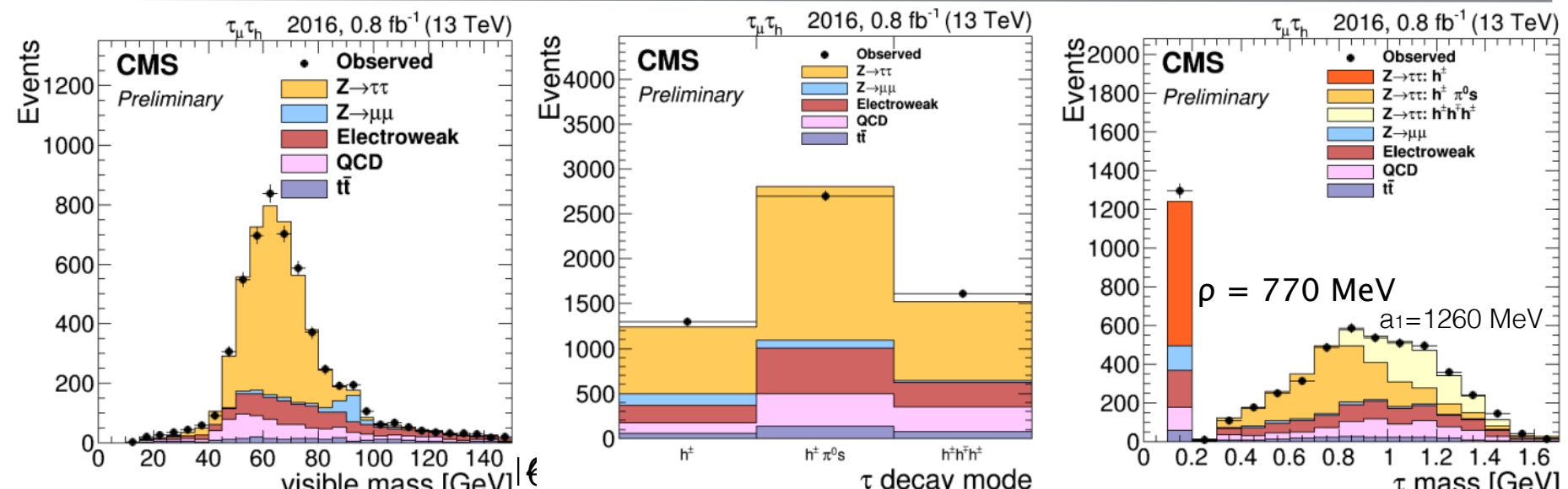
τ_h Reconstruction at CMS

Tau Reconstruction uses a Cut-Based **Hadron Plus Strips (HPS)** Algorithm to Reconstruct **1-prong**, **1-prong + π^0** and **3-prong** Taus from “Particle Flow” Charged Hadron and e/gamma Candidates

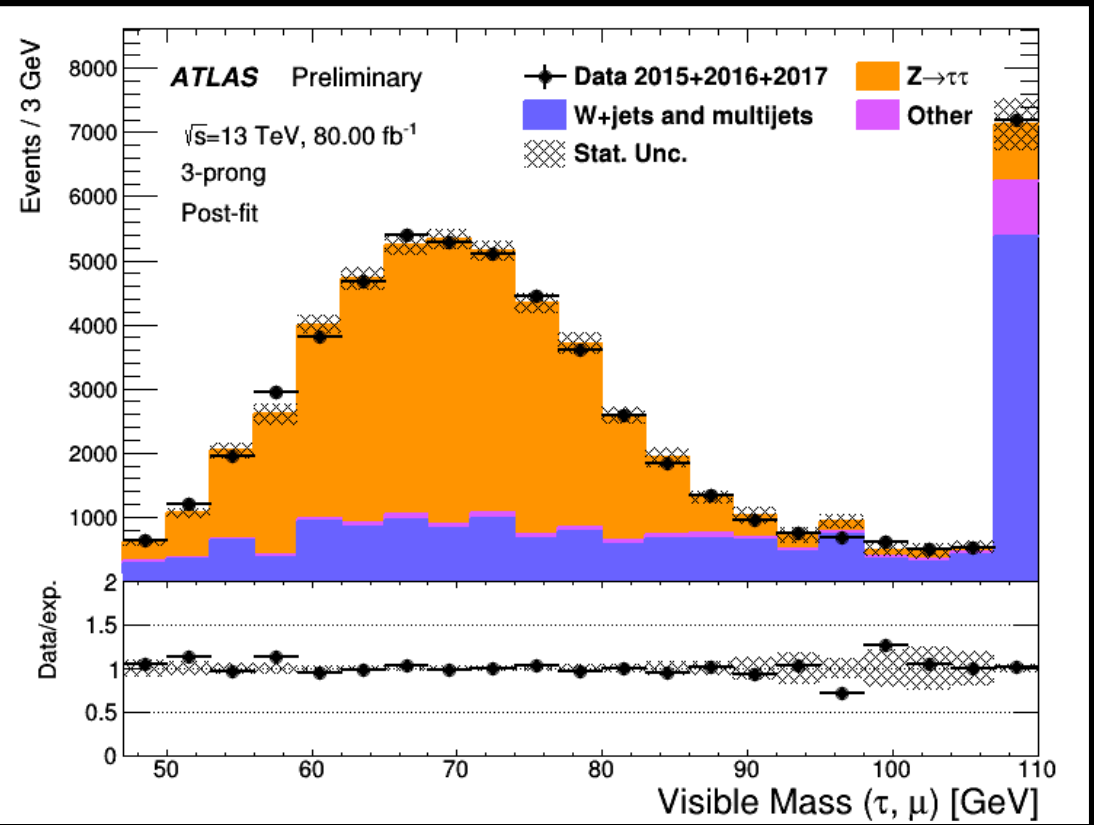
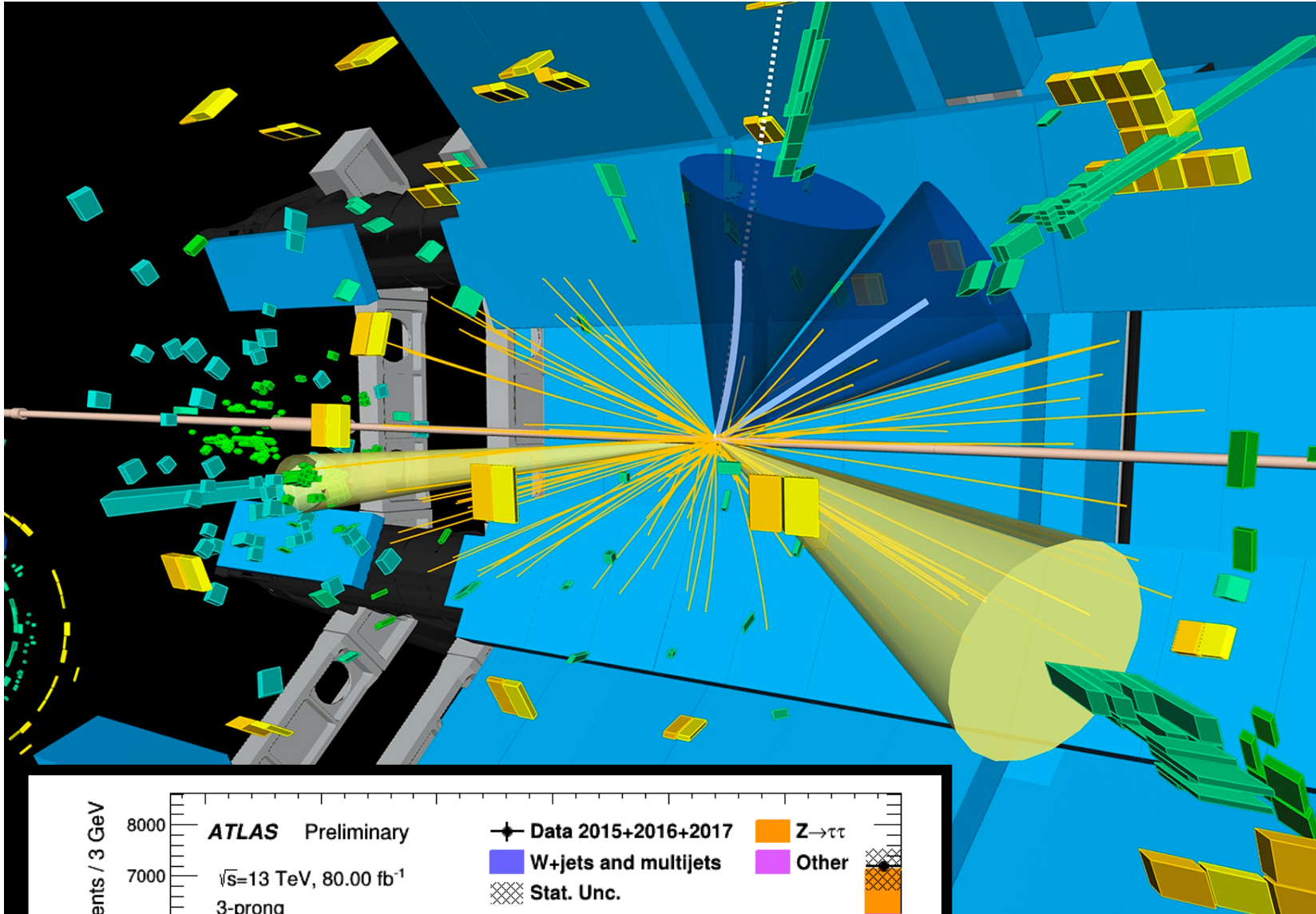


New for Run II 1-prong + π^0 :
Take into account the expected size of the strip based on the e/gamma p_T

13TeV Performance



τ_h Reconstruction ATLAS

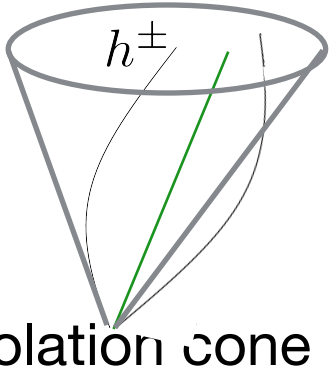


- Tau candidates are seeded by jets
 - A tau vertex is chosen as the candidate track vertex with the largest fraction of momentum from tracks associated ($\Delta R < 0.2$)
 - Tracks are selected based on their position and impact parameters
-
- Provided requirements are passed the tracks are then associated to core ($0 < \Delta R < 0.2$) and isolation ($0.2 < \Delta R < 0.4$) regions around the tau candidate.



Tau ID at CMS

For Jet, τ_h Discrimination we have developed a **cut-based** and an **MVA based** approach

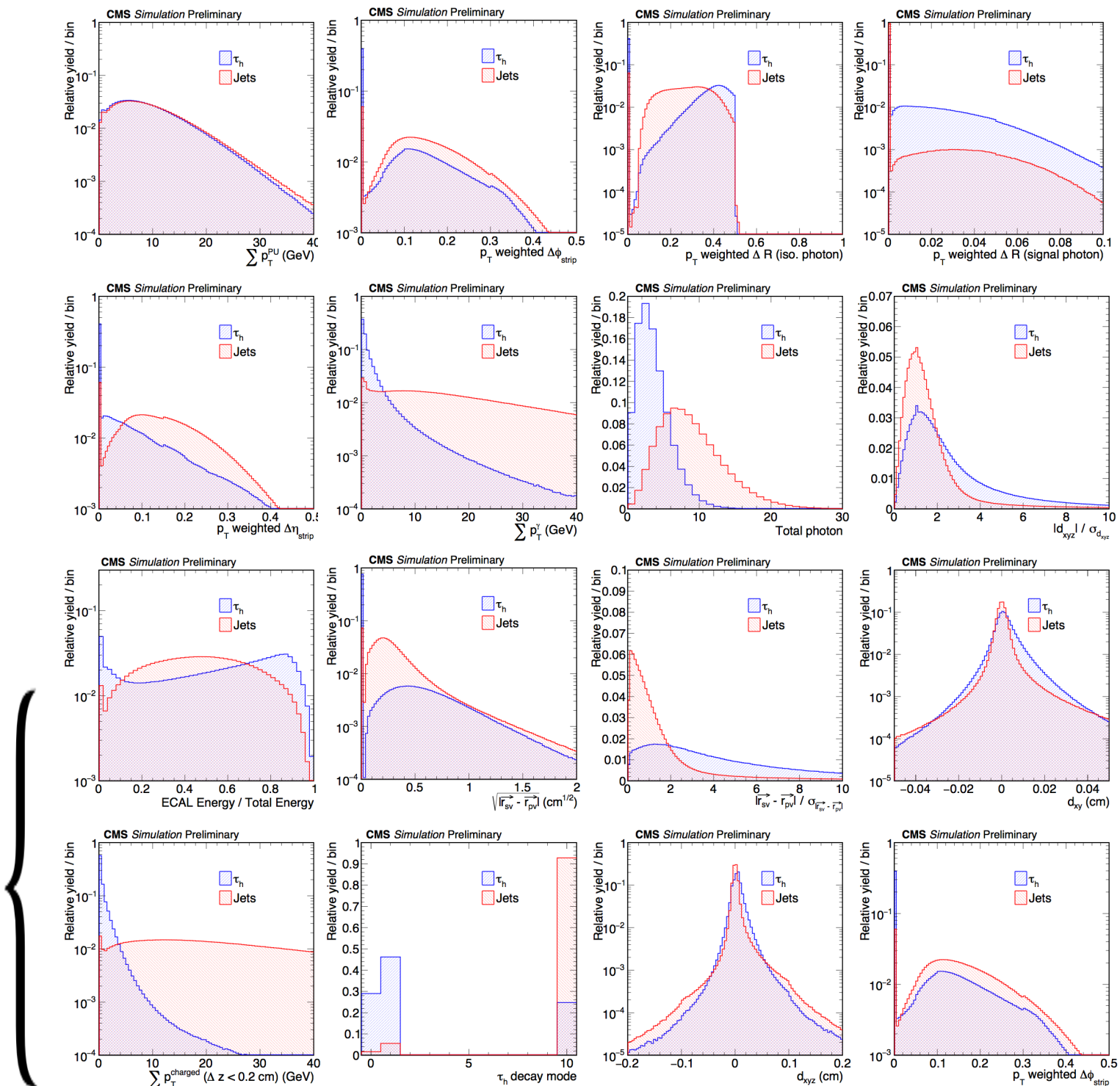


cut-based
calculated
using the
particles found
within the τ_h Isolation cone

$$I_{\tau_{had}} = \sum P_T^{charged}(\Delta z < 2 \text{ mm}) + \max(P_T^\gamma - \Delta\beta, 0)$$

MVA-based (a few highly discriminant):

- Signed impact parameter + significance of leading track (i.e. **Life Time Variables**)
- Number of photons
- Photon Energy Sum
- Decay Mode
- Shape Variables

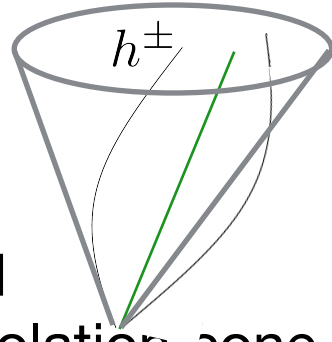


Inputs to the MVA-based jet discriminators

Tau ID at CMS 2016

For Jet, τ_h Discrimination we have developed a **cut-based** and an **MVA based** approach

cut-based
calculated
using the
particles found
within the τ_h Isolation cone



$$I_{\tau_{had}} = \sum P_T^{charged}(\Delta z < 2 \text{ mm}) + \max(P_T^\gamma - \Delta\beta, 0)$$

MVA-based (a few highly discriminant):

- Signed impact parameter + significance of leading track (i.e. **Life Time Variables**)
- Number of photons
- Photon Energy Sum
- Decay Mode
- Shape Variables

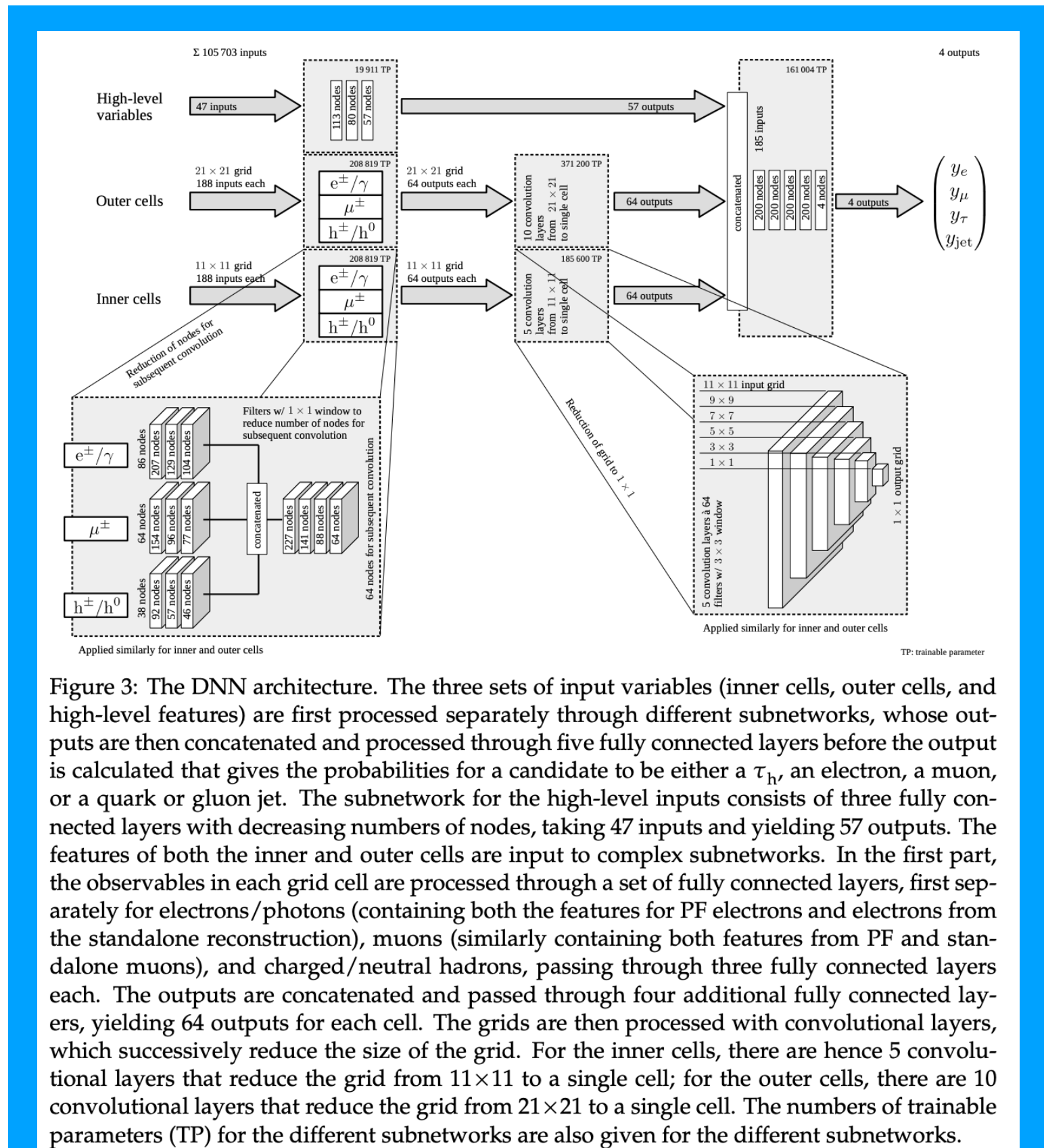


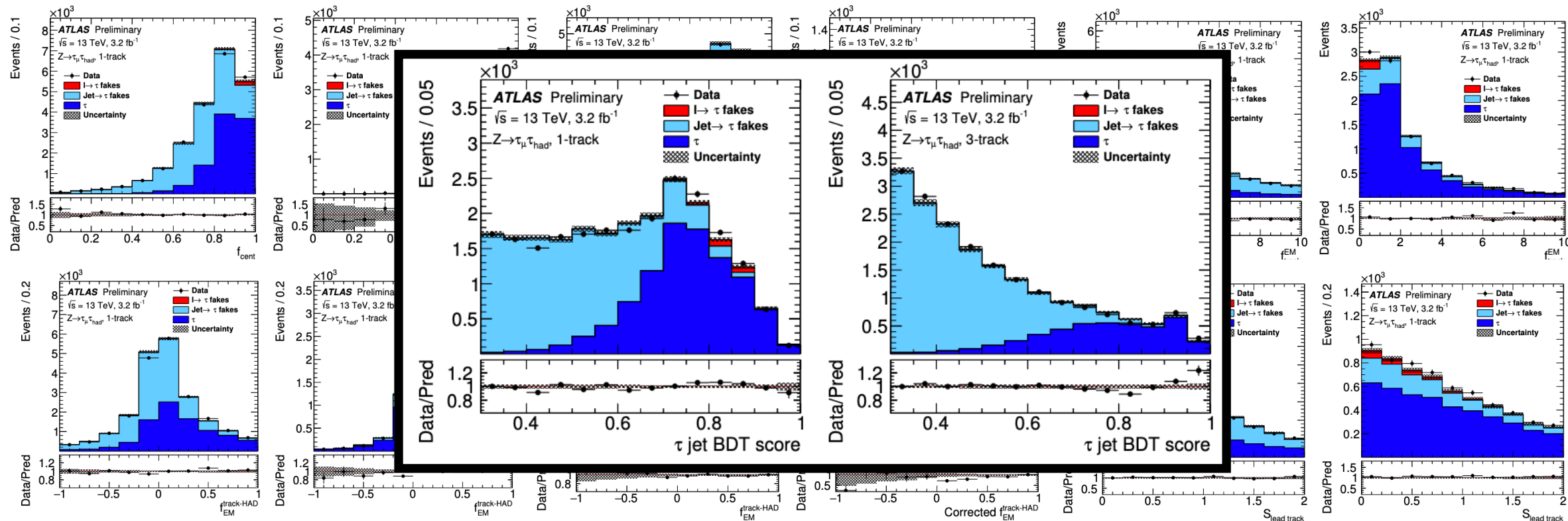
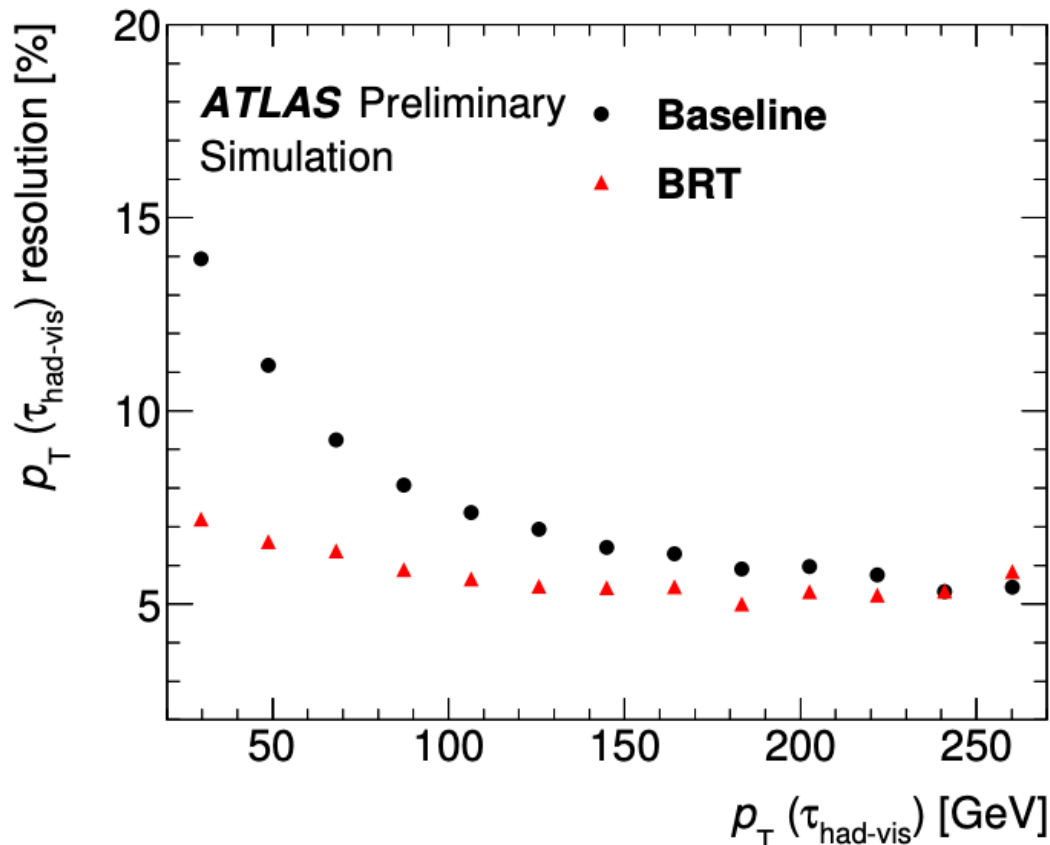
Figure 3: The DNN architecture. The three sets of input variables (inner cells, outer cells, and high-level features) are first processed separately through different subnetworks, whose outputs are then concatenated and processed through five fully connected layers before the output is calculated that gives the probabilities for a candidate to be either a τ_h , an electron, a muon, or a quark or gluon jet. The subnetwork for the high-level inputs consists of three fully connected layers with decreasing numbers of nodes, taking 47 inputs and yielding 57 outputs. The features of both the inner and outer cells are input to complex subnetworks. In the first part, the observables in each grid cell are processed through a set of fully connected layers, first separately for electrons/photons (containing both the features for PF electrons and electrons from the standalone reconstruction), muons (similarly containing both features from PF and standalone muons), and charged/neutral hadrons, passing through three fully connected layers each. The outputs are concatenated and passed through four additional fully connected layers, yielding 64 outputs for each cell. The grids are then processed with convolutional layers, which successively reduce the size of the grid. For the inner cells, there are hence 5 convolutional layers that reduce the grid from 11x11 to a single cell; for the outer cells, there are 10 convolutional layers that reduce the grid from 21x21 to a single cell. The numbers of trainable parameters (TP) for the different subnetworks are also given for the different subnetworks.

CMS has since updated to a Deep Neural Network

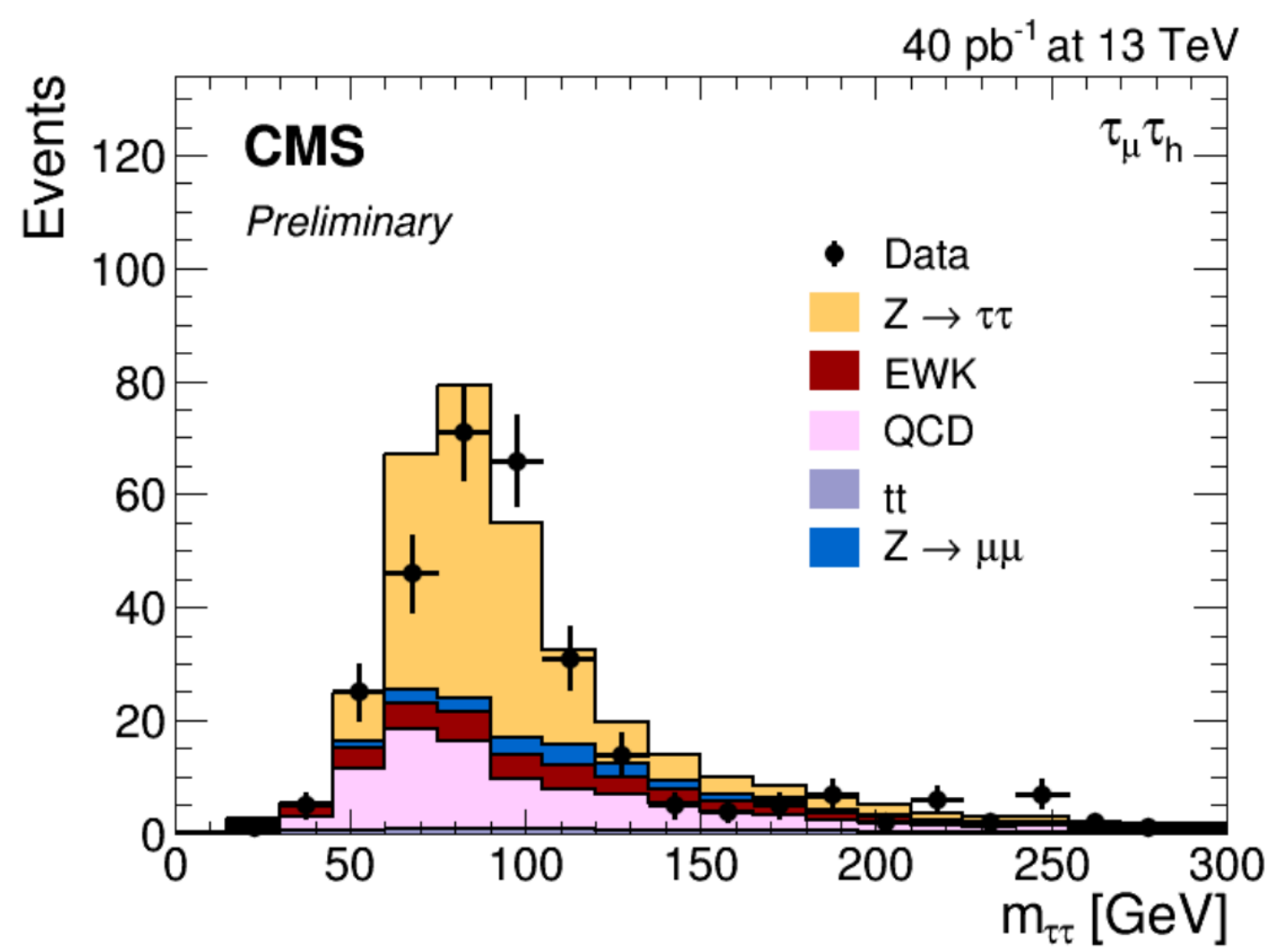
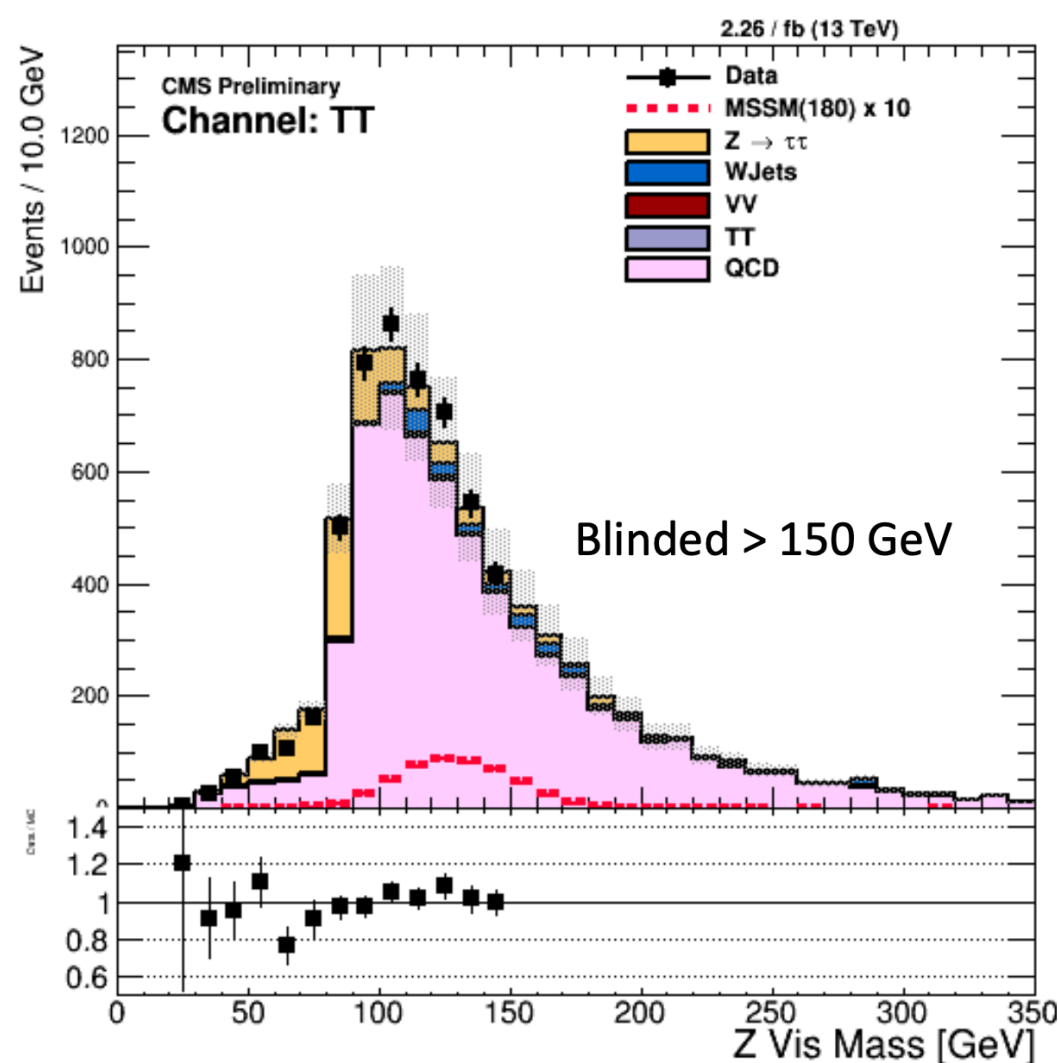


Tau Calibration & ID at ATLAS

- Energy is calibrated using an MVA regression “BRT”-method
 - Takes as input “Tau Particle Flow” objects along with an baseline Energy estimate
 - τ_h are discriminated from jets using a BDT

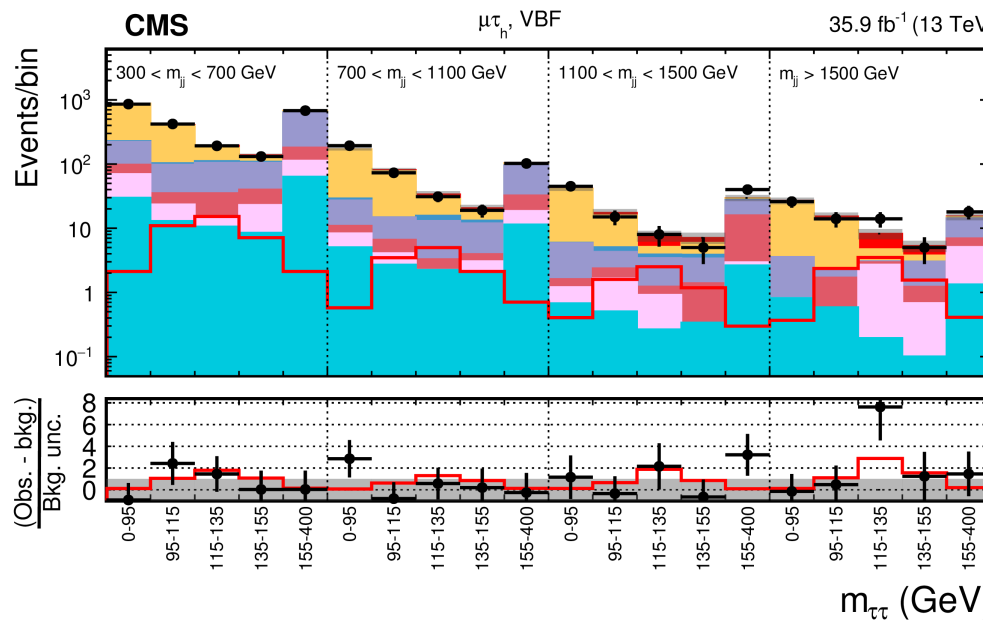
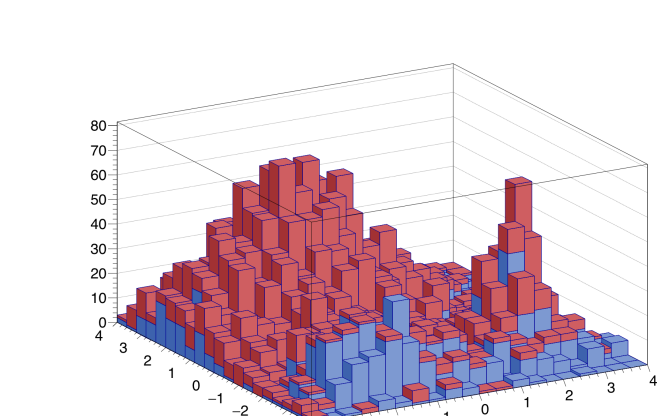


First look at 2015 Data



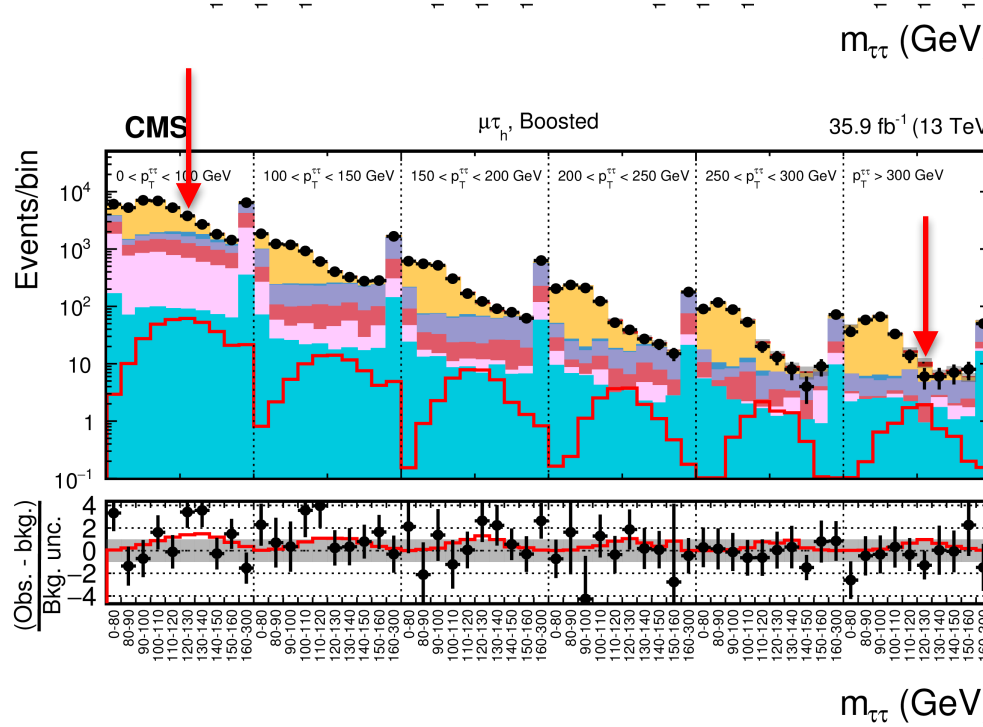
Analysis Strategy

- CMS: 2D Distributions + Control Regions
- ATLAS: Categories + Control Regions



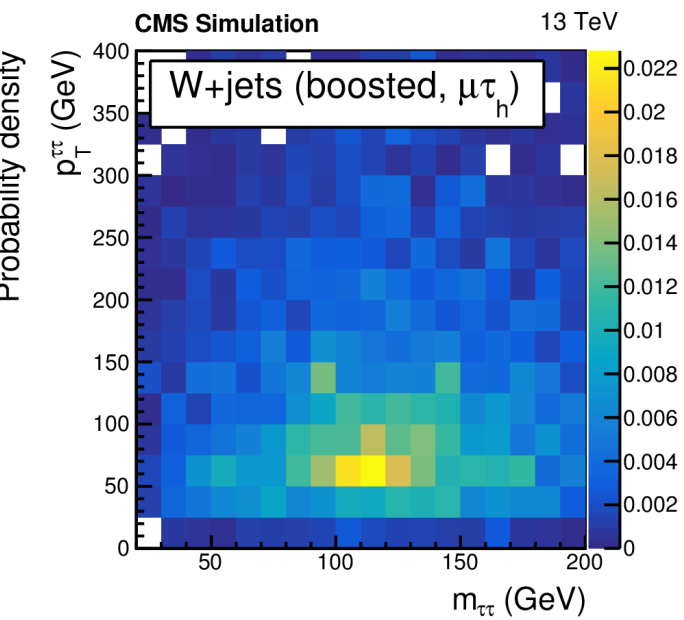
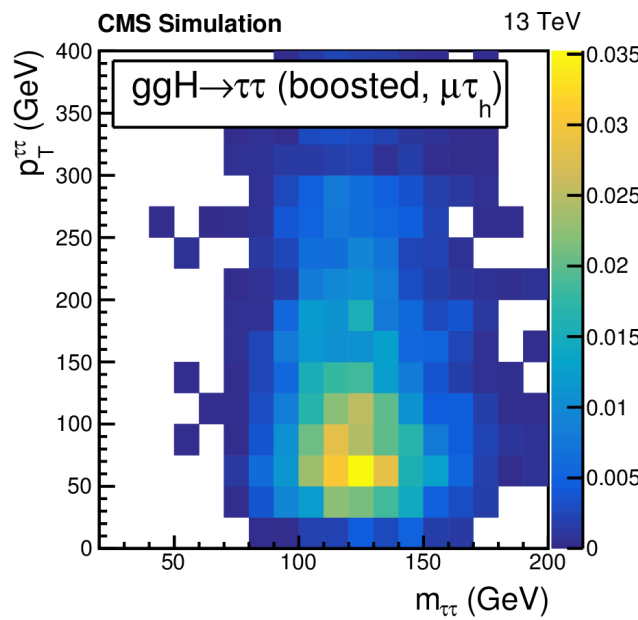
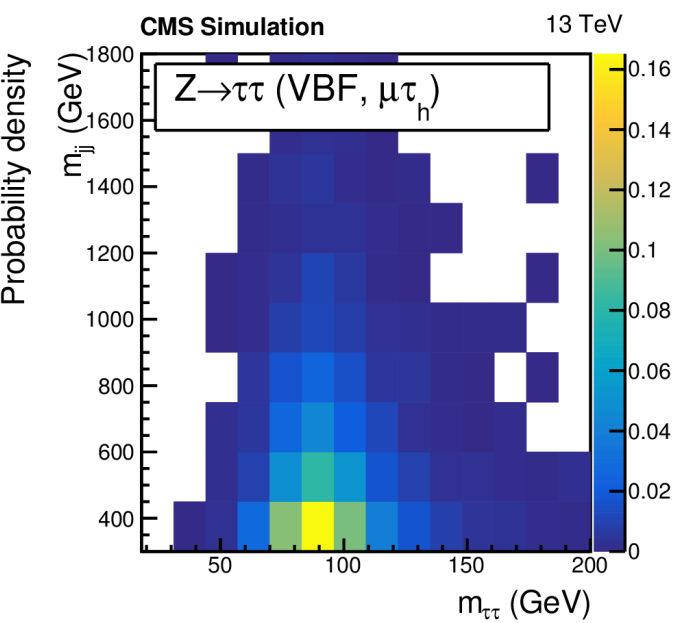
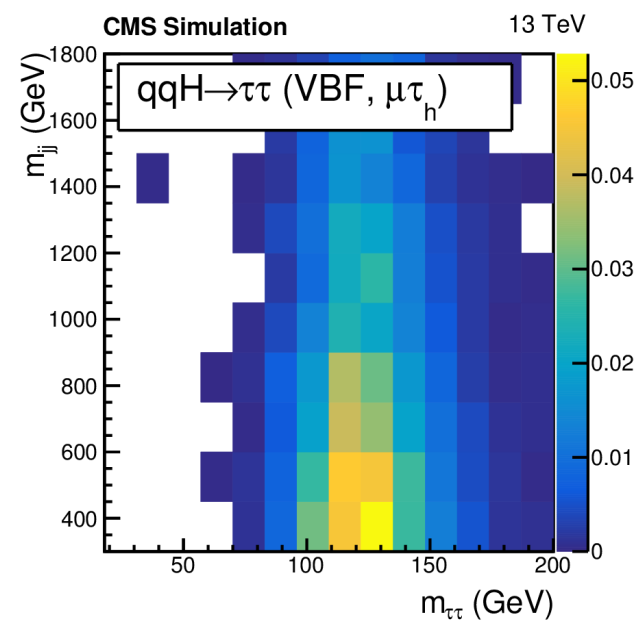
Legend:

- Observed
- $H \rightarrow \tau\tau (\mu = 1.09)$
- $Z \rightarrow \tau\tau$
- $Z \rightarrow \mu\mu/\text{ee}$
- $t\bar{t} + \text{jets}$
- $W + \text{jets}$
- QCD multijet
- Others
- Total unc.
- $H \rightarrow \tau\tau (\mu = 1.09)$
- $\text{Obs.} - \text{bkg.}$
- $H \rightarrow \tau\tau$
- Bkg. unc.
- Bkg. unc.



Legend:

- Observed
- $H \rightarrow \tau\tau (\mu = 1.09)$
- $Z \rightarrow \tau\tau$
- $Z \rightarrow \mu\mu/\text{ee}$
- $t\bar{t} + \text{jets}$
- $W + \text{jets}$
- QCD multijet
- Others
- Total unc.
- $H \rightarrow \tau\tau (\mu = 1.09)$
- $\text{Obs.} - \text{bkg.}$
- $H \rightarrow \tau\tau$
- Bkg. unc.
- Bkg. unc.



Categorization CMS

Four $\tau\tau$ Final States (Channels):

$e\tau, \mu\tau_h, \tau_h\tau_h, e\mu$

Three Categories for signal extraction, using 2D distributions:

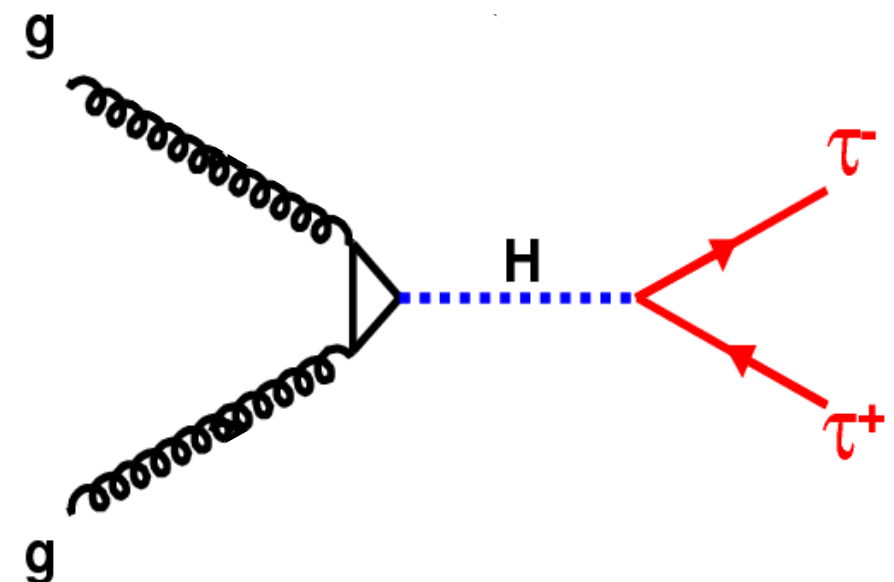
0 jet*: M_{vis} vs. $\tau/\mu p_T$
or M_{vis} vs. τ DM

VBF: SVMass vs. M_{jj}

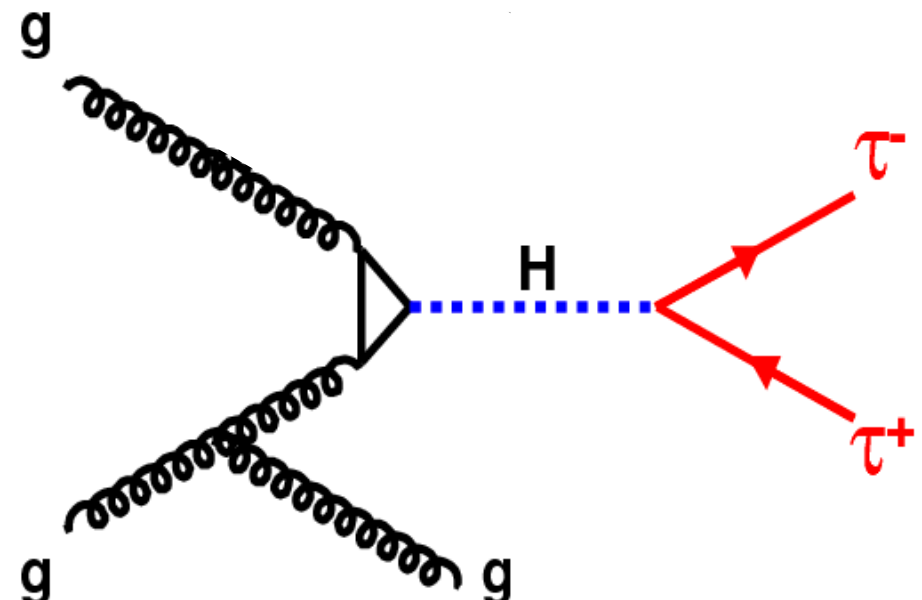
Boosted: SVMass vs. Higgs p_T

0-Jet

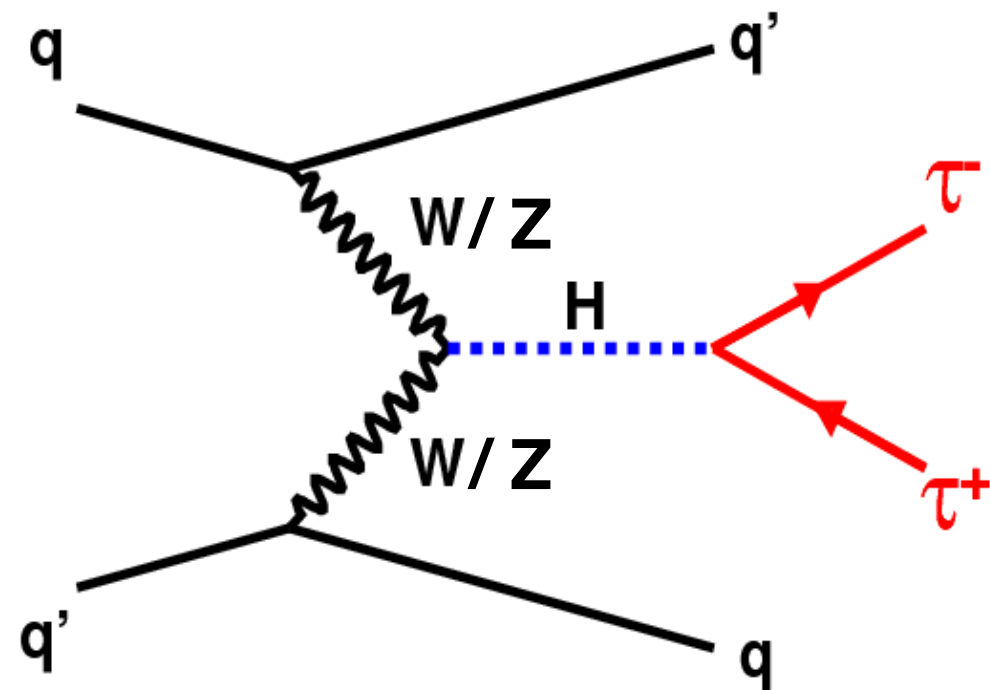
Background normalization



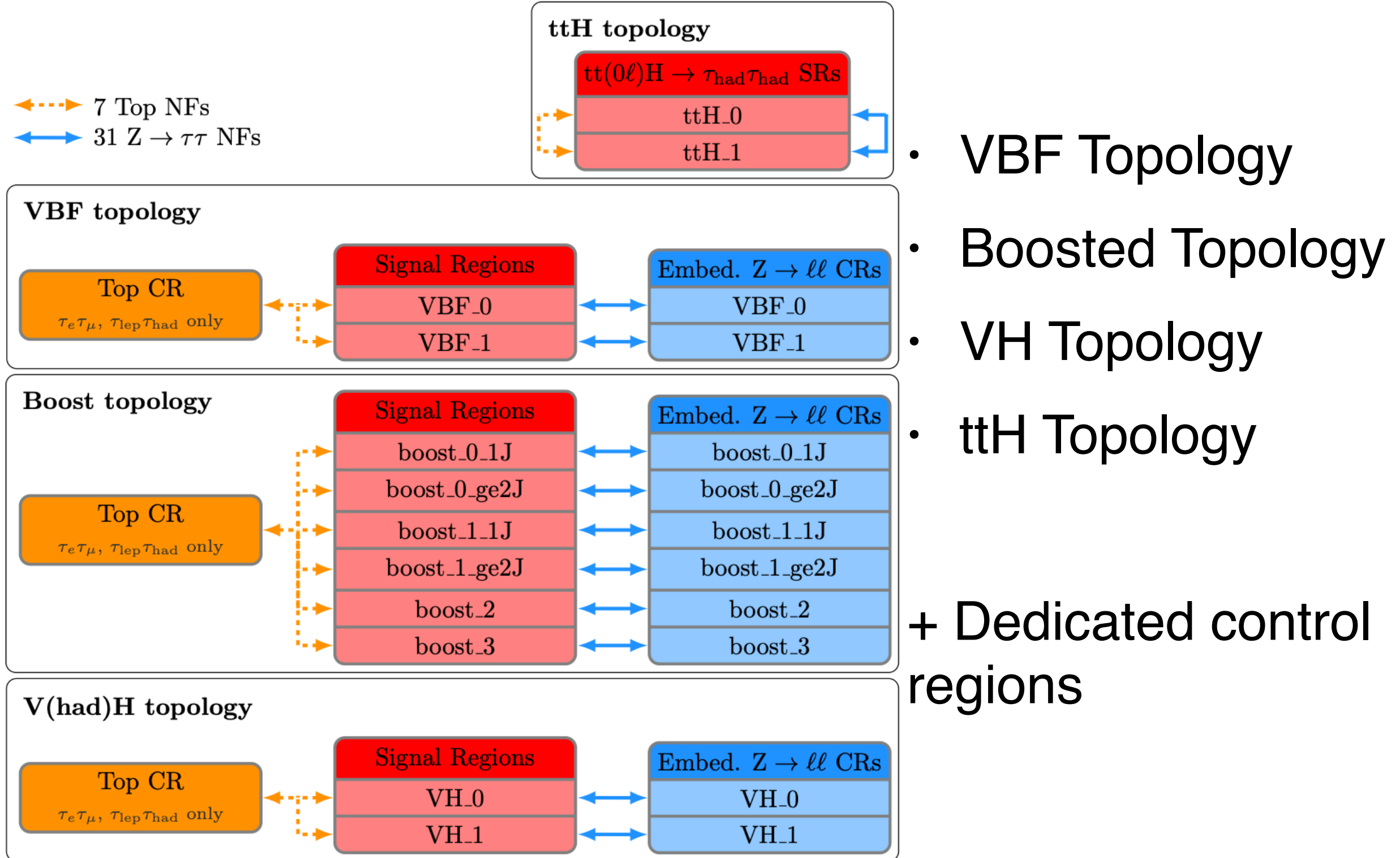
1-Jet Boosted higgs



2-Jet VBF



Categorization ATLAS

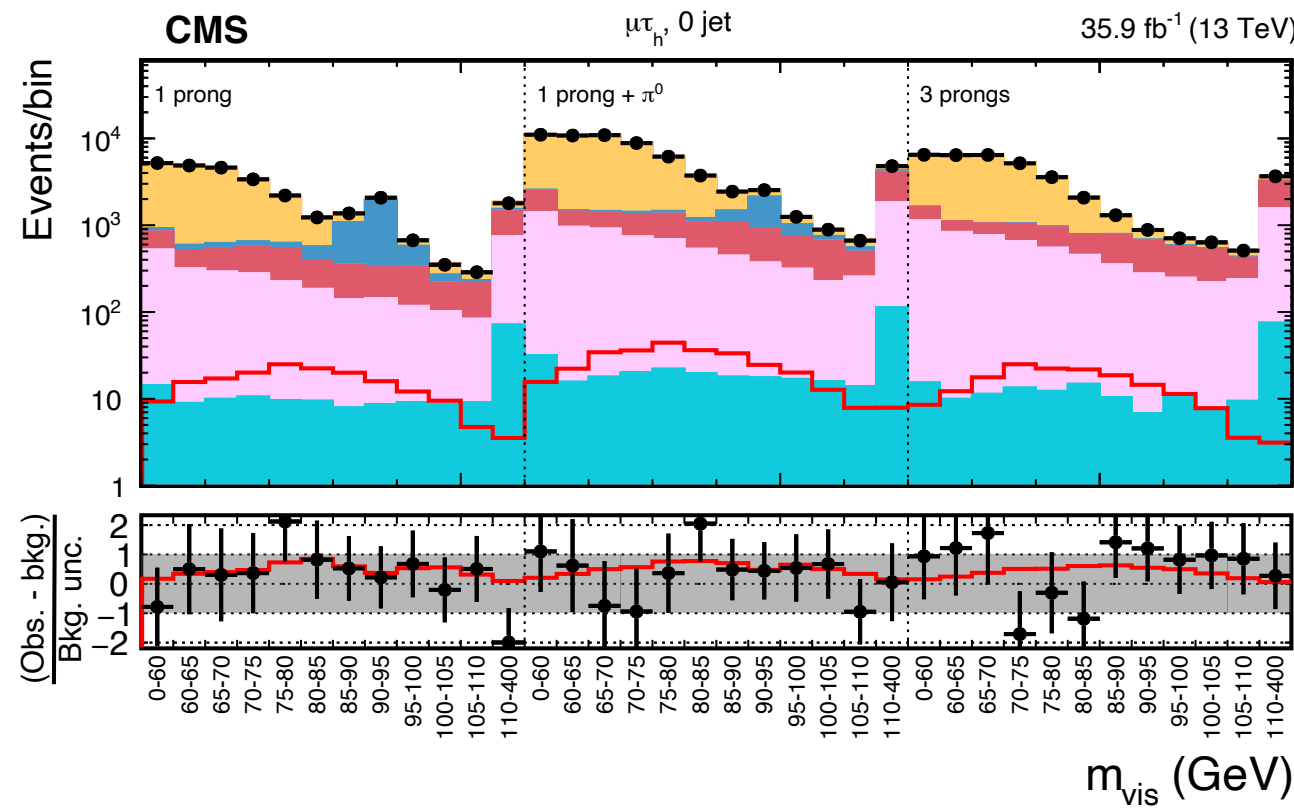


- VBF Topology
 - Boosted Topology
 - VH Topology
 - ttH Topology
- + Dedicated control regions



CMS H $\tau\tau$ Observation

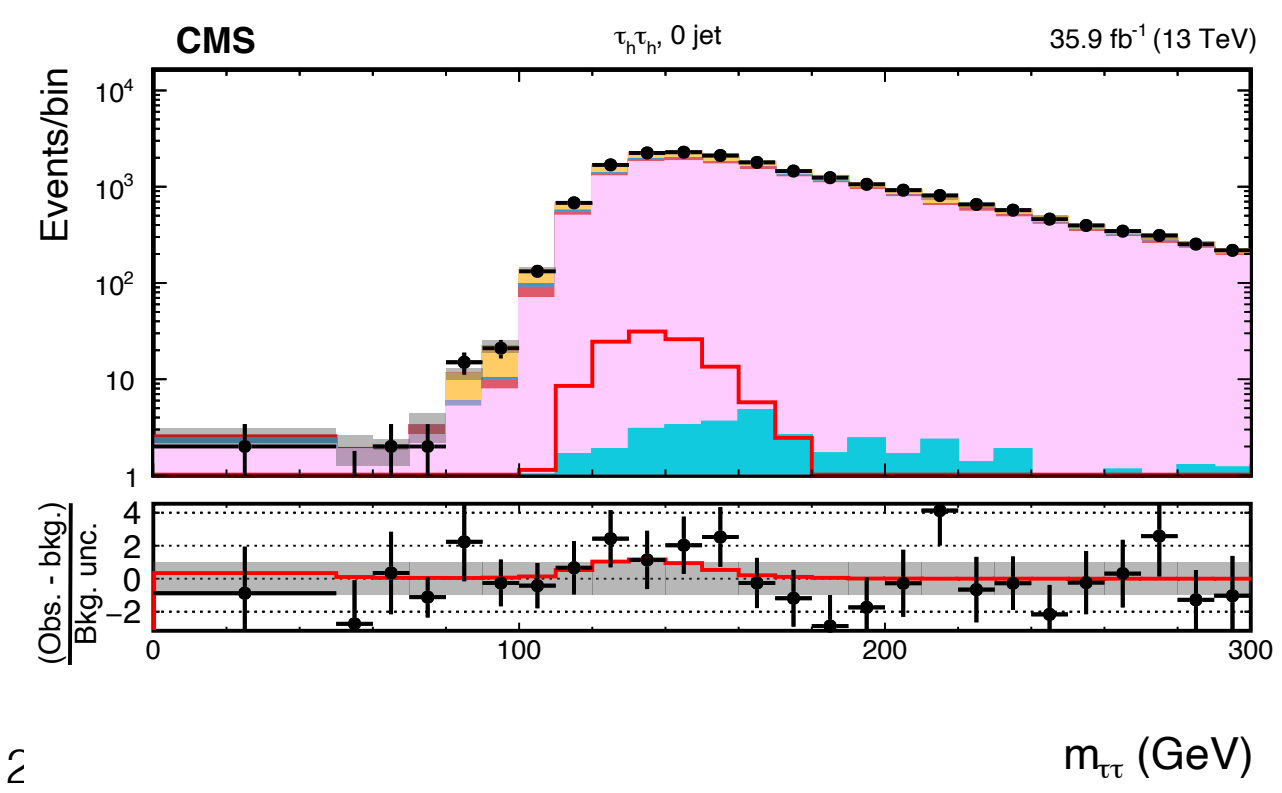
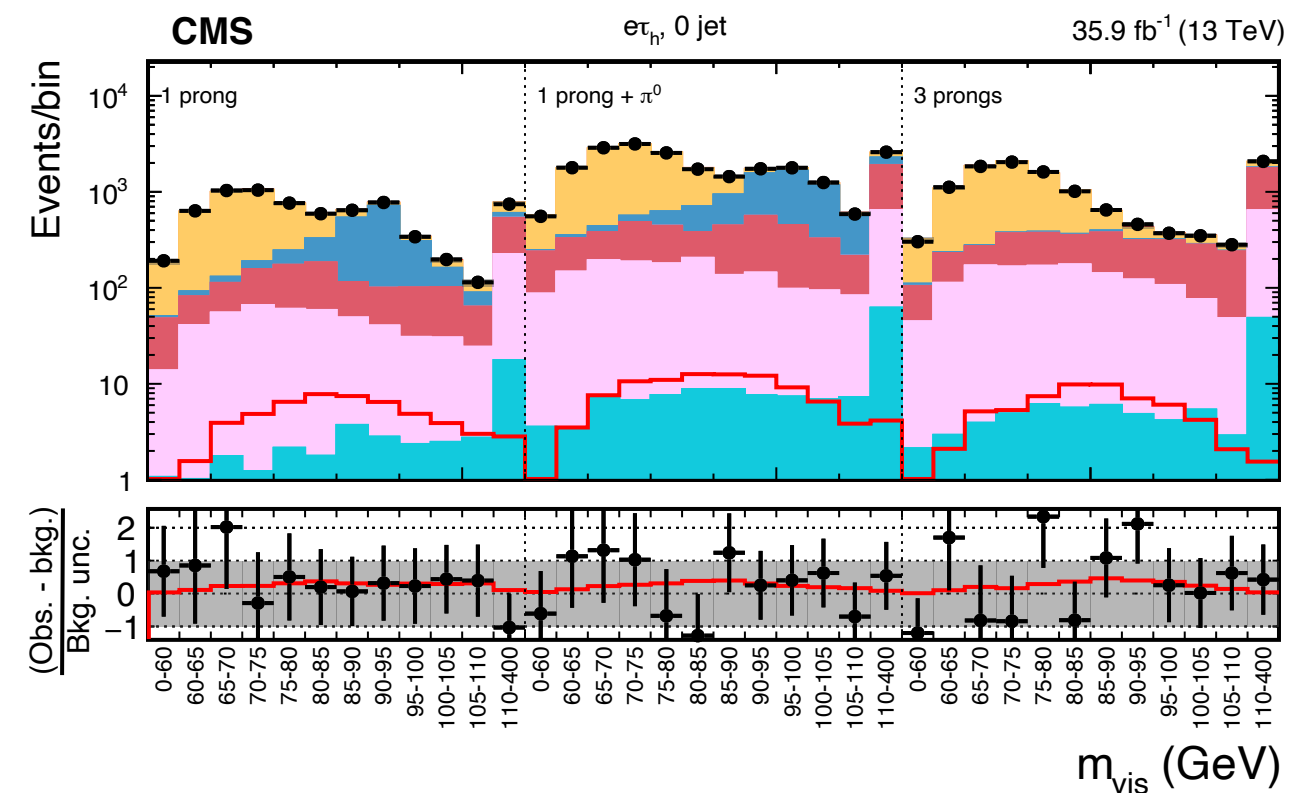
Two Dimensional Distributions:



- Observed
- $H \rightarrow \tau\tau (\mu = 1.09)$
- $Z \rightarrow \tau\tau$
- $Z \rightarrow \mu\mu/\text{ee}$
- $t\bar{t} + \text{jets}$
- $W + \text{jets}$
- QCD multijet
- Others
- Total unc.
- $H \rightarrow \tau\tau (\mu = 1.09)$

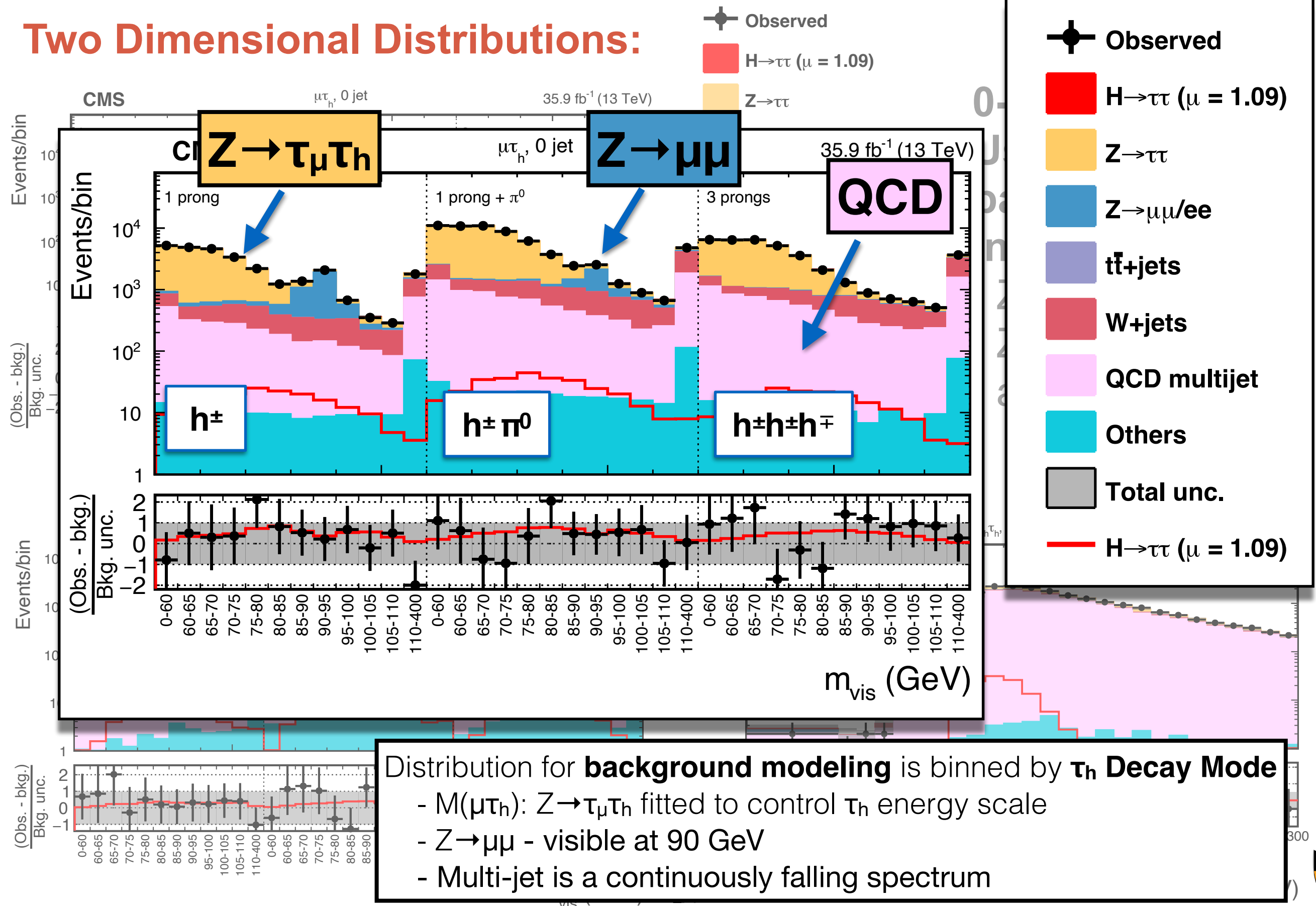
**0-Jet Category
Used to Model
backgrounds
including**

$Z \rightarrow \tau\tau$
 $Z \rightarrow \text{ee} / Z \rightarrow \mu\mu$
and QCD



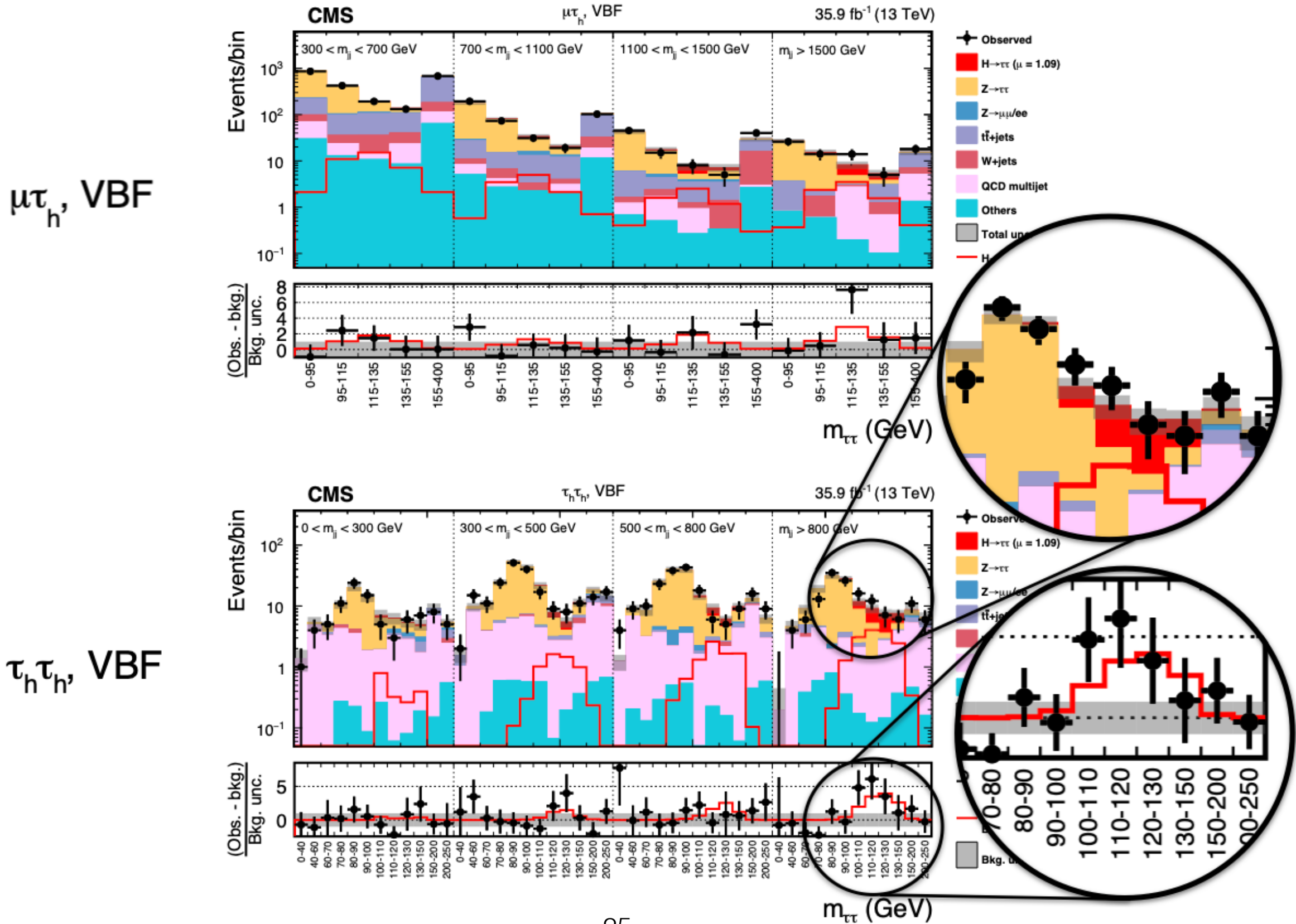
CMS H $\tau\tau$ Observation

Two Dimensional Distributions:

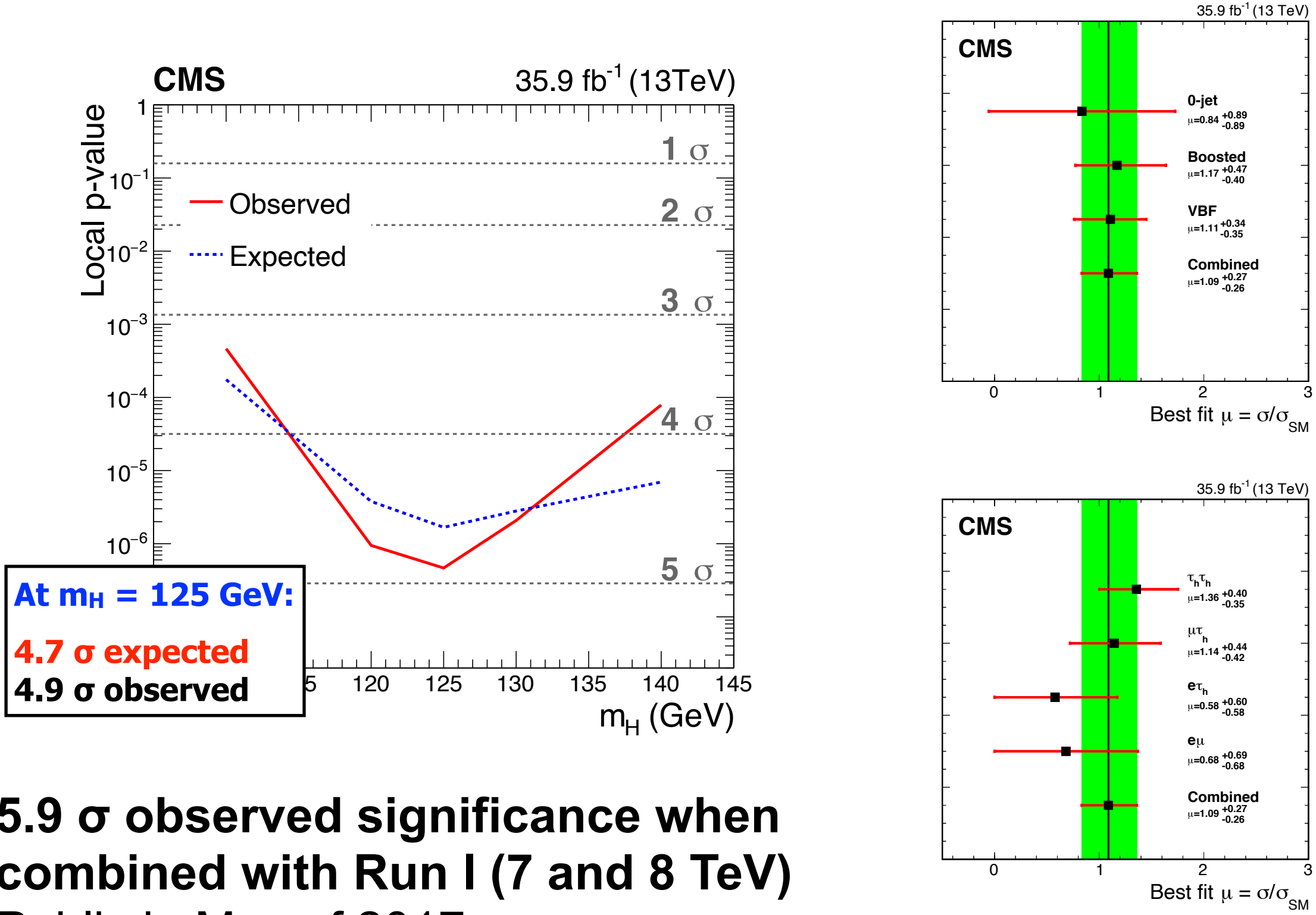


CMS H $\tau\tau$ Observation

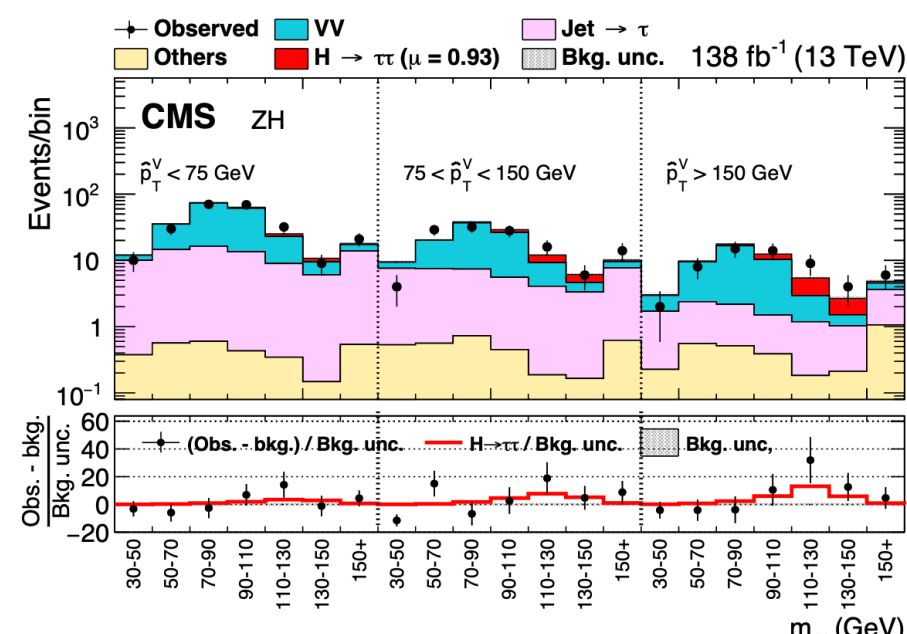
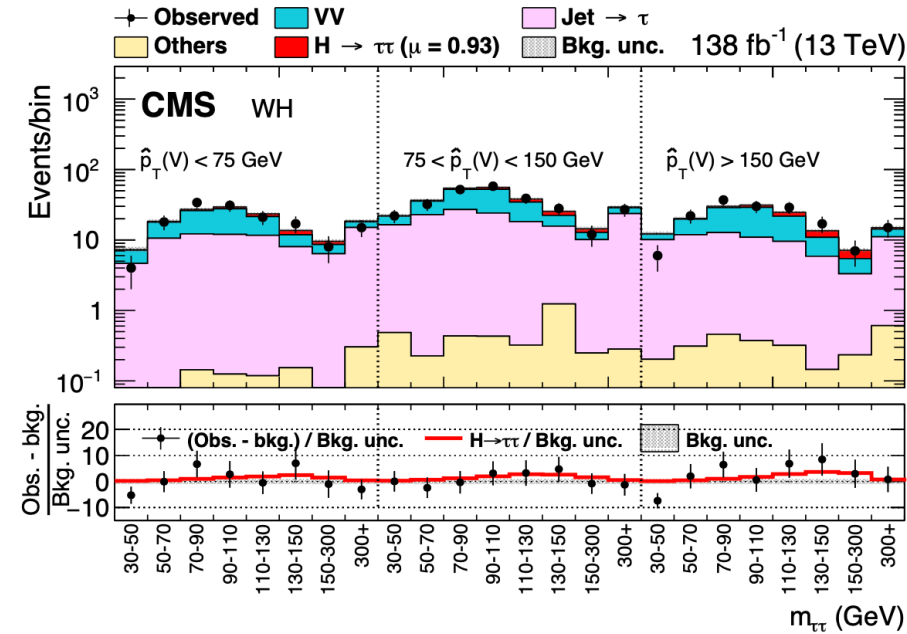
VBF High Signal Region:



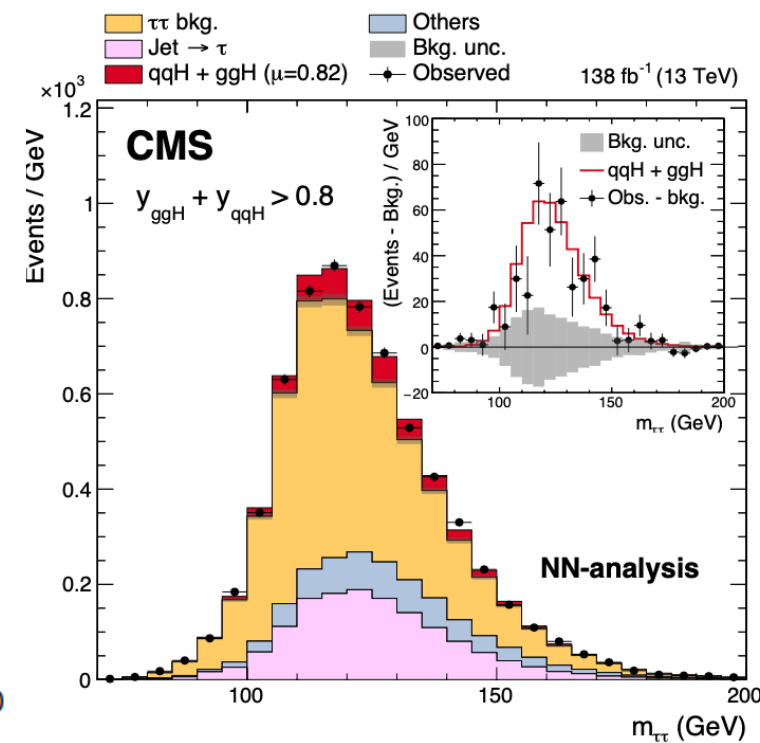
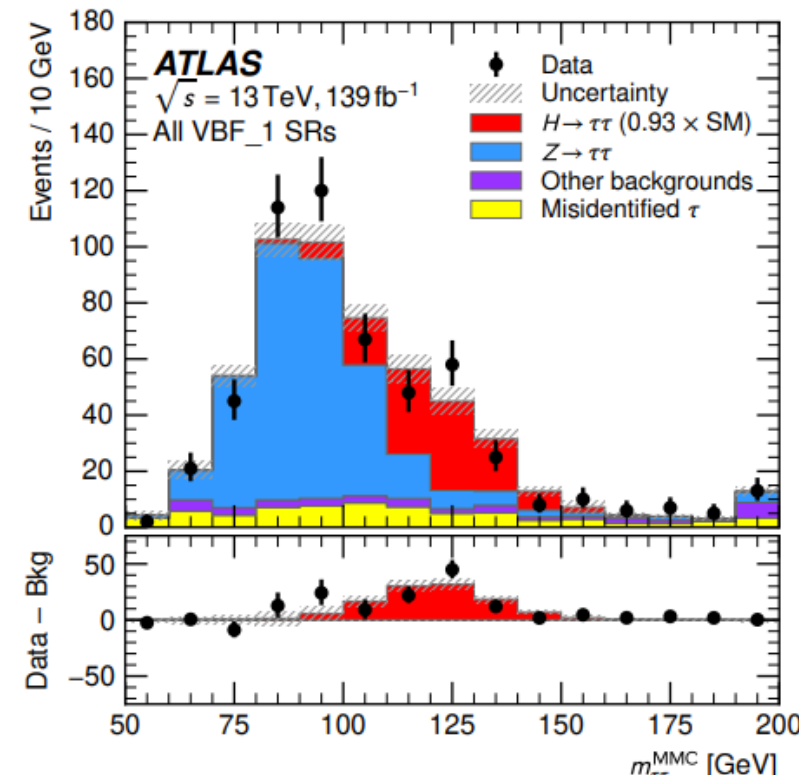
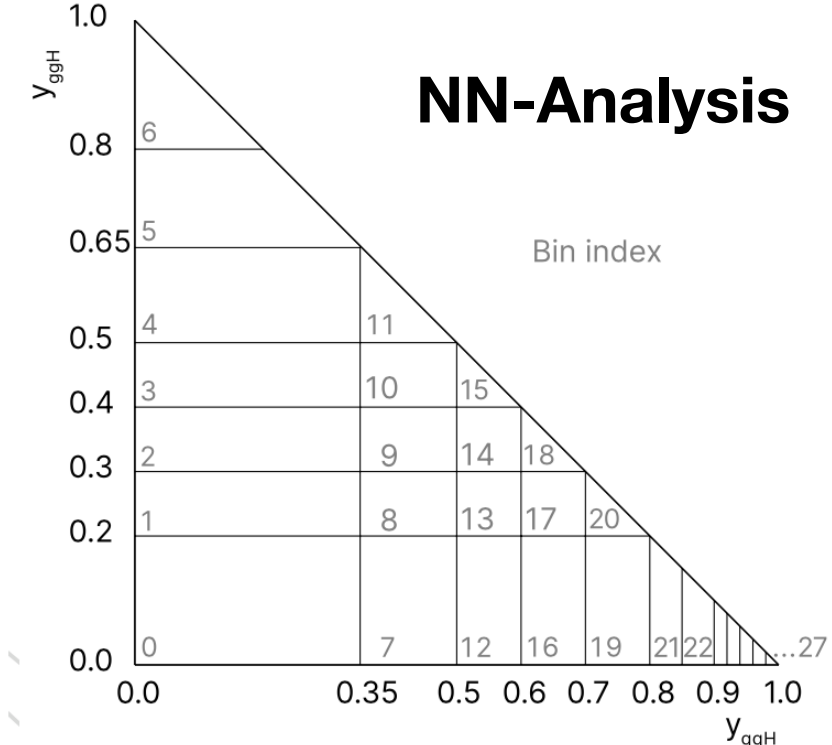
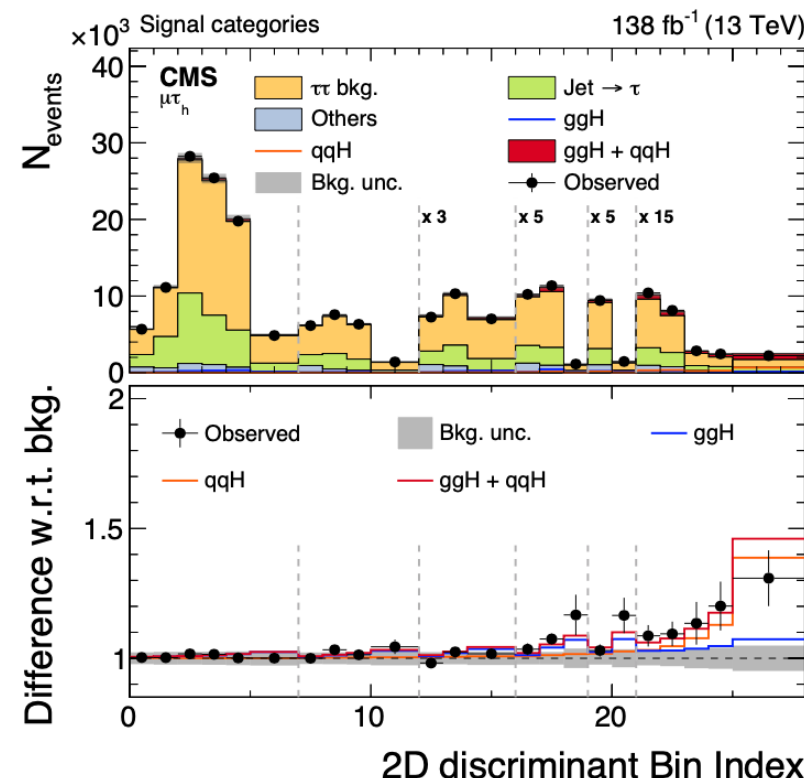
CMS H $\tau\tau$ Observation



More with Higgs $\tau\tau$ STXS



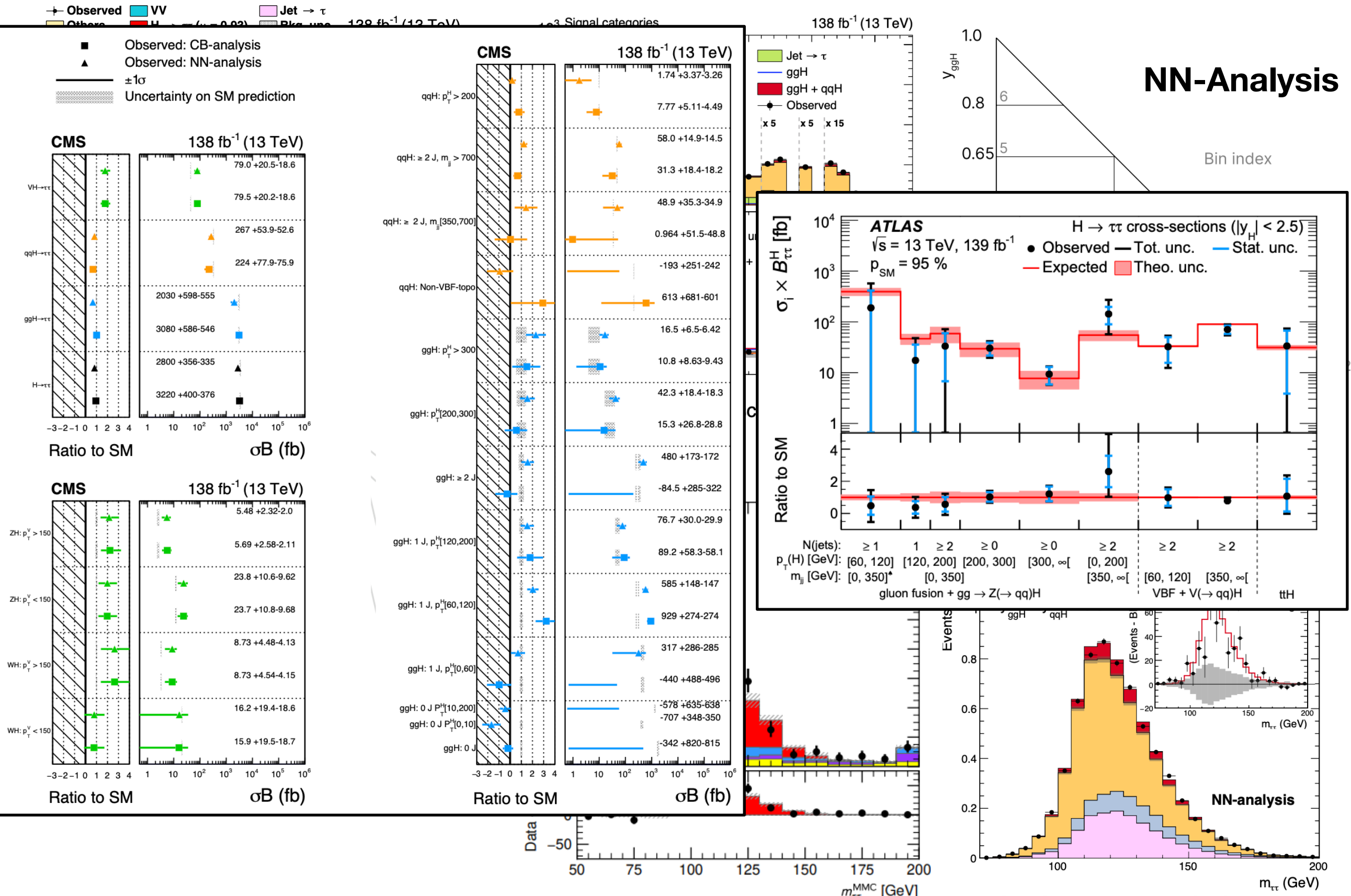
VH-channel



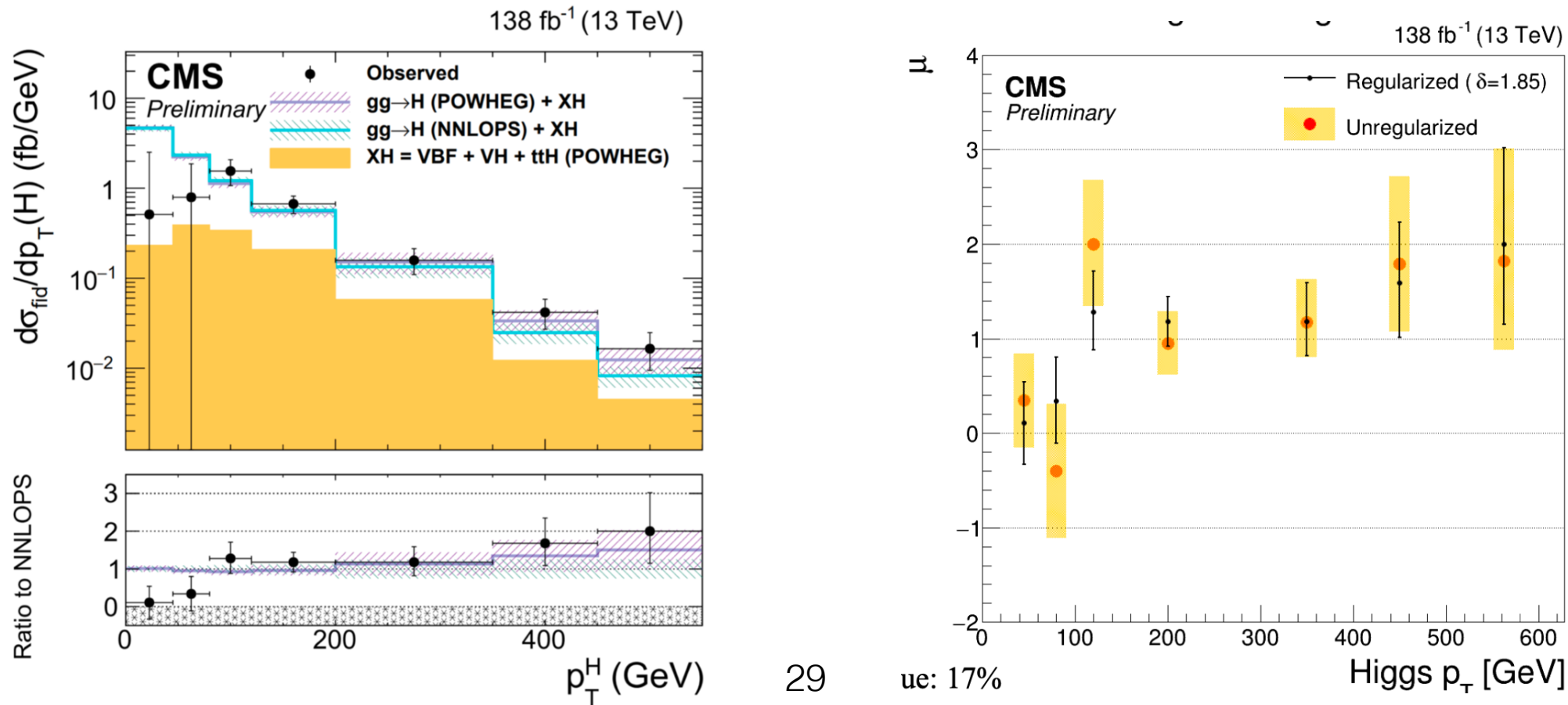
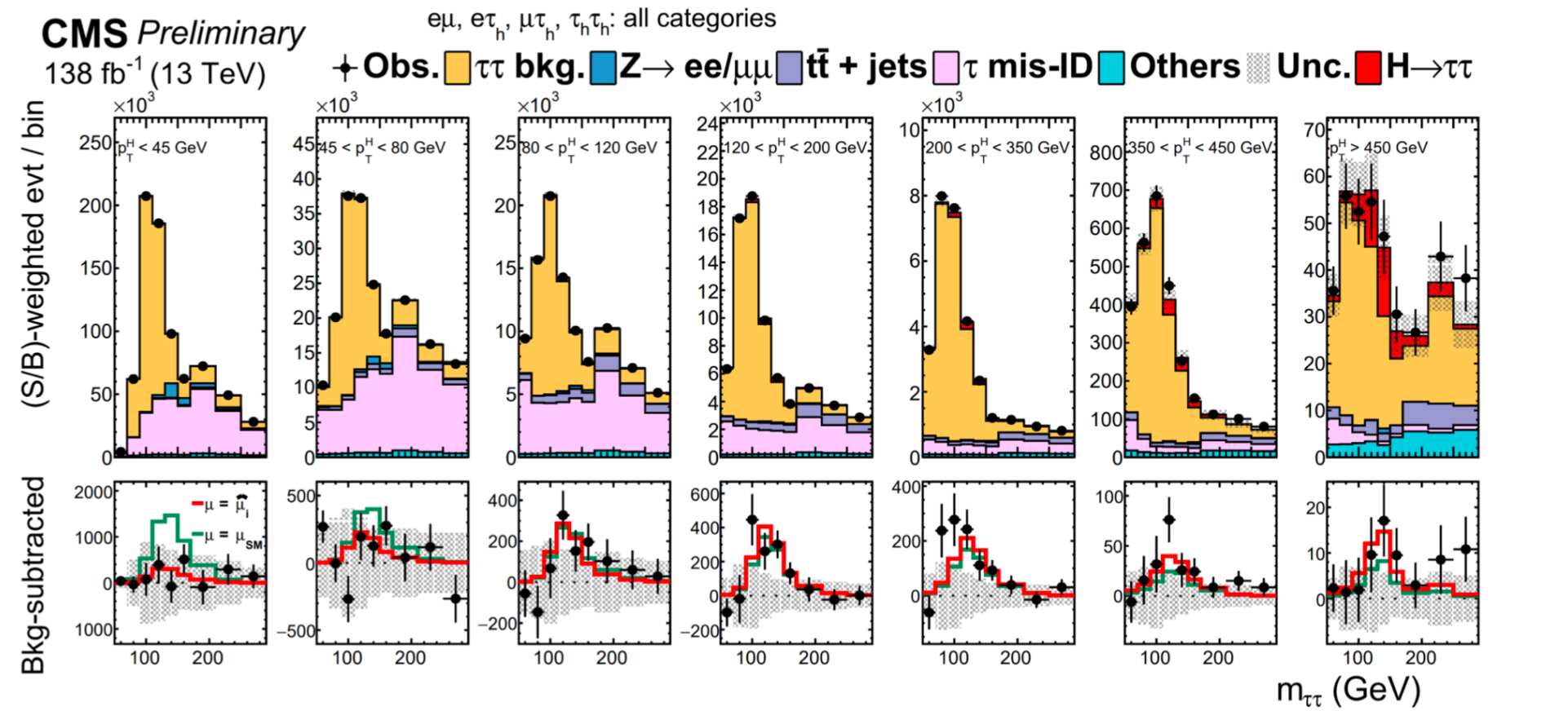
More with Higgs tt STXS

July 1, 2022

I.Ojalvo **H \rightarrow tt** Higgs Discovery Birmingham

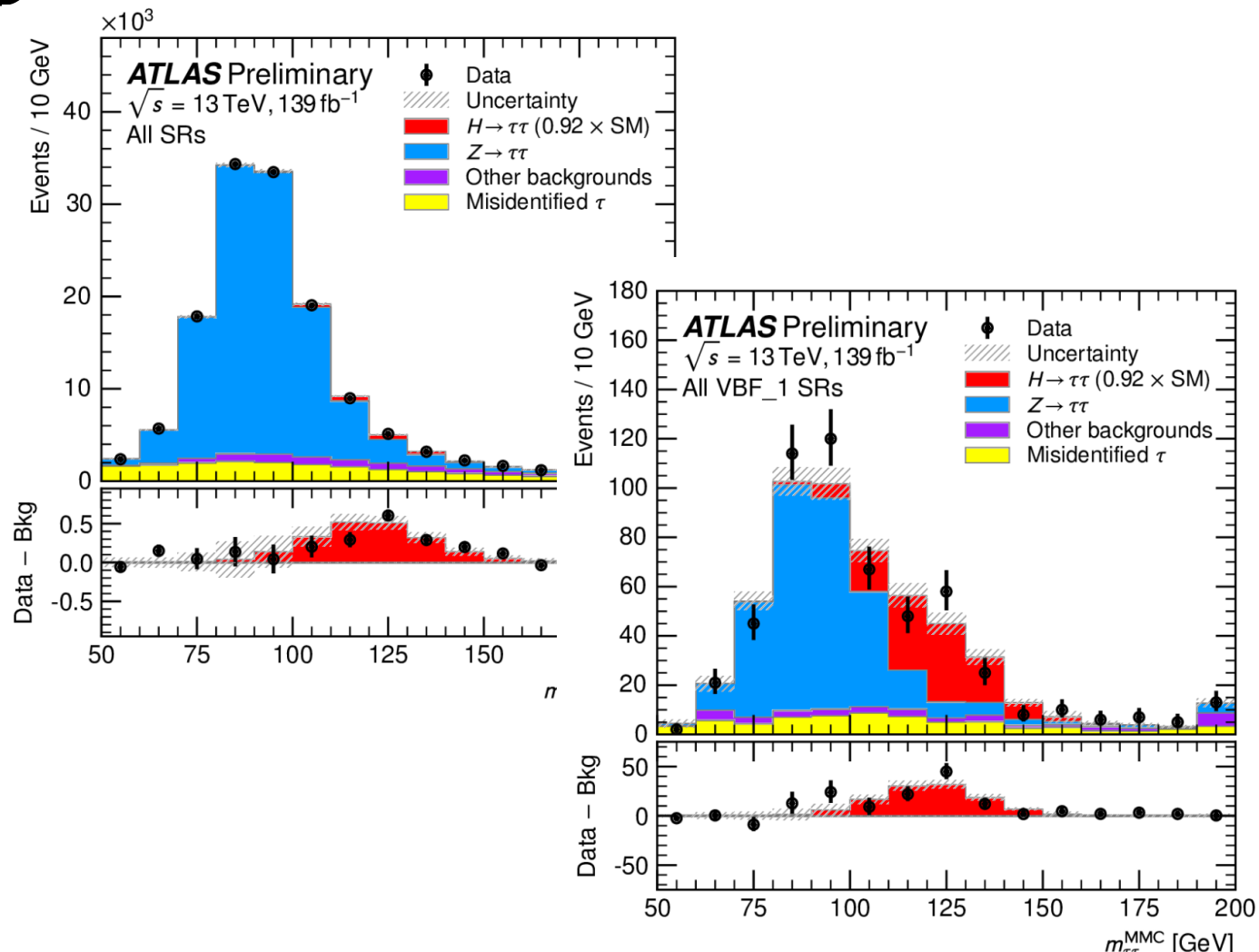
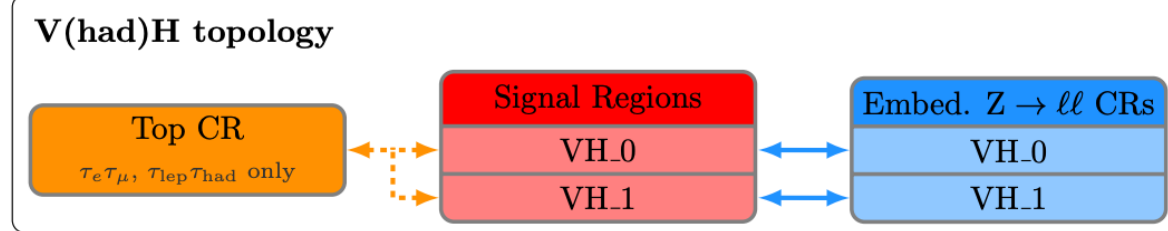
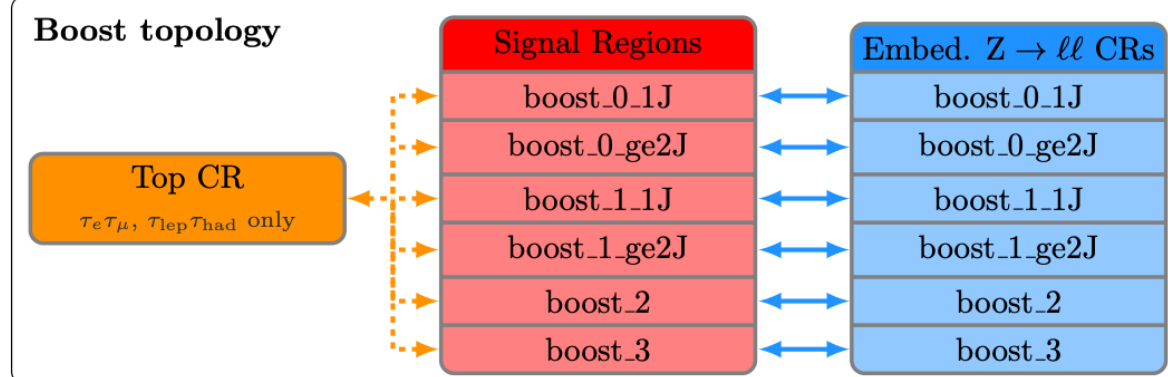
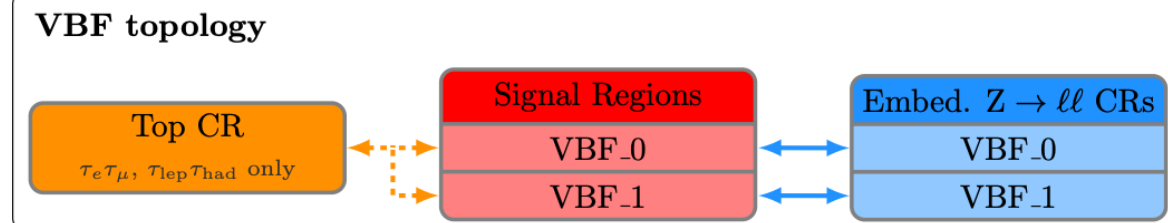
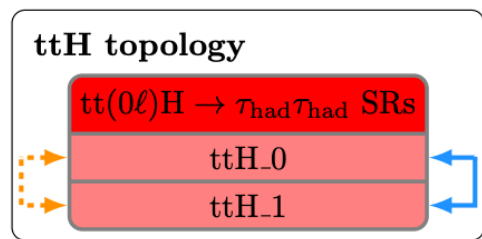


Differential $H \rightarrow \tau\tau$



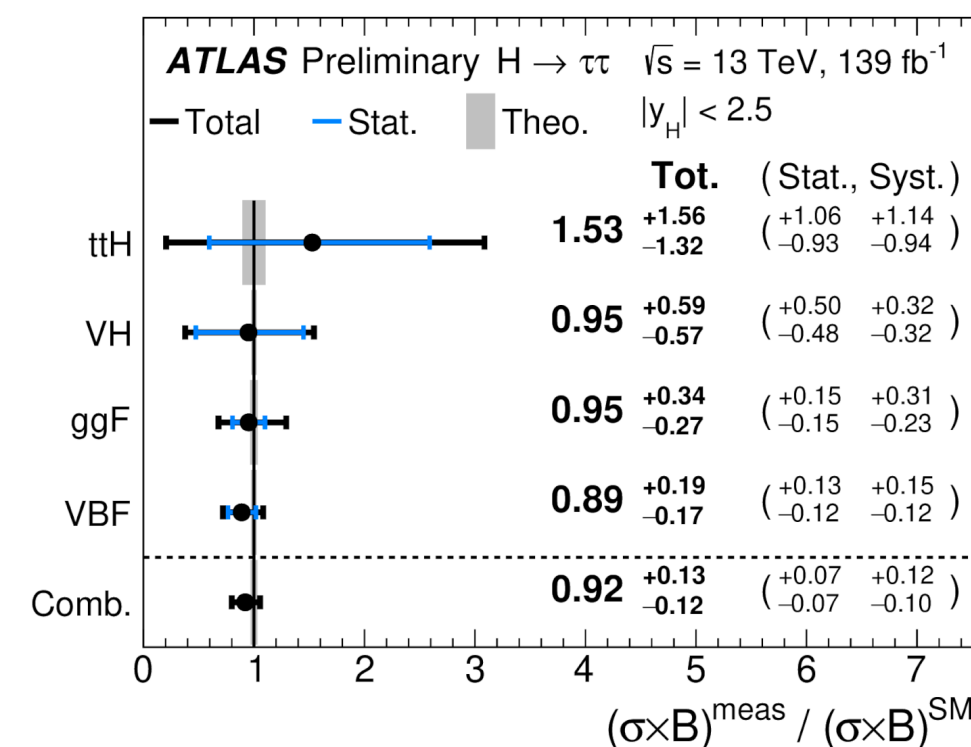
ATLAS Higgs Observation

7 Top NFs
31 $Z \rightarrow \tau\tau$ NFs

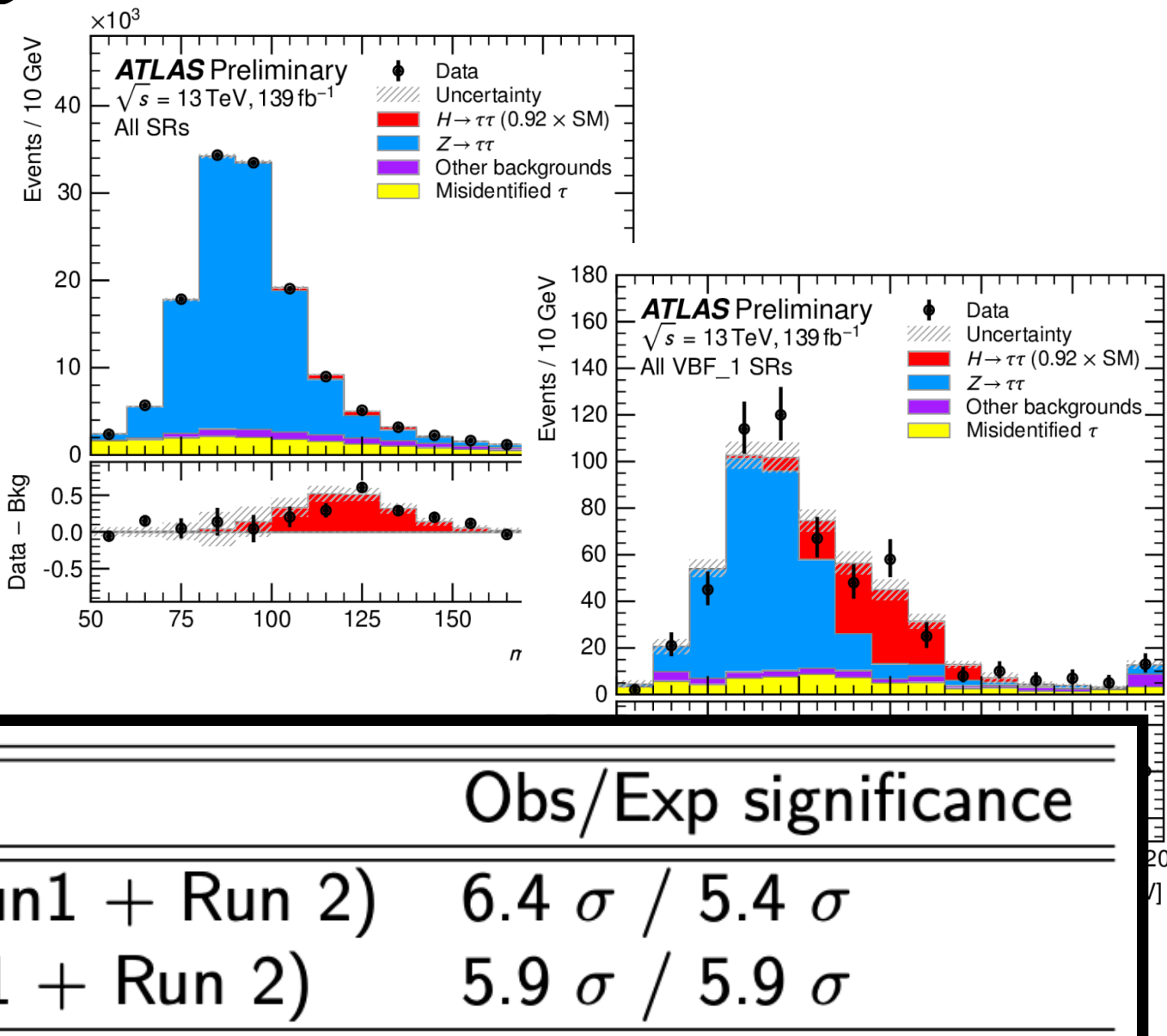
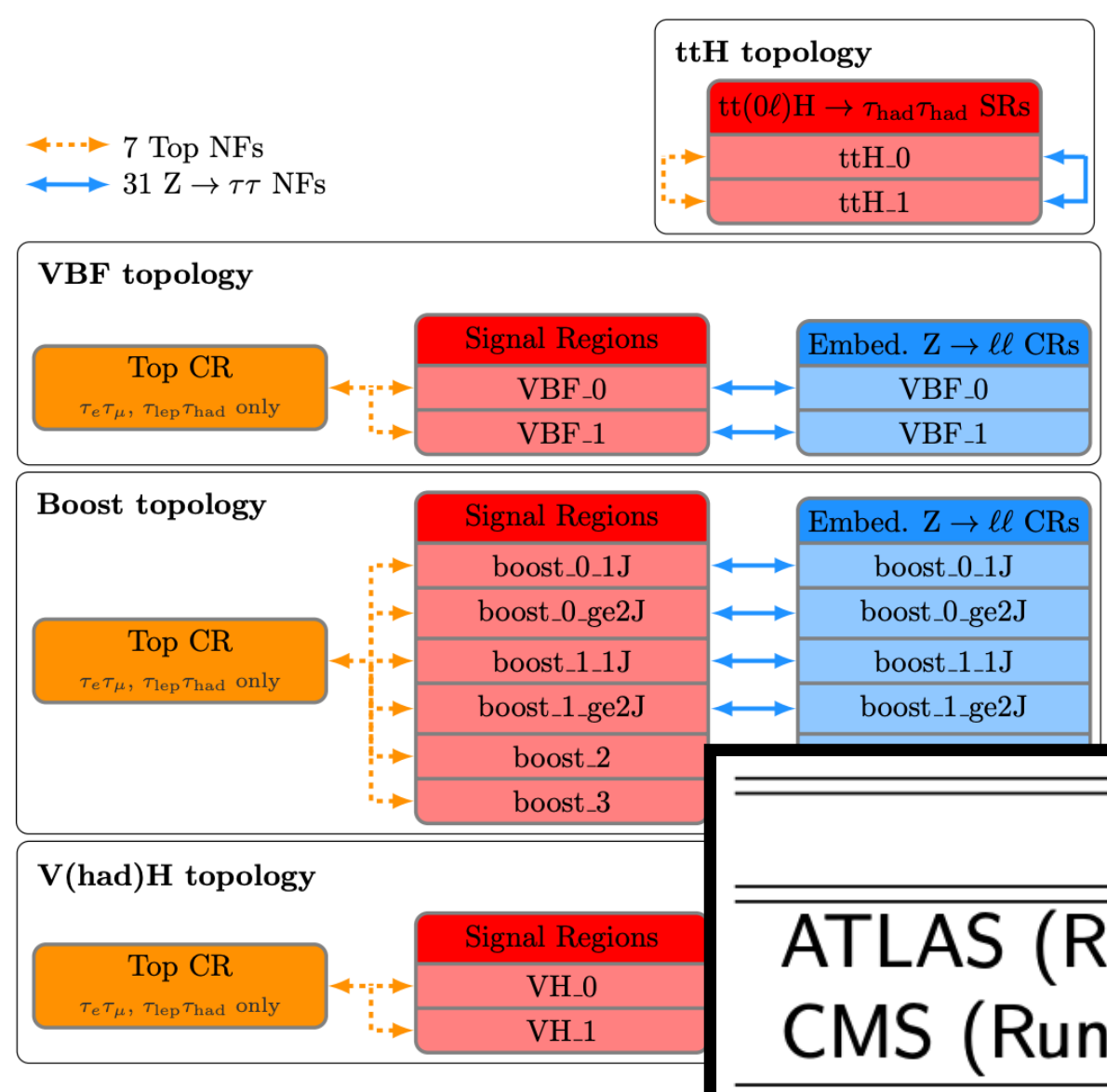


Equally Complex Story at ATLAS

- 24 Signal and Control Regions
- Using a Missing Mass Estimator to reconstruction the di-tau mass
- November 2018, Run-1 + 2016 Data

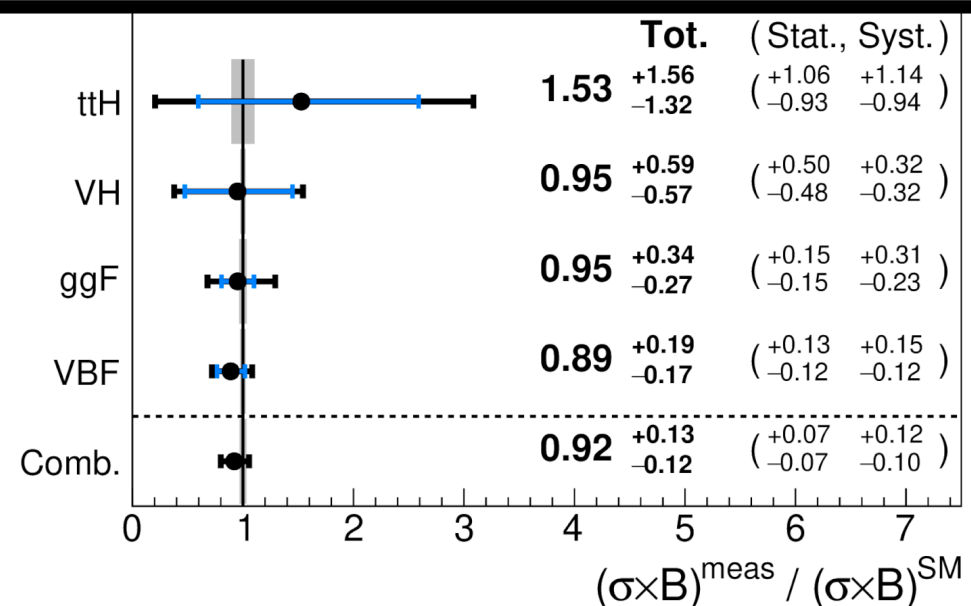


ATLAS Higgs Observation



Equally Complex Story at ATLAS

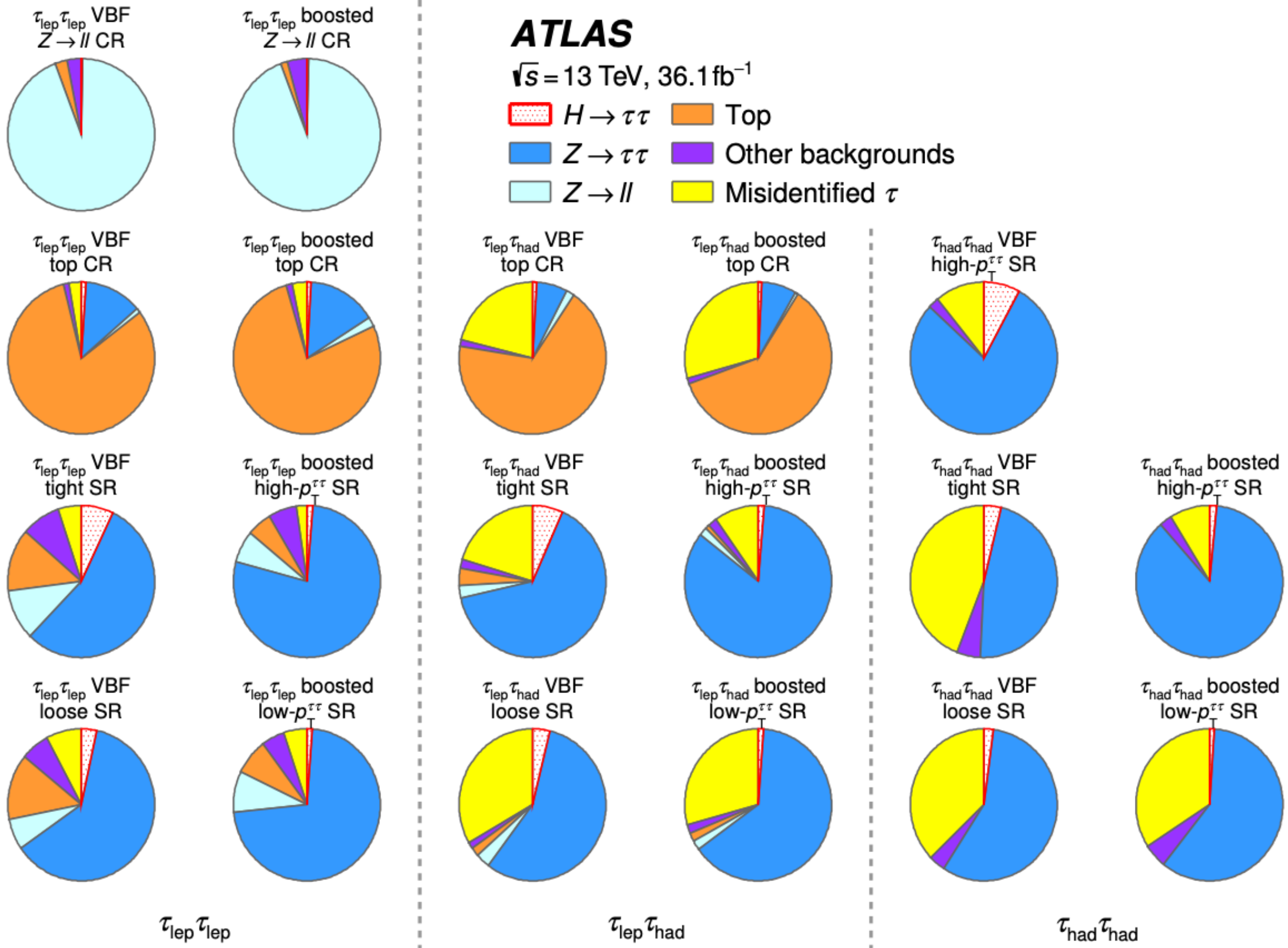
- 24 Signal and Control Regions
- Using a Missing Mass Estimator to reconstruction the di-tau mass
- November 2018, Run-1 + 2016 Data



In 1975 the discovery of the Tau was new land in the sea of two generations. Perhaps the Tau will lead us out of the sea of the Standard Model.

- *Martin Perl*





BRT variables

Number of primary vertices, n_{PV}

Number of primary vertices in the event.

Average interactions per crossing, μ

Average number of interactions per bunch crossing.

Cluster shower depth, λ_{centre}

Distance of the cluster shower centre from the calorimeter front face measured along the shower axis.

Cluster second moment in λ , $\langle \lambda^2 \rangle$

Second moment of the distance of a cell, λ , from the shower centre along the shower axis.

Cluster first moment in energy density, $\langle \rho \rangle$

Cluster first moment in energy density $\rho = E/V$, where E and V represent the energy and volume of the cluster, respectively.

Cluster presampler fraction, $f_{\text{presampler}}$

Fraction of cluster energy deposited in the barrel and endcap presamplers.

Cluster EM-like probability, P_{EM}

Classification probability of the cluster to be EM-like, as described in Ref. [28].

Number of associated tracks, n_{track}

Number of tracks associated with the $\tau_{\text{had-vis}}$.

Number of reconstructed neutral pions, n_{π^0}

Number of reconstructed neutral pions associated with the $\tau_{\text{had-vis}}$.

Relative difference of pion energies, γ_π

Relative difference of the total charged pion energy, E_{charged} , and the total neutral pion energy, E_{neutral} : $\gamma_\pi = (E_{\text{charged}} - E_{\text{neutral}})/(E_{\text{charged}} + E_{\text{neutral}})$.

Calorimeter-based pseudorapidity, η_{calo}

Calorimeter-based (baseline) pseudorapidity.

Interpolated transverse momentum, $p_{\text{T}}^{\text{interp}}$

Transverse momentum interpolated from calorimetric corrections to energy measurement and TPF reconstruction.

Ratio of p_{T}^{LC} to $p_{\text{T}}^{\text{interp}}$, $p_{\text{T}}^{\text{LC}}/p_{\text{T}}^{\text{interp}}$

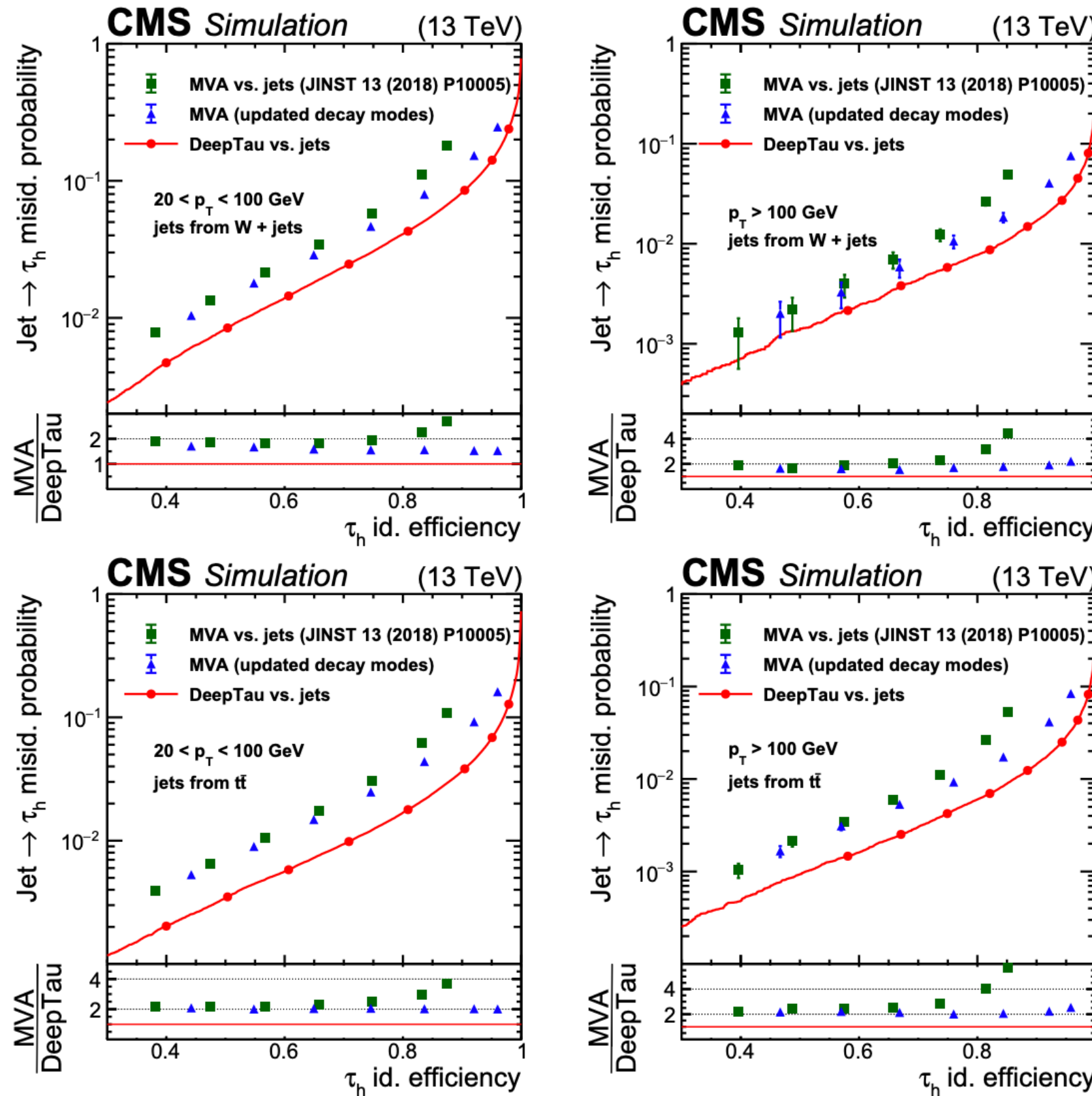
Ratio of the local hadron calibration transverse momentum to $p_{\text{T}}^{\text{interp}}$.

Ratio of $p_{\text{T}}^{\text{TPF}}$ to $p_{\text{T}}^{\text{interp}}$, $p_{\text{T}}^{\text{TPF}}/p_{\text{T}}^{\text{interp}}$

Ratio of the TPF reconstruction transverse momentum, $p_{\text{T}}^{\text{TPF}}$, to $p_{\text{T}}^{\text{interp}}$.



Backup



Why use τ 's to study physics Beyond the Standard Model?

- In **2HDM** τ 's can have enhanced couplings to down type quarks and leptons
- $H^\pm \rightarrow \tau^\pm \nu$
- Insight into the Flavor puzzle:
Large branching fraction for the study of **Lepton Flavor Violation**
- **W'**, **Z'** - Universality is not guaranteed in these models
- Enhanced couplings for **Long Lived Particles**

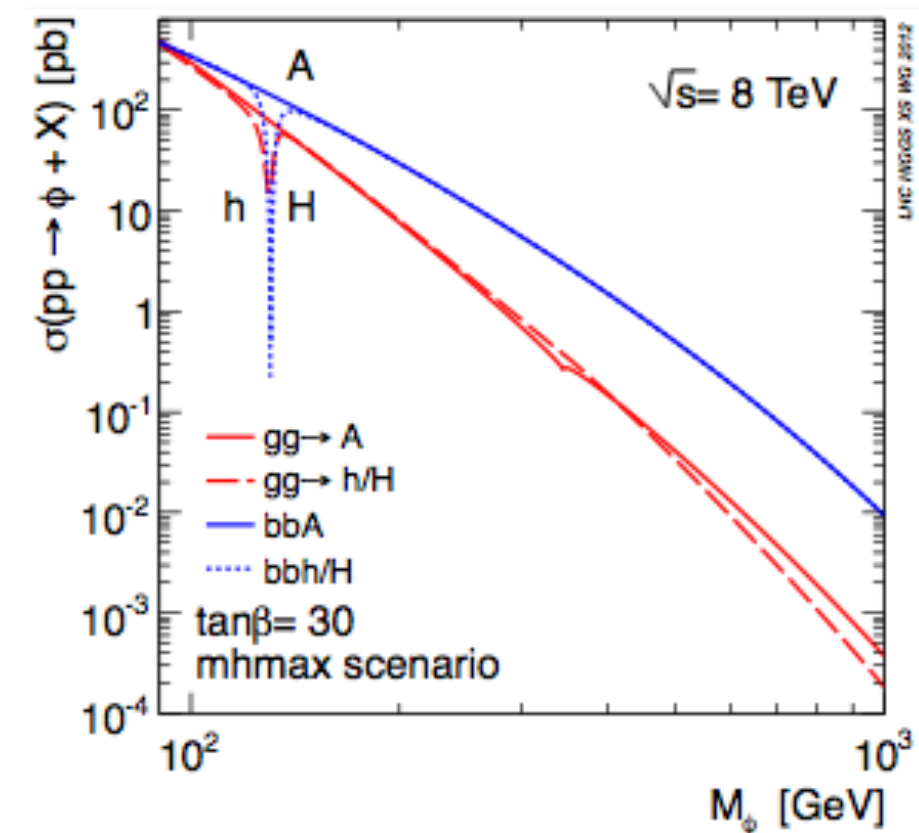
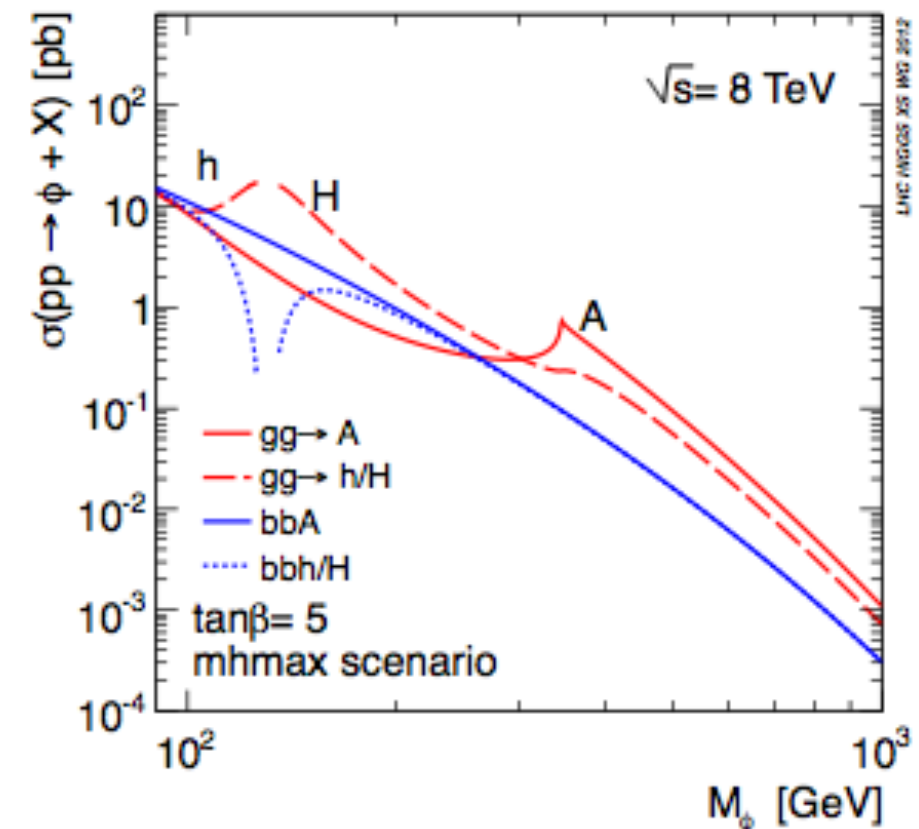


Table 3: Primary tau triggers used in the 2016 pp data taking period. For each trigger, the typical offline selection is indicated, together with the online selections at L1 and the HLT. The online thresholds are matching in the same order to the offline thresholds. When an online selection is not applicable, ‘-’ is indicated. ‘i’ indicates that an isolation requirement is applied at trigger level. The trigger rates are reported for an instantaneous luminosity of $1.2 \times 10^{34} \text{ cm}^{-2}\text{s}^{-1}$ and are not unique, that is they do not account for overlaps with other triggers. The L1Topo 2 τ triggers are those commissioned in 2016.

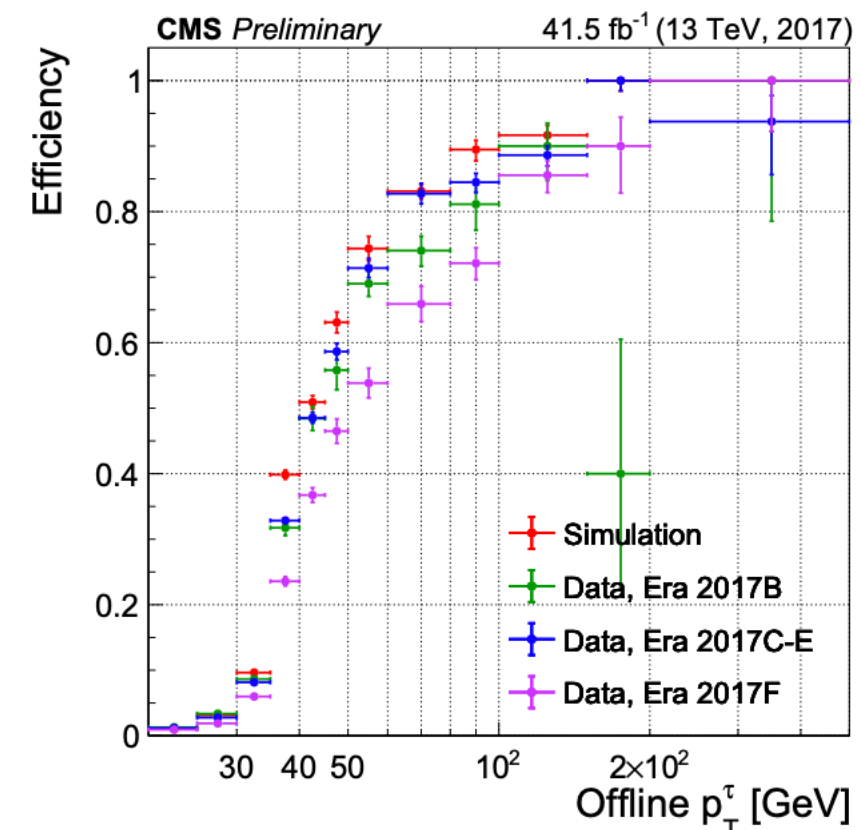
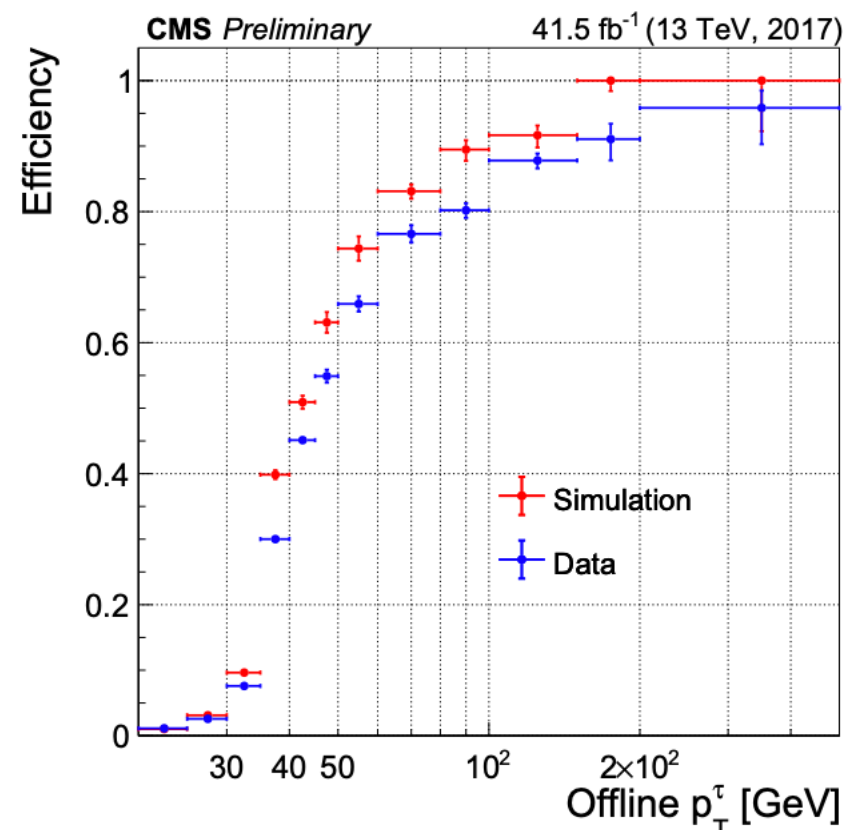
Trigger	Typical offline selection	Trigger selection		Trigger rate at $1.2 \times 10^{34} \text{ cm}^{-2}\text{s}^{-1}$	
		L1	HLT	L1 [kHz]	HLT [Hz]
τ	$p_T^\tau > 170 \text{ GeV}$	60	160	5.2	15
2 τ	$p_T^\tau > 40, 30 \text{ GeV}$, $p_T^{\text{jet}} > 80 \text{ GeV}$	20i,12i,25	35,25,-	6.7	35
$\tau+e$	isolated e , $p_T^e > 18 \text{ GeV}$, $p_T^\tau > 30 \text{ GeV}$, $p_T^{\text{jet}} > 80 \text{ GeV}$	15i,12i,25	17i,25,-	3.4	9
$\tau+\mu$	isolated μ , $p_T^\mu > 15 \text{ GeV}$, $p_T^\tau > 30 \text{ GeV}$, $p_T^{\text{jet}} > 80 \text{ GeV}$	10,12i,25	14i,25,-	1.7	7
$\tau+E_T^{\text{miss}}$	$p_T^\tau > 40 \text{ GeV}$, $E_T^{\text{miss}} > 150 \text{ GeV}$, $p_T^{\text{jet}} > 70 \text{ GeV}$	20i,45,20	35,70,-	1.8	8
2 τ with L1Topo	$p_T^\tau > 40, 30 \text{ GeV}$, $\Delta R(\tau, \tau) < 2.6$	20i,12i,2.9	35,25,-	5.9	39
	$p_T^\tau > 40, 30 \text{ GeV}$, $\Delta R(\tau, \tau) < 2.6$, $p_T^{\text{jet}} > 80 \text{ GeV}$	20i,12i,2.9,25	35,25,-,-	3.8	24

Trigger Efficiency of 2017 Data versus Simulation

CMS-DP-2018-009

$di\tau_h$ Trigger Efficiency

- The τ_h leg efficiencies of the following $di\tau_h$ trigger is shown for 2017 data and Drell-Yan events
 - HLT_DoubleTightChargedIsoPFTau35_Trk1_TightID_eta2p1_Reg_CrossL1_v
 - HLT_DoubleMediumChargedIsoPFTau40_Trk1_TightID_eta2p1_Reg_CrossL1_v
 - HLT_DoubleTightChargedIsoPFTau40_Trk1_eta2p1_Reg_CrossL1_v
- It has a medium/tight isolation, and seeded by $\mu + \text{Iso } \tau_h$ L1 trigger



- Dead pixel modules (Era 2017B) and DC-DC converter problems (Era 2017F) reduces the efficiency
- Perform tracking mitigation in Era 2017D to recover the reduced efficiency due to dead pixel modules
- Isolation of tau leptons at Level 1 seed and higher isolation at HLT level results in a sharper turn-on



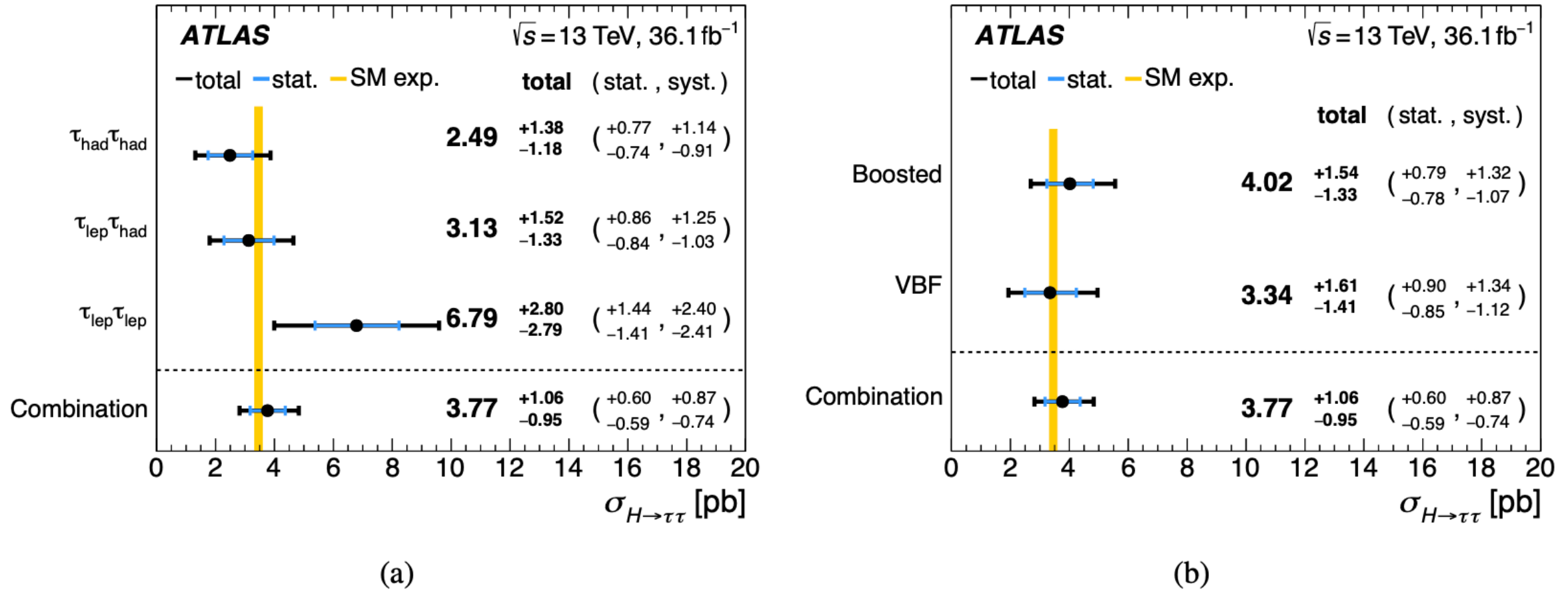


Figure 7: The measured values for $\sigma_{H \rightarrow \tau\tau}$ when only the data of (a) individual channels or (b) individual categories are used. Also shown is the result from the combined fit. The total $\pm 1\sigma$ uncertainty in the measurement is indicated by the black error bars, with the individual contribution from the statistical uncertainty in blue. The theory uncertainty in the predicted signal cross section is shown by the yellow band.

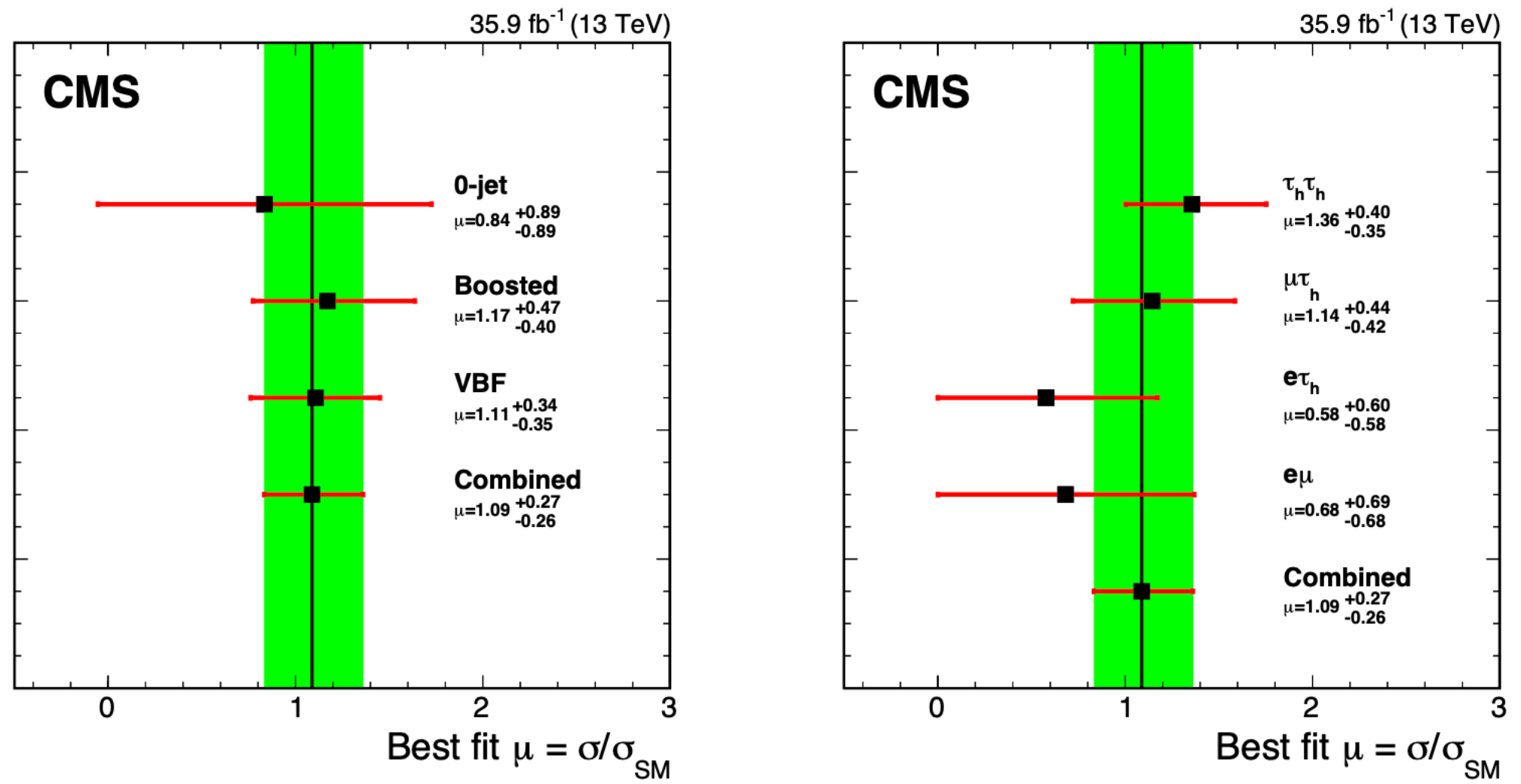
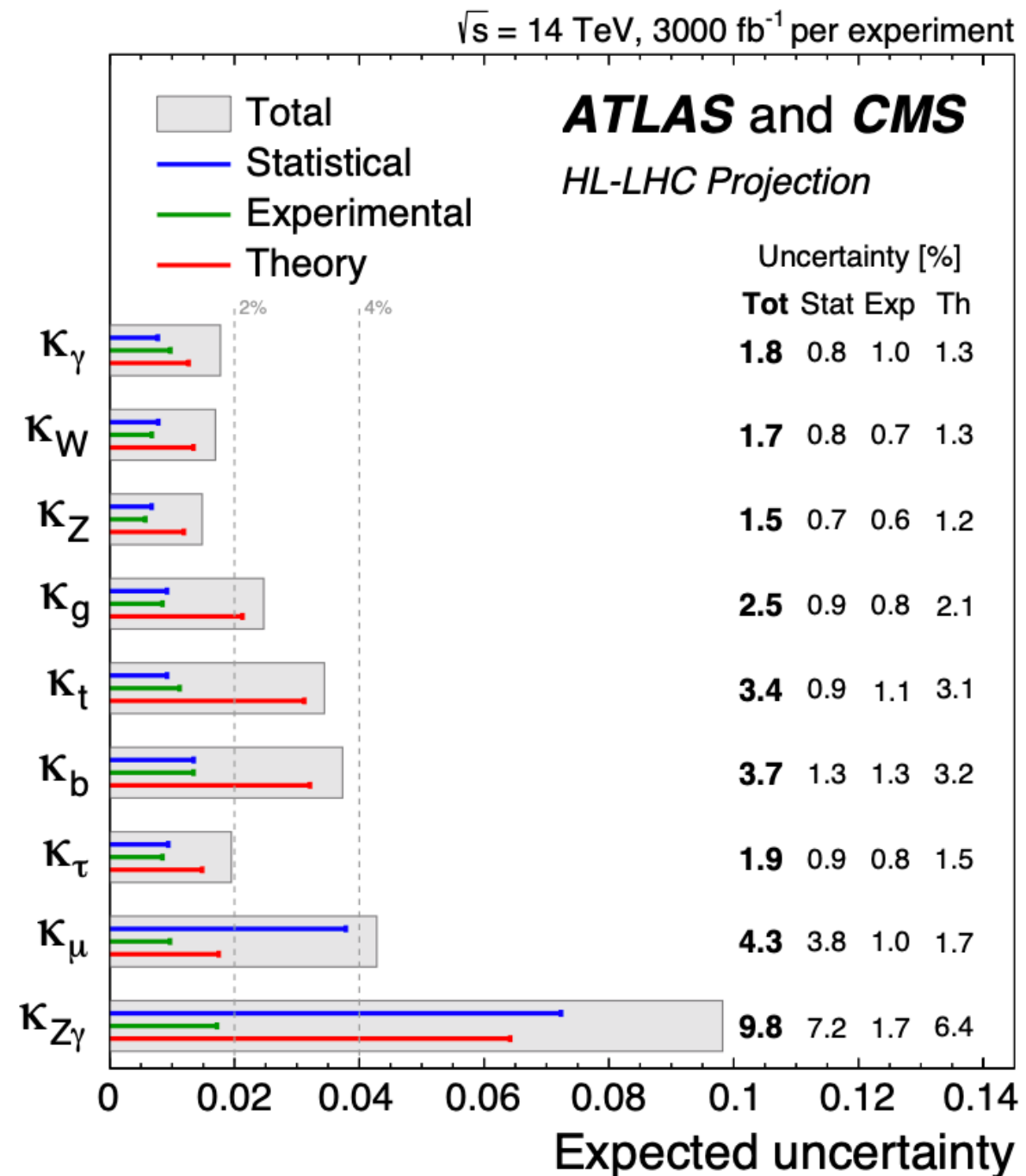
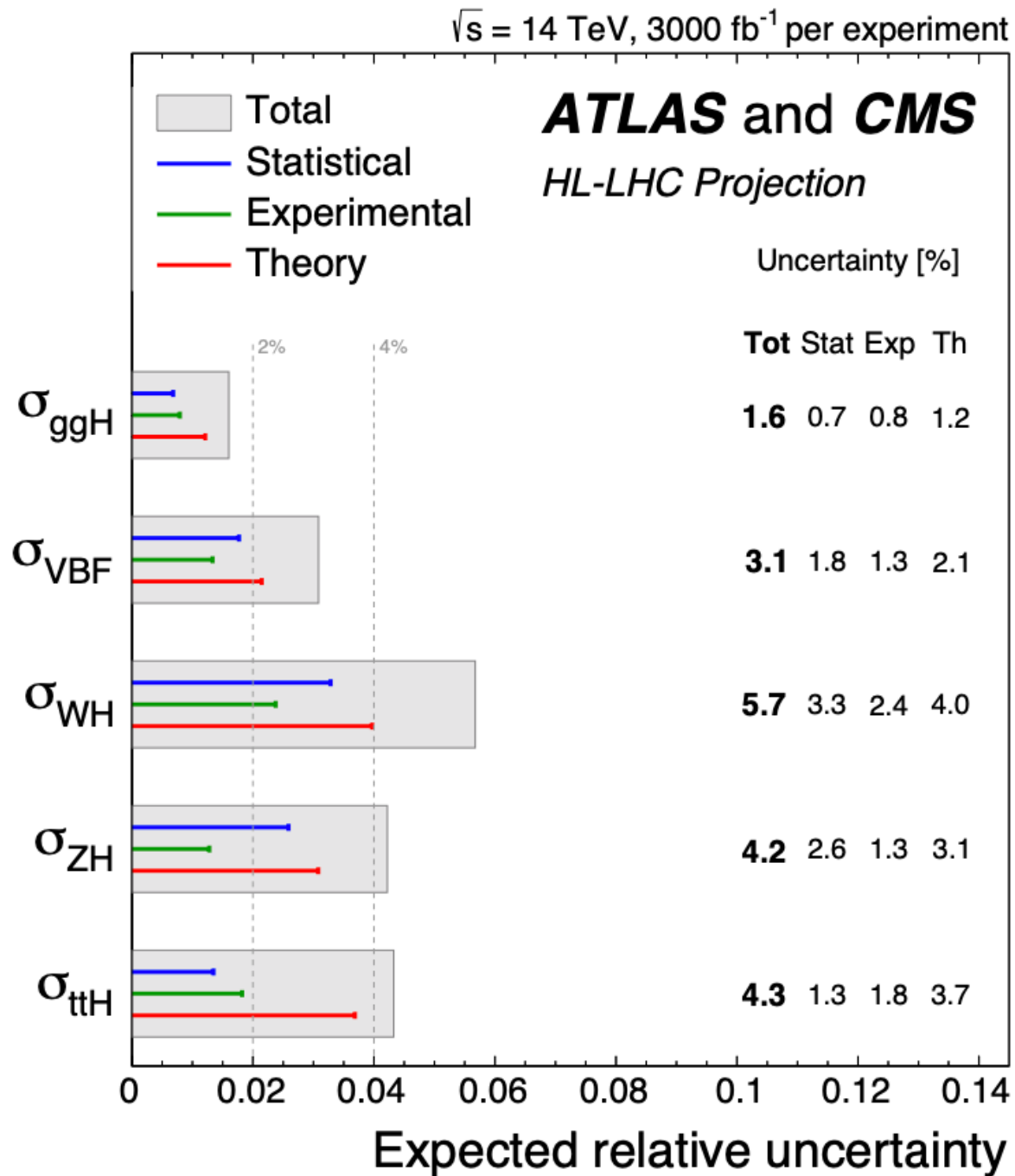


Figure 21: Best fit signal strength per category (left) and channel (right), for $m_H = 125.09$ GeV. The constraints from the global fit are used to extract each of the individual best fit signal strengths. The combined best fit signal strength is $\mu = 1.09^{+0.27}_{-0.26}$.

What can we expect at the HL-LHC?



HLT Taus at CMS

Level 2

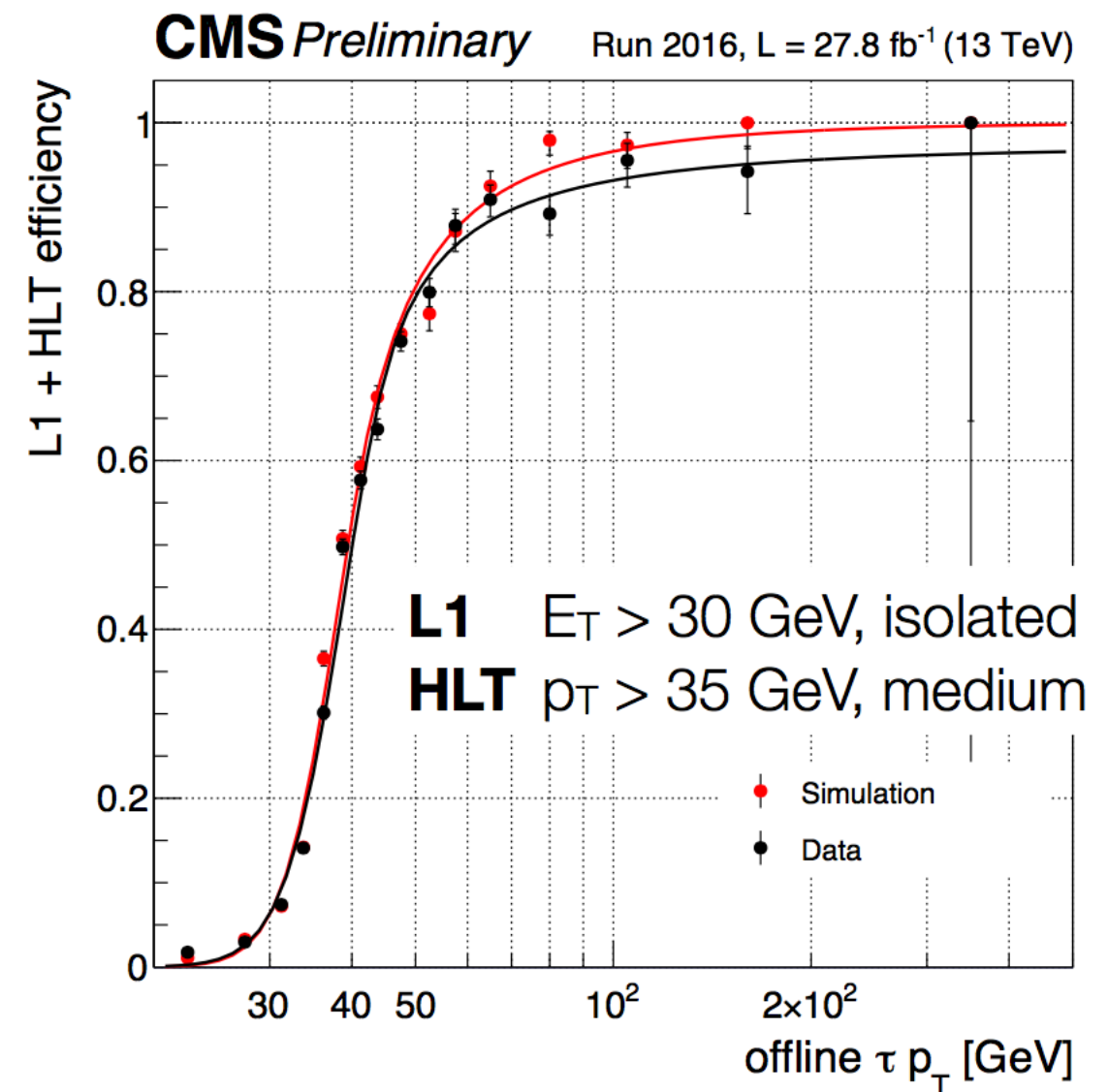
Narrow CaloJets are formed around
“Level 1 Seeds”

Level 2.5

Pixel based Isolation is required
around the CaloJet

Level 3

Offline-like Tau Reconstruction
proceeds with HLT Particle Flow
▶ Less stringent than Offline Reco



- ▶ For each step if a minimum requirement (typically p_T or isolation) is not met then processing is **Halted** -> (Allowing for a new event to be processed)
- ▶ If all of the **requirements are met** then the **event is saved** for **offline analysis**



What Could We Achieve??

Higgs Self Coupling

collider	single- H_{SM}	$H_{\text{SM}}H_{\text{SM}}$	combined
HL-LHC [15]	100-200%	50%	50%
ILC ₂₅₀ /C ³ -250 [16, 10]	49%	—	49%
ILC ₅₀₀ /C ³ -550 [16, 10]	38%	20%	20%
CLIC ₃₈₀ [17]	50%	—	50%
CLIC ₁₅₀₀ [17]	49%	36%	29%
CLIC ₃₀₀₀ [17]	49%	9%	9%
FCC-ee [18]	33%	—	33%
FCC-ee (4 IPs) [18]	24%	—	24%
FCC-hh [19]	—	2.9-5.5%	2.9-5.5%
$\mu(3 \text{ TeV})$ [13]	—	15-30%	15-30%
$\mu(10 \text{ TeV})$ [13]	—	4%	4%

Table 2-4. Sensitivity at 68% probability on the Higgs cubic self-coupling at the various future colliders. Values for single Higgs determinations below the first line are taken from [20]. The values quoted here are combined with an independent determination of the self-coupling with uncertainty 50% from the HL-LHC.

